16 Interior Noise

Lead authors

John S. Mixson
NASA Langley Research Center
Hampton, Virginia

John F. Wilby
Atlantic Applied Research Corp.
Los Angeles, California

Introduction

Interior noise is an important consideration in the design and operation of virtually all aerospace flight vehicles. Noise is a natural by-product of powerful propulsion systems, high-speed aerodynamic flow over vehicle surfaces, and operation of onboard systems such as air conditioners. The noise levels produced can be intense enough to result in an unacceptable interior noise environment through effects such as passenger discomfort, interference with communication, crew fatigue, or malfunction of sensitive electronic equipment. Control of the noise environment requires substantial special effort, and the noise control measures usually result in penalties such as added structural weight, reduced cabin volume, or reduced performance. Interior noise control therefore requires a continuing search for means to reduce both the noise levels and the associated penalties, especially for new higher performance vehicles.

A variety of noise sources and transmission paths contribute to cabin noise. Sources such as propellers, inlet and exhaust systems of reciprocating or turbofan engines, turbomachinery, and turbulent airflow over the aircraft surfaces generate noise that impinges directly on the exterior of the fuselage and transmits into the cabin. This noise is referred to as "airborne noise." Sources such as engine unbalance forces transmitted through engine mounts and engine exhaust or propeller wakes impinging on wing or tail surfaces generate vibrational energy that is transmitted along the airframe structure and radiated into the cabin as acoustic noise. This noise is referred to as "structure-borne noise." Other important noise sources such as helicopter gearboxes, air-conditioning systems, and hydraulic systems used to operate landing gear or flaps are located within the fuselage of the aircraft. In general, any one of these sources can produce excessive noise; therefore all must be considered in a noise control design. Several sources may contribute about equally. Then, reducing noise from only one source to a level below that from several others has minimal effect since total acoustic power changes by only a small percentage (ref. 1, pp. 40–44). A balanced noise control treatment, therefore, would reduce the excessive noise from each source-path combination, so that all contribute about equally and the combined noise satisfies the acceptability criteria.

Interior sound levels can be controlled by reducing the noise generated by the source, by reducing the noise during transmission through airborne and

structure-borne paths, and by reducing the noise transmitted within the cabin. In some cases the interior noise sensation can be reduced, for example, by the use of ear protectors by occupants. In this chapter the emphasis is on the mechanisms of transmission through airborne and structure-borne paths and the control of cabin noise by path modification. Methods for identifying the relative contributions of the various source-path combinations are also discussed because of the need to concentrate treatment on the dominant combinations and to avoid weight penalties associated with treatment of nondominant source-path combinations. The mechanisms of source noise generation and control are discussed in other chapters of this book. However, features of the source noise that have important effects on interior noise and its control are discussed in the next section. The interior environment required for acceptability also has a major effect on the control of transmitted noise because of the penalties that have been mentioned. The effects of noise on equipment result from the vibrations that are induced; procedures are available for design and test of equipment to withstand vibrations (ref. 2). Human response to noise environments is described in detail in another chapter of this book. However, some aspects of passenger comfort of particular interest to interior noise control are described in the following paragraphs.

Noise is one of many factors that influence the comfort of passengers. Other factors include vibration, temperature, seat size and hardness, cabin air pressure, and air ventilation and quality. In spite of interactions that may occur between noise and the other factors (ref. 3), noise requirements are usually considered separately. In general, the noise level should be low enough to provide a feeling of comfort, and the noise spectrum should allow speech communication and be without excessive low-frequency "booming" or high-frequency "hissing." Noises that are annoying or alarming are undesirable, even though they may be low in level for normal operation of the aircraft. Occasionally, the noise level in the cabin may have large spatial variations that may also be undesirable. The penalties associated with noise control may be significant; therefore passenger requirements should be known accurately and the noise reduction provided should be only sufficient to satisfy those requirements.

Three parameters are in common use to quantify the subjective aspects of interior noise. The overall sound pressure level (OASPL, dB) adds most audible frequency components equally. The A-weighted sound level reduces the contributions of very low- and high-frequency components and has been found to correlate closely with the subjective response of human laboratory subjects and aircraft passengers. Speech interference level (SIL) includes only the frequencies between 350 Hz and 5623 Hz and relates to the quality of voice communication. Laboratory studies using simulated cabin noise indicate that 50 percent of the subjects reported feelings of annoyance when the A-weighted level exceeded about 82 dB or when the SIL exceeded 70 to 75 dB (ref. 4). Modern turbofan-powered aircraft having A-weighted sound levels in the range from 75 to 82 dB during cruise and associated SIL in the range from 55 to 70 dB have gained wide acceptance by travelers and are sometimes considered a standard of comparison. Values of SIL in that range are considered acceptable for large transports because nearby passengers can converse comfortably, while distant conversations that might intrude are masked. For smaller, executive class aircraft, a lower SIL is desirable so that all passengers can converse as a group. Laboratory studies have indicated that strong tones, such as those produced by propellers, tend to cause increased annoyance (ref. 5). Surveys of interior noise levels in existing

general aviation and commercial propeller and jet aircraft show that the A-weighted sound levels vary from about 67 dB to about 103 dB (ref. 4), suggesting that a range of levels is acceptable depending on the particular application. Surveys in buses, trains, and automobiles show that the A-weighted levels vary from about 60 dB to about 90 dB, so the levels in the quieter aircraft are in the same range as those in ground transportation.

The character and level of the noise differ for different aircraft and for different times during the flight. These differences affect the interior noise control efforts required. For example, the noise levels generated by full-power engine operation during takeoff and by reverse thrust during landing can exceed levels during cruise, but the takeoff and landing phases are of sufficiently short duration that the passengers can accept the additional noise without undue discomfort. Because the cruise portions of flight are of relatively long duration, the associated noise levels must be controlled for a steady state level of passenger comfort. The different durations and operating conditions for different aircraft types and flight conditions permit different noise control requirements. The most stringent requirements are usually associated with long flights that may last 12 to 16 hours. Somewhat higher noise levels are acceptable on shorter flights, but some short distance operations may involve high speeds at low altitudes which can lead to higher source noise levels and a requirement for more sound-reducing treatment. Thus, interior noise control must take account of the ultimate operational use of the aircraft, as well as the noise sources, transmission paths, and passenger comfort requirements.

Sources of Interior Noise

The source characteristics required for interior noise analysis include both magnitude and phase of the sound pressure and their distributions in frequency and space over the surface of the vehicle. These characteristics differ significantly for the different sources of interest; in some cases the sound pressures are deterministic,[1] and in other cases random. Empirical models have been developed for the pressure fields from many of the sources on an airplane (ref. 7). The different characteristics can have important effects on the noise transmitted through a fuselage, as illustrated in figure 1. These results were obtained in a theoretical study of the noise transmitted through a cylindrical aircraft fuselage of typical frame and stringer-stiffened skin construction and having a diameter of about 1.68 m (ref. 8). The source noise characteristics were carefully modeled to match available experimental data and the fuselage structure and interior were the same for both curves. For this example, fuselage noise reduction is defined as the difference between the maximum exterior SPL on the fuselage surface and the SPL transmitted through to the interior. Figure 1 shows that noise reduction is higher for the propeller source by as much as 15 dB. These differences result from the spatial distributions of source pressure magnitude and phase, which govern the total acoustic force on the fuselage and the efficiency of that force in causing motion of the fuselage structure.

[1] Deterministic pressures are those that can be described by an explicit mathematical relation, such as $\cos \omega t$ (ref. 6), where ω is circular frequency and t is time.

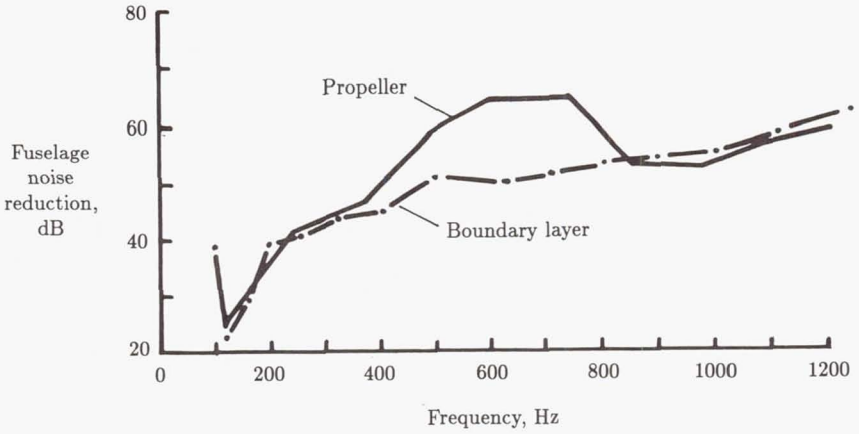

Figure 1. Predicted fuselage noise reduction for a general aviation aircraft showing effect of source character on fuselage noise transmission. (From ref. 8.)

Boundary Layer Noise

The noise generated by airflow over the aircraft surfaces is important for virtually all classes of aircraft. For the smaller aircraft with less streamlining, more exposed struts, and light structure, airflow noise is important at higher frequencies. For the larger, jet-powered, well-streamlined aircraft, high speed flows generate significant levels of turbulent boundary layer noise that usually constitutes the most important source of cabin noise during cruise. Considerable information on turbulent boundary layer pressure fluctuations is available in the literature from both wind tunnel and flight studies.

Fluctuating pressures acting on the fuselage surface beneath the boundary layer have been measured in flight of a large jet aircraft operating at speeds from 138 to 242 m/sec at an altitude of 7620 m (ref. 9). Figure 2 shows that the spectrum of the pressure is broadband and contains significant components at frequencies from below 100 Hz to above 2000 Hz. Increasing airspeed from Mach 0.45 to Mach 0.78 increases spectral density by a factor of 5, which is equivalent to about 7 dB. Since the overall root-mean-square (rms) pressure varies, approximately, as the flight dynamic pressure or the square of the flight speed, an increase of 9 to 10 dB might be expected. However, this increase is not reproduced directly in the spectrum level because the energy is distributed over a wider frequency range at the higher speed. At the aft location in figure 2, the spectral density is higher than at the forward location, but only at frequencies below about 1000 Hz. The increase is a factor of about 3.5, equivalent to 5 dB. It is due in part to a shift of energy to lower frequencies as the boundary layer thickness increases farther aft, but it also may be influenced, for the example chosen, by the presence of low-frequency jet noise contributions on the rear of the fuselage. The variations along the fuselage are large enough to influence the design of interior acoustic treatments. These flight data were used, together with

data from several laboratory studies, to develop a general empirical equation for predicting fluctuating pressure spectra (ref. 9).

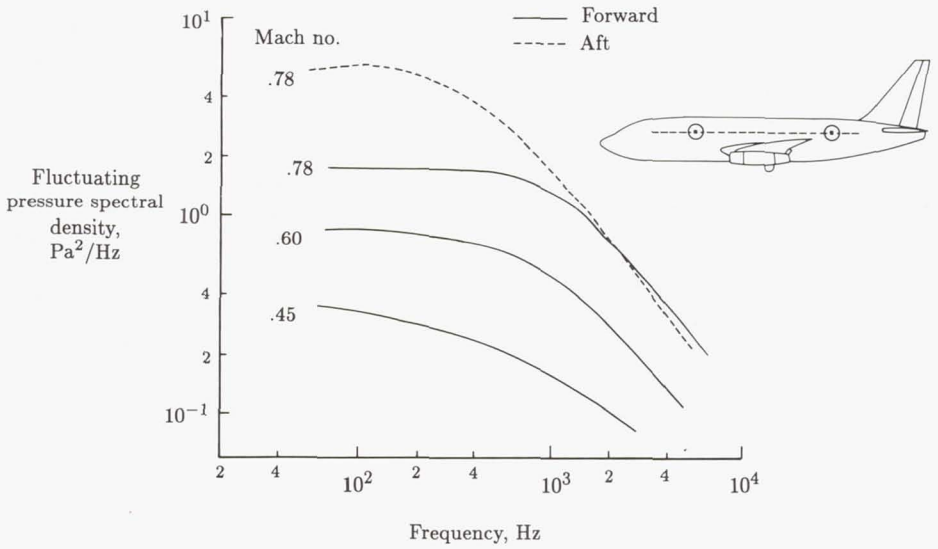

Figure 2. Spectral density of fluctuating pressure on the exterior of a large jet aircraft in flight. Boundary layer source. (From ref. 9.)

The flight data were also analyzed to determine the point-to-point correlation (in the time domain) or cross spectral density (in the frequency domain) of the pressures. Cross spectral density of a random pressure field plays an important role in determining the effective force acting on a structure, and hence, the response. Flight and wind tunnel measurements indicate that a boundary layer pressure field is convected in the direction of the flow and the coherence decreases as the separation distance between the measuring points increases. The convection speed U_c is about 70 percent of the flight speed, so that as the aircraft speed increases, there is the possibility that "hydrodynamic coincidence" will occur. When hydrodynamic coincidence occurs, the phase speed of the fluctuating pressures matches the structural bending wave speed. As a result, the structural vibration and interior sound pressure levels increase significantly. For example, figure 3 presents vibration spectra measured at the center of a fuselage skin panel on a large jet-powered airplane (ref. 10). The vibration spectral densities have been normalized with respect to the exterior boundary layer pressure spectral densities. If there were no change in correlation of the pressure field, the vibration would be expected to scale directly with exterior pressure and the two spectra in figure 3 would lie on top of each other; this is not the case. In the frequency range from 800 to 1500 Hz, the response at a flight Mach number of 0.60 is higher, by up to 7 dB, than that at a Mach number of 0.78, and at frequencies above about 2000 Hz, the converse is true. It has been shown that this effect is associated with correlation changes and coincidence conditions (ref. 10). Similar results can be seen in the sound pressures measured in the cabin. Note that, at least for subsonic flight, hydrodynamic coincidence occurs

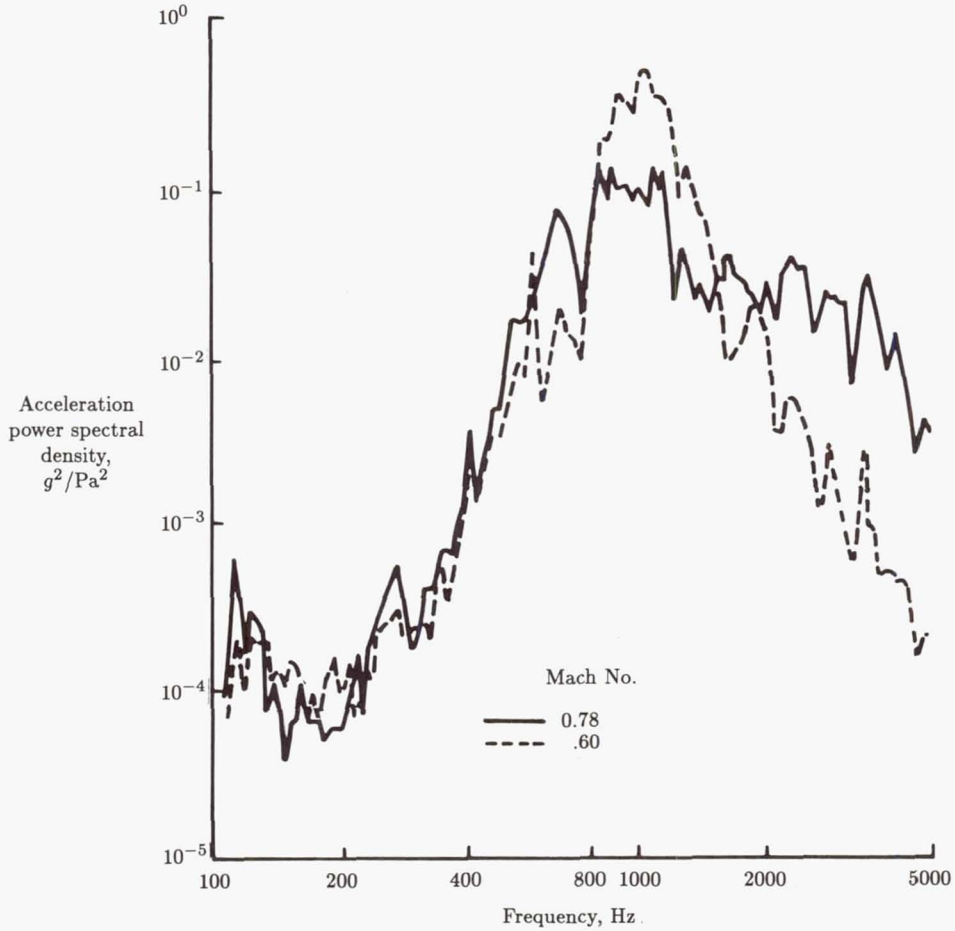

Figure 3. Fuselage panel acceleration spectra for unit excitation showing influence of pressure coherence. (From ref. 10.)

at frequencies lower than the acoustical critical frequency which, for the example shown, is about 10 000 Hz.

The correlation characteristics of turbulent boundary layer pressure fields have been incorporated into several empirical mathematical models of the pressure cross spectral density function (refs. 7 and 8). The models have been used to predict fuselage vibration (ref. 11) and airplane interior sound levels (ref. 8). The decaying and convecting nature of the pressure field is shown (in the separable form) by the cross spectral density function $S_p(\overline{x}_1, \overline{x}_2, \omega)$:

$$S_p(\overline{x}_1, \overline{x}_2, \omega) = S_p(\overline{x}, \omega) \exp(-a_x|x_2 - x_1|) \times \exp(-a_y|y_2 - y_1|) \exp[-ib\omega(x_2 - x_1)/U_c]$$

where the pressure field is taken to be homogeneous, with an auto spectral density function $S_p(\overline{x}, \omega)$. Coherence decay parameters a_x and a_y can be functions of frequency, convection velocity, and boundary layer thickness.

Propeller Noise

A single propeller generates a noise field that is highly tonal in frequency content and highly directional in spatial distribution. The noise-generating mechanisms are associated with the thickness of the blades passing through the air and with the aerodynamic pressures on the blades that produce the steady thrust and torque. As a consequence, the sound pressures are deterministic and are completely correlated at all points in the sound field. The boundary layer turbulence in the airflow over the blade surfaces also generates a broadband random noise, but this source is generally low level. The noise level generated by a propeller is influenced by factors such as power produced, tip speed (rotational and forward), number of blades, blade shape, and distance from the propeller. The effects of these factors have been studied experimentally (ref. 12). Also, nonuniformity of the airflow into the propeller can generate increased noise. Nonuniform inflow occurs when a propeller is operated at nonzero angle of attack, in the wake from a wing or strut, or at near-zero forward speed. Theoretical methods are available to predict test results with good accuracy and to include complicating factors such as nonuniform inflow and interaction with a fuselage (refs. 13 and 14).

The spectrum of exterior noise on a twin-engine aircraft is illustrated in figure 4. These results were measured in flight using a flush-mounted microphone on the port side of the aircraft (ref. 15). Each engine was run at a different rpm, so the contribution from each propeller can be seen. The tone at the blade-passage frequency of about 75 Hz has the highest level; succeeding tones decrease at a rate of about 3 dB per harmonic. The first few tones greatly affect passenger comfort and are difficult to control by sidewall treatment, especially at the lower frequencies. Blade-passage frequencies fall in the range from 75 to 125 Hz for light aircraft and in the range from 160 to 250 Hz for the new high-speed turboprops. The overall level and falloff rate vary with operating condition, altitude (ref. 15), and propeller tip speed (ref. 13). The propeller tones decrease with frequency faster than the boundary layer noise; therefore at high frequency the boundary layer noise is dominant.

Propeller directional characteristics are illustrated in figure 5. These results were obtained for a model of a blade designed for operation at Mach 0.8 (ref. 16). Design helical tip speed is slightly greater than Mach 1.0. The test results were obtained in flight with the model propeller mounted on a pylon atop a jet-powered aircraft and with microphones flush-mounted in the skin of the aircraft. The figure shows that the OASPL is highest near the plane of rotation of the propeller and decreases rapidly in both forward and aft directions. This directivity pattern suggests that fuselage noise control treatment (ref. 15) is required primarily near the region of highest noise. For a transport aircraft concept designed for 155 passengers, the propeller noise is estimated to require extra treatment over about 28 percent of the cabin length (ref. 17). For smaller general aviation aircraft (see fig. 4), treatment may be required over a greater percentage of the cabin length. The noise distribution pattern can be expected to be broader for larger propeller diameter and for greater clearance between the propeller and the fuselage. In addition, the directional characteristics

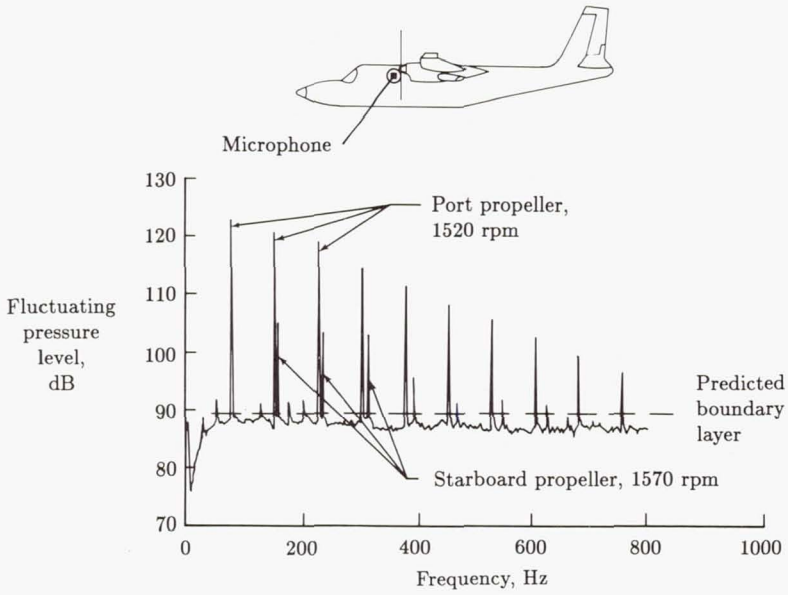

Figure 4. Spectrum of fluctuating pressure on exterior of a light twin-engine aircraft in flight. Altitude = 9100 m; Speed = 154 m/sec. (From ref. 15.)

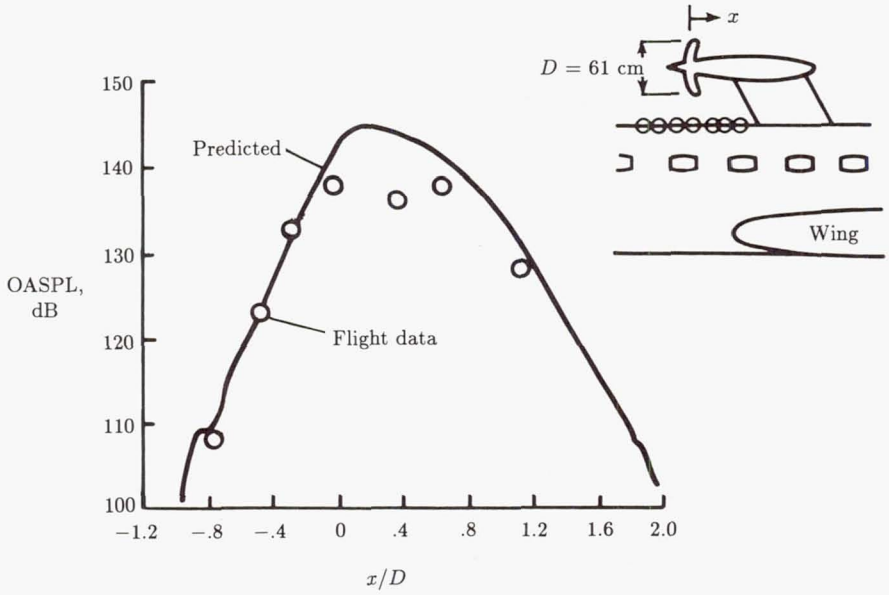

Figure 5. Overall sound pressure level generated by scale model of high-speed propeller. Measured on carrier aircraft at Mach 0.8. (From ref. 16.)

may be affected by operational factors such as flight speed, by interactions with the fuselage flow field, and by interaction with a second propeller in a counterrotating configuration. For a propeller of a light aircraft the higher frequency harmonics were found to decrease faster with distance than the lower frequency harmonics (ref. 18). In the circumferential direction the noise level also decreases rapidly, and in general the noise level on the opposite side of the aircraft is lower by a large amount (fig. 4 indicates about 15 dB).

Phase characteristics are illustrated in figure 6 for the same high-speed propeller model studied in figure 5. The results of figure 6 apply to tests carried out in an acoustic wind tunnel with a massive steel cylinder to simulate a fuselage (ref. 19). Tunnel airflow was carefully managed to minimize turbulence flowing into the propeller, and propeller rotational speed was increased to produce the correct supersonic helical tip speed since the tunnel flow speed was less than design flight speed. The figure shows that large variations in phase angle occur on the cylinder. Such phase variations could have an important effect on the fuselage response and resultant noise transmission. The propeller of figure 6 was located with a tip clearance of 0.8 propeller diameter from the cylinder. For general aviation aircraft, tip clearance is often much less and may be of the order of 0.1 propeller diameter. The measured phase characteristics of one such configuration were found to describe a traveling wave field, rotating in the circumferential direction at a speed approximately equal to the propeller tip speed (ref. 20).

Cabin noise characteristics can be affected in an important way by interactions between the noise fields of several propellers and by interactions of a propeller noise field with the fuselage. For example, when two propellers are operated at slightly different rpm values, beating interference between the two sources occurs, and the noise level in the cabin rises and falls in a manner that is easily detectable and possibly annoying (ref. 21). Many aircraft are equipped with an electromechanical phasing device that is intended to control rpm and phase in an attempt to reduce these fluctuations. It has been proposed that the phase be adjusted to minimize the cabin noise, with the thought that acoustic interference might be used to obtain a noise level below that which results from each propeller separately. The interaction of the propeller noise with the fuselage dynamics is not well understood but is being studied (ref. 22). The noise reduction that may be possible has been estimated in a flight study of a large four-engine aircraft (ref. 23). Some of the results are illustrated in figure 7. Interior noise levels were measured at six longitudinal positions for a flight where the four propellers were controlled only by a mechanical governor that allowed slow angular drift of the relative propeller positions. The data were analyzed to determine the cabin noise levels associated with 5832 combinations of relative phase positions of the four (four-bladed) propellers at 5° angular steps for each propeller. The lowest space-averaged acoustic pressure level was 94 dB and the highest was 103 dB. Larger differences are observed in figure 7 at some fuselage locations. The combination giving the 94-dB average, referred to as "optimum phase," also resulted in noise levels well below the maxima at most of the individual locations. These results indicate that substantial benefits can be obtained throughout the cabin when the propeller phase angles can be accurately controlled.

The interaction of a single propeller with the fuselage has been studied for a twin-engine commuter class aircraft (ref. 24). Interior noise levels were obtained in flight and ground tests with each engine at a different rpm to identify the contribution

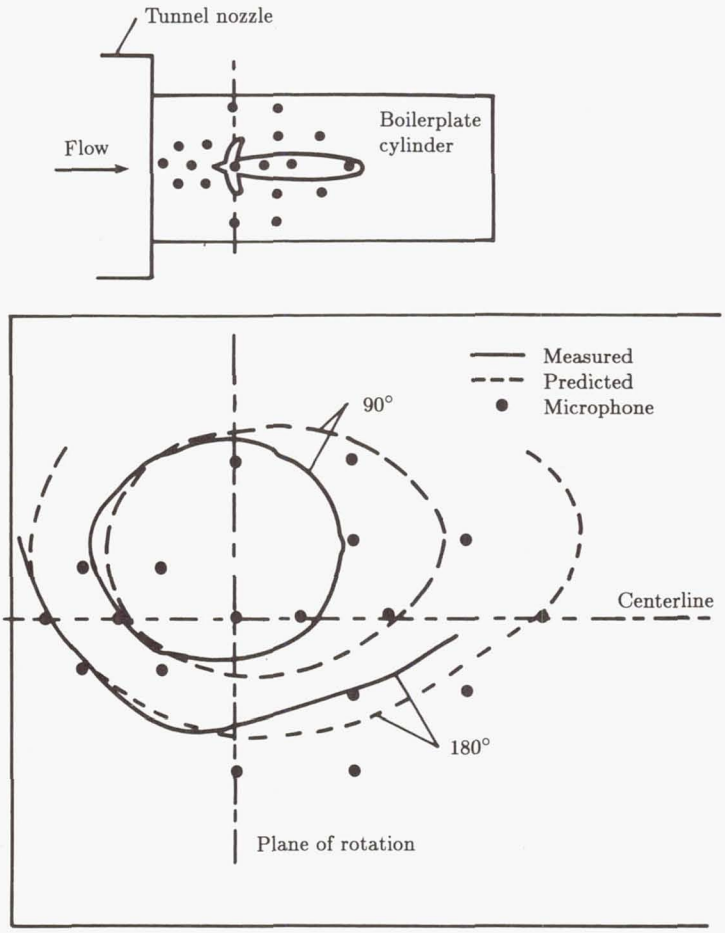

Figure 6. Phase angle distribution of blade-passage harmonic of scale model of high-speed propeller. (Based on ref. 19.)

from each propeller. As the aircraft was configured, the right propeller tip was moving upward as it passed near the fuselage while the left propeller tip was moving downward. Interior levels, obtained by averaging the microphones at left and right seat positions just aft of the propeller plane, indicated that the up-sweeping propeller produced as much as 10 dB less cabin noise in individual blade-passage harmonics than did the down-sweeping propeller. This effect is thought to be associated with nonsymmetries of the fuselage structure and the propeller noise field with respect to the fuselage upper and lower halves. Nonuniform inflow and installation effects may also contribute (ref. 25). These measured cabin noise reductions are significant, but the mechanisms involved are not well understood.

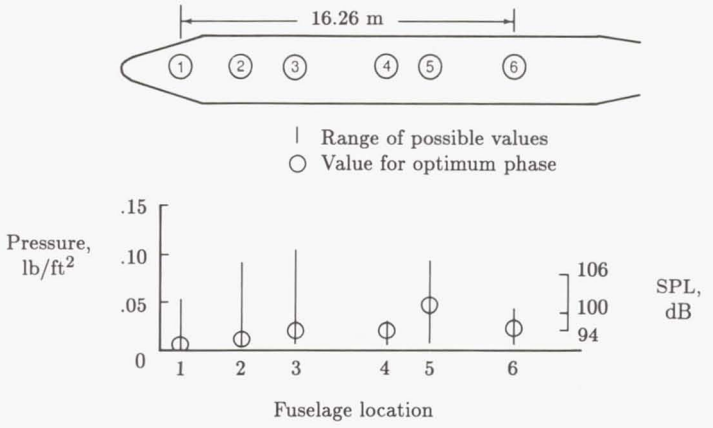

Figure 7. Variation of interior noise level with propeller phase angle for four-engine aircraft. Calculated for blade-passage frequency of 68 Hz. (From ref. 23. Copyright AIAA; reprinted with permission.)

Other Sources of Cabin Noise

The noise radiated by the exhaust from a jet engine has been studied extensively and methods are available for predicting the acoustic near field on an airframe (ref. 7). The impact of jet noise on the cabin environment is reduced greatly by the use of high-bypass engines with low-velocity exhaust and by locating the engines at outboard or aft positions. The influence of jet noise on the fuselage of an airplane with wing-mounted jet engines has been investigated in reference 26. A related phenomenon is associated with the noise from rocket exhausts on space vehicles, such as the Space Shuttle at lift-off (ref. 11). For jet and rocket exhaust noise, the acoustic field on the airframe is random and has a trace velocity in some direction over the structure. Thus, the cross spectral density function can be represented analytically in a manner similar to that used for turbulent boundary layers, but with different values for the coherence decay parameters and convection velocity. Because of the differences in the cross spectral density function, jet noise is often a more efficient exciter of structural vibration at low frequencies than is a subsonic turbulent boundary layer. Acoustic loadings associated with powered-lift configurations have been investigated for STOL (short takeoff and landing) aircraft applications in reference 27. Reciprocating engine exhaust noise and forward-radiated noise from a jet engine fan inlet can sometimes influence cabin noise.

Engine unbalance forces and other sources of engine vibration are known to cause cabin noise (refs. 28 and 29), but information for modeling these sources for cabin noise prediction is not available. It has been postulated that the wake of a propeller striking a wing (or empennage) could be a source of structural vibration with subsequent noise transmission into the airplane cabin. Wind tunnel measurements have been made of the fluctuating pressures produced by a high-speed propeller model on a simulated wing surface placed in the propeller wake (ref. 30). The pressure spectrum was found to be rich in blade-passage harmonics and the pressure levels were found to exceed by more than 15 dB the maximum direct noise which

would strike the fuselage. The mechanisms of acoustic transmission through wing structures have not yet been clearly defined.

Sources of cabin noise in a large helicopter are indicated in figure 8 (ref. 31). The main and tail rotors are located outside the fuselage and can generate significant cabin noise. Main-rotor noise extends into the very low-frequency range. For this helicopter, the main gearbox generates intense tones at frequencies of about 1350 Hz and 2750 Hz, where the human ear is quite sensitive and passenger annoyance may result. Other internal equipment, such as pumps and drive shafts, also contributes to the cabin noise.

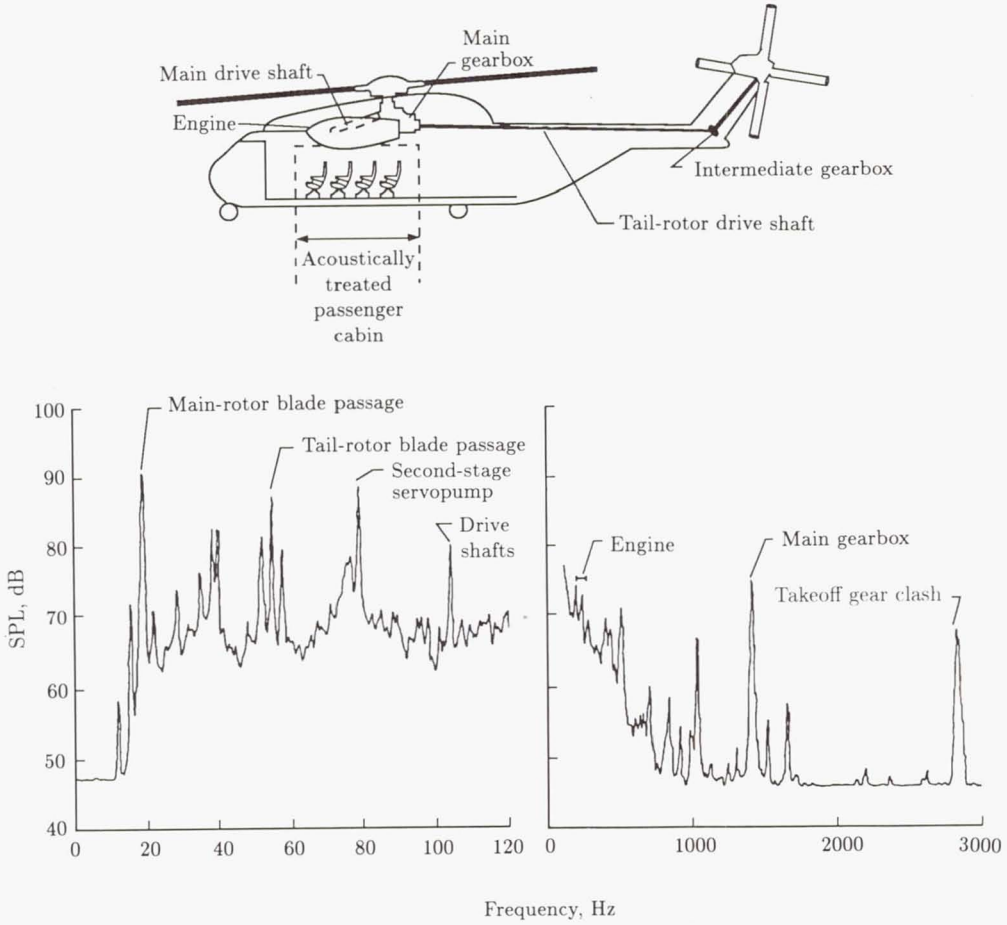

Figure 8. Sources of interior noise in a large helicopter. (From ref. 31.)

Airborne Noise

Airborne noise is defined as that part of the cabin noise that is transmitted through the fuselage sidewall from sources that exert pressures directly on the exterior of the fuselage. Such noise is a major contributor to the cabin noise in

virtually all aircraft and consequently has been studied extensively. The elements to be considered include the source noise characteristics, the noise transmission through the fuselage structure and attached acoustic treatment (or "trim"), and the distribution and absorption of the noise within the cabin. Aircraft noise sources and their effect on sidewall transmission were described in the previous section on sources. This section focuses on noise transmission into the cabin, with emphasis on aircraft structural characteristics, theoretical methods for understanding and predicting airborne noise, and approaches for controlling it. The actual application of these noise control approaches to aircraft is discussed in a later section of this chapter.

Aircraft Sidewall Transmission

Cabin Noise in Flight

Some effects of the sidewall transmission characteristics are evident in the measured cabin noise shown in figure 9 (ref. 15). Both the propeller tones and the boundary layer noise appear in the cabin, with the propeller harmonics dominating, as they do in the exterior noise shown in figure 4. The largest magnitudes occur at the first two propeller tones; these tones occur at low frequencies where noise control is difficult. The appearance of an engine tone in the cabin sound levels but not in the exterior noise suggests the presence of structure-borne noise for this source. Both the propeller tones and the boundary layer noise levels inside the cabin vary in an irregular manner with frequency, in contrast to the smoother variations exhibited by the exterior noise levels. These variations are evidence of the frequency-dependent transmission characteristics of the fuselage, probably associated with fuselage shell and panel modal activity. The levels in the cabin are significantly lower than the levels on the exterior, indicating that the sidewall provides substantial noise reduction. While the boundary layer noise is much less than the propeller noise in the low-frequency range shown in figure 9, at the higher frequencies, which contribute to speech interference, the boundary layer noise may make a major contribution, even for a propeller-driven aircraft (ref. 32).

Sidewall Noise Reduction

The noise transmission properties of aircraft sidewalls have been studied in flight and ground tests. Transmission is characterized in terms of noise reduction which is defined for this chapter as the difference between two noise levels measured simultaneously at positions inside and outside the aircraft.[2] For the results shown in figure 10, the measurements were made in the plane of the propellers, where

[2] The use of transmission loss (TL), as is customary in architectural acoustics, is not appropriate to characterize aircraft sidewall noise transmission in flight for several reasons. The incident and transmitted acoustic powers required by the definition of TL (ref. 1) cannot be determined in general for aircraft noise sources. The source noise implied by the use of TL is a diffuse, reverberant field (ref. 33). As indicated in figure 1, source characteristics have an important effect on the transmitted noise, and so the transmission of reverberant sound can be expected to differ from the transmission of aircraft sources. Finally, TL does not include the effects of the receiving space (the aircraft cabin) on the transmitted noise. These effects can be significant.

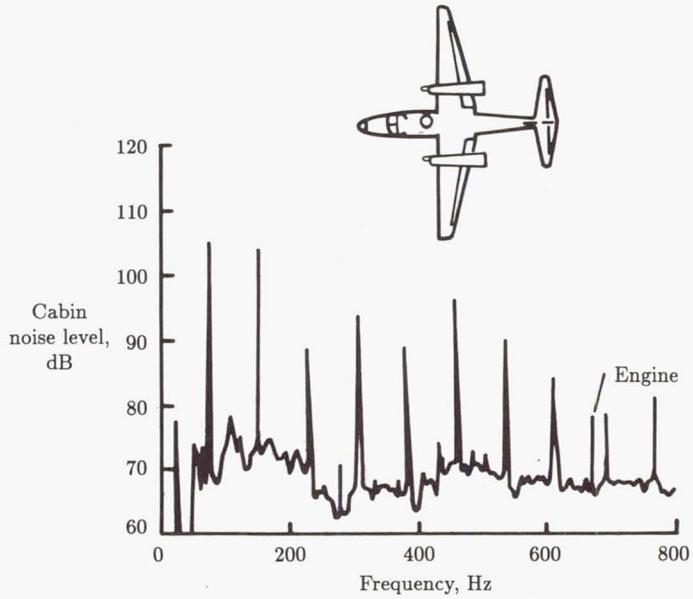

Figure 9. Cabin noise spectrum in flight of a light twin-engine aircraft. No cabin noise control treatment. (From ref. 15.)

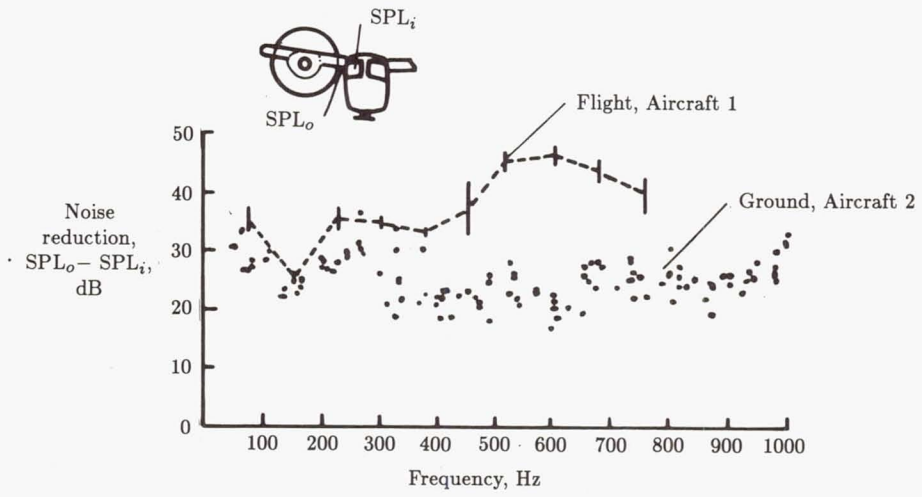

Figure 10. Reduction in propeller noise transmitted through light aircraft sidewalls. Aircraft 1: Weight of 5079 kg, pressurized, no interior treatment (ref. 15). Aircraft 2: Weight of 3175 kg, unpressurized, fiberglass treatment (ref. 34).

both outside and inside noise levels are expected to be maximum with respect to other locations. The two aircraft in the study had similar configurations as shown in figure 10, but differed somewhat in size and weight. The exterior noise was measured by a microphone mounted flush with the surface at about mid-window height, and the interior noise was measured at about ear height for a passenger seat on the side of the aircraft near the window.

The vertical bars in figure 10 indicate data measured in flight on aircraft 1 (ref. 15). The engines of this aircraft operated at (virtually) a single rpm, so results are shown only at the propeller blade-passage frequency and at its harmonics. The height of the bars indicates the range of noise reduction values measured at the various flight conditions. Altitude varied from 3000 m to 8500 m, and cabin pressure, flight speed, and engine power differed somewhat at different altitudes.

Measurements made with aircraft 2 stationary on a runway (ref. 34) are also shown in figure 10. Noise reduction was calculated at each of approximately 10 propeller tones. Operation of the (reciprocating) engine at several different rpm values resulted in the almost continuous distribution of data points.

For the ground tests the noise reduction has a minimum value of about 20 dB in the range from 300 to 600 Hz and increases for lower and higher frequencies. Noise reduction measured in flight is slightly higher than ground measurements for frequencies below 400 Hz and is substantially higher (about 20 dB) at higher frequencies. For both ground and flight tests, the noise reductions at low frequency (below 300 Hz) are significantly higher than the value of about 10 dB that would be expected from architectural experience (i.e., from transmission loss). The trend and magnitude of the noise reductions shown in figure 10 are thought to be strongly influenced by the highly directional nature of the propeller noise field (illustrated in fig. 5) and by interaction with the dynamic wave properties of the sidewall structure (ref. 35). Other variables that may also affect the noise reduction include pressurization, transmission loss and absorption by fiberglass or other treatment, and the position where the interior noise is measured.

Mass and Stiffness Effects

Changes in sidewall noise reduction due to addition of mass or stiffness to the sidewall structure are illustrated in figure 11, from a laboratory test of a light aircraft fuselage using a horn to simulate propeller noise (ref. 36). Skin stiffness was increased by bonding aluminum honeycomb panels to the inner side of the fuselage skin. The stiffness treatment provided more noise reduction than an equal weight of mass treatment in most of the frequency range shown. The increase in noise reduction due to addition of mass can be estimated from (ref. 37)

$$\Delta \mathrm{NR} = 20 \log(1 + m_t/m_s) \tag{1}$$

where m_t is the added treatment mass and m_s is the original skin mass, provided that the sidewall is sufficiently massive that $(\pi m_s f/\rho c)^2 >> 1$, where f is frequency and ρc is the characteristic acoustic impedance. For the aircraft of figure 11 with 2 kg/m^2 of added mass, the noise reduction estimate is about 5.4 dB for frequencies above about 200 Hz, which is in approximate agreement with the results presented. The effect of added stiffness has been shown to be beneficial in some, but not all,

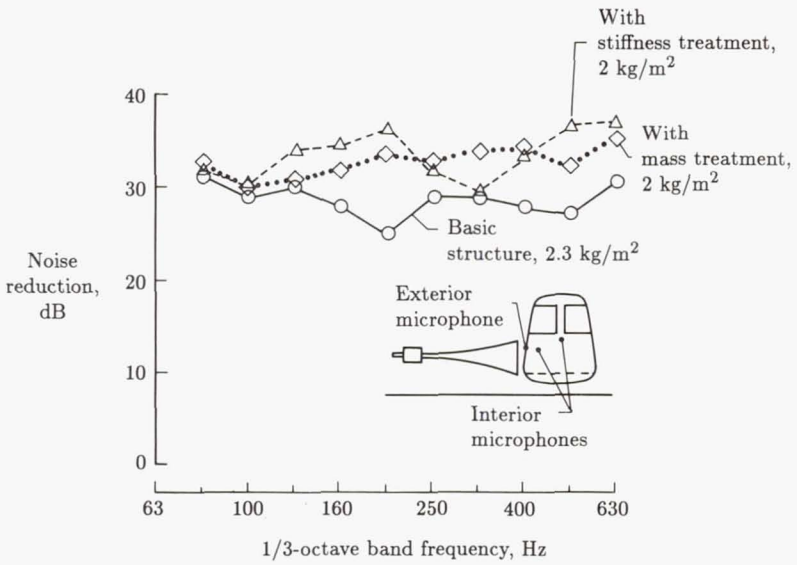

Figure 11. Measured noise reduction due to mass and stiffness treatments for cabin noise control. Mass and stiffness added to fuselage sidewall structure. (From ref. 36.)

laboratory studies, but no flight test results are documented to demonstrate the benefits. Addition of stringers and ring frames is another method of adding stiffness.

Add-On Treatment

The effect on cabin noise level of add-on acoustic treatment is illustrated in figure 12 (ref. 32). Add-on treatments consist primarily of fiberglass wool and impervious layers, which may vary from lightweight to heavy, and are usually installed so that they have minimum contact with the fuselage skin and ring frames. Their acoustic function is to provide an additional barrier to the noise, rather than to modify the sidewall structural behavior as the mass and stiffness treatments do (fig. 11). The fiberglass also provides thermal insulation and the innermost impervious mass layer usually serves as the decorative panel that gives the passenger cabin a finished appearance. These treatments are characterized in terms of insertion loss, defined as the reduction in cabin noise that results from the installation of the treatment. This approach is used because cabin noise levels can be measured conveniently in flight, but exterior noise levels required for noise reduction measurements usually are difficult to measure, especially in an aircraft to be delivered to a customer. Insertion loss is determined from two flights, one with and one without the treatment; therefore flight conditions must be repeatable so that only the change in treatment affects the noise level. Such repeatability of flight conditions can be difficult to obtain (ref. 15), and the best results have been obtained when special flights are dedicated to the noise study.

Fiberglass provides little insertion loss at low frequencies, but is quite effective at high frequencies; its light weight is a great advantage. Cabin absorption is an

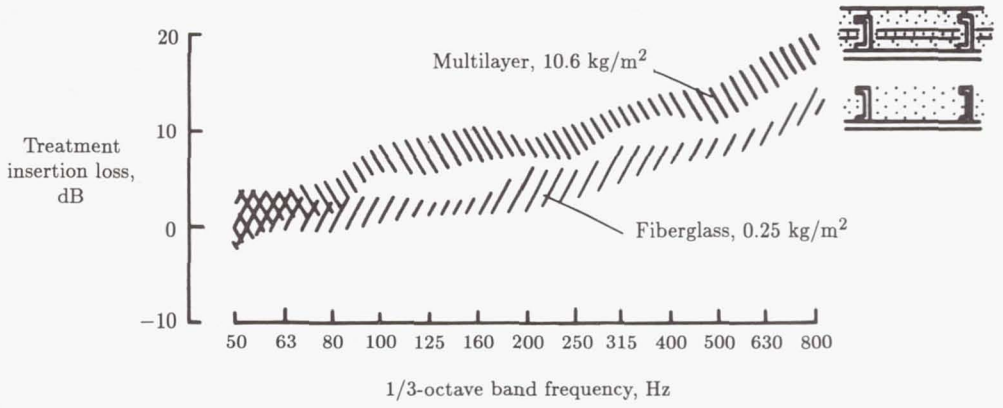

Figure 12. Insertion loss of add-on sidewall treatment for cabin noise control measured in flight of a light twin-engine propeller aircraft (ref. 32). Insertion loss equals SPL before treatment minus SPL after treatment.

important factor in the results shown in figure 12. The multilayer treatment weighs significantly more than the fiberglass, but the extra insertion loss provided, about 5 dB, can be important to cabin comfort. The insertion loss values of figure 12 were found to be approximately predictable from values of sidewall noise transmission and absorption measured under laboratory conditions (ref. 32).

The insertion loss provided by a treatment depends not only on the treatment itself but also on the fuselage configuration (including other treatments) to which the treatment is added (ref. 38). Development of lightweight and effective add-on treatments is of major importance in aircraft cabin noise control.

General Modal Theory

Modal analysis forms the basis of many of the theoretical methods that have been used for the prediction of aircraft interior noise. The basic principles, developed in general without specifying a particular aircraft (ref. 39), are described in the following sections for the cabin and structure.

General Modal Analysis of Cabin Acoustics

Let the aircraft cabin occupy a volume V and be surrounded by a wall surface, of which the portion with area A_F is flexible while the remainder of area A_R is rigid; neither surface provides much absorption. If the air within the cabin is at rest prior to motion of the wall, the acoustic pressure p satisfies the wave equation and associated boundary conditions:

$$\nabla^2 p - \ddot{p}/c_o^2 = 0 \tag{2}$$

$$\partial p/\partial n = \left\{ \begin{array}{ll} -\rho_o \ddot{w} & (\text{On } A_F) \\ 0 & (\text{On } A_R) \end{array} \right\} \tag{3}$$

The dot denotes differentiation with respect to time t, ρ_o and c_o are the equilibrium density and acoustic velocity within the cabin, and w is the displacement of the

flexible portion of the wall in the normal direction. The acoustic pressure is expressed in the modal series

$$p(\bar{x},t) = \rho_o c_o^2 \sum_n P_n(t) F_n(\bar{x})/M_{an} \tag{4}$$

where $\bar{x}$ is the position coordinate vector, P_n are generalized coordinates, F_n are the acoustic mode shapes of the volume when all the walls are rigid, and M_{an} are the generalized masses of the acoustic modes.[3] The wave equation (2) can be transformed into a set of ordinary differential equations in time by using Green's theorem, the modal series equation (4), and the orthogonality properties of the acoustic mode functions $F_n(\bar{x})$. The result for the undamped nth acoustic mode is

$$\ddot{P}_n(t) + \omega_{an}^2 P_n(t) = \frac{-1}{V} \int_{A_F} F_n(\bar{x}) \ddot{w}(\bar{x},t)\, dA \tag{5}$$

where ω_{an} is the natural frequency of the nth acoustic mode. Solution of equation (5) for each mode produces the coefficients P_n that enter equation (4) along with the mode functions F_n to give the cabin acoustic pressure. In general the acoustic response is coupled with the structural motion $\ddot{w}(\bar{x},t)$ through the structural equations of motion, to be discussed subsequently. Solution of these coupled structural-acoustic equations is quite complex; therefore solutions have been found for only a few systems (ref. 39). Fortunately the effects of the acoustic pressure on the structural motion are small for most aircraft applications, so the structural equations can be solved uncoupled from the acoustics. The resulting structural motions $\ddot{w}(\bar{x},t)$ can then be inserted as known quantities into the right side of equation (5), which can then be solved directly using known methods for single-degree-of-freedom undamped systems with a known forcing function.

The effects of acoustic damping can be included in several ways. When one of the walls of the cabin is highly absorbent, it is often characterized by a simple point-impedance model which states that

$$p = Z_A \dot{w}_A \qquad (\text{On } A_A) \tag{6}$$

where the subscript A is used to refer to the absorbent wall characteristics; that is, w_A is the absorbent wall displacement and Z_A is the absorbent wall impedance. The boundary condition equation (6) can be combined with equation (3) to obtain the boundary condition for the absorbing wall:

$$\partial p/\partial n = -\rho_o \dot{p}/Z_A \qquad (\text{On } A_A) \tag{7}$$

This boundary condition can be used instead of equation (3) in the Green's theorem derivation to obtain a damping term proportional to $\dot{P}_n$ that adds to the left side of equation (5). The resulting equation has been used to study the relation between wall impedance Z_A, acoustic damping, and reverberation time (ref. 41). The damping

[3] Since the normal modes F_n satisfy the homogeneous boundary condition (eq. (3)) on the entire wall surface, the normal derivative of pressure (eq. (4)) does not converge uniformly on the flexible portion of the wall surface. Equation (4), is suitable, however, for calculating the pressure itself throughout the cavity and everywhere on the wall surface, including the flexible portion (ref. 40).

term couples all the acoustic modes[4] and increases the complexity of the solution; therefore this approach is not often used in practice. An alternative approach is simply to add to the left side of equation (5) a modal damping term that combines the coordinate velocity $\dot{P}_n$ with a modal damping coefficient that is to be determined experimentally (ref. 42). The exact form of this damping term is determined by analogy with a damped single-degree-of-freedom system. The acoustic modes remain uncoupled and the solution is straightforward.

Prediction of Acoustic Modes

Clearly, acoustic modes and their prediction are important in predicting interior noise using modal theory. As illustrated in figure 13, acoustic mode predictions are accurate for the lower frequency modes of rectangular parallelepiped enclosures having hard, nonabsorbing walls and geometries that are not too complicated. The results of figure 13 were obtained using a subspace mode coupling method (ref. 39), which was also found to predict test results for a variety of other enclosure shapes.[5] Finite element analysis has also been shown to predict hard-wall acoustic modes accurately for three-dimensional analysis (ref. 43) of a large reverberant chamber, a very irregularly shaped model of an automobile compartment (ref. 44), and a model of a general aviation aircraft cabin (ref. 45). Reasonable predictions of acoustic modes have also been obtained using finite element analysis for an enclosure and a light aircraft fuselage having flexible walls (refs. 45 and 46).

Other methods have been used to predict acoustic modes in volumes of various shapes in aerospace vehicles. A perturbation method was applied to the closed-form analysis of rectangular parallelepiped volumes in order to describe the acoustic characteristics of the Space Shuttle payload bay (ref. 47), closed-form solutions have been obtained for cylindrical cavities, and the finite difference method was used to predict acoustic modes in a cylindrical fuselage with a floor (ref. 48). The mode shape shown in figure 14 was calculated with the finite difference method and shows the distortion of the modal node pattern caused by the presence of the floor.

Addition of acoustic damping in the form of absorption material on the walls greatly affects the acoustic character of the enclosure. As illustrated in figure 15, the addition of fiberglass lining all but eliminates the resonant response peaks of the acoustic modes (ref. 49). A simplified analysis for this situation has been proposed. There are few reports in the literature on acoustic characteristics of furnished aircraft cabins, but occasionally evidence of standing waves has been found (refs. 50 and 51). Mathematically, the addition of damping on the walls can cause the modes to be complex (having real and imaginary components) and greatly increase the difficulty of the solution. Theoretical analysis of a cylindrical enclosure indicates that wall damping equivalent to a Sabine acoustic absorption coefficient of 25 percent is sufficient to suppress the acoustic mode resonances (ref. 52). Absorption coefficient values of such magnitude have been reported for furnished aircraft cabins (ref. 4).

[4] Conditions that allow neglect of the modal coupling due to damping have been defined (refs. 39–41). A method for estimating acoustic damping from wall impedance is also described.

[5] The experimental studies revealed a sound suppression effect by which sound levels in a large enclosure can be reduced by constructing a smaller enclosure around the moving portion of the wall so that the smaller enclosure resonates at the frequency at which the wall is moving.

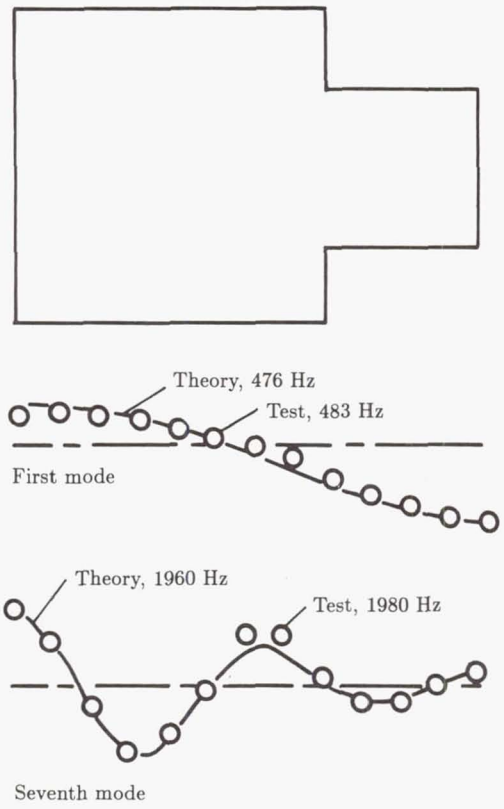

Figure 13. Longitudinal pressure distribution for acoustic modes in a hard-wall enclosure. (From ref. 39.)

General Modal Analysis of Structural Response

When the structure is represented by a linear mathematical model, the structural response, including acoustic interaction, may be analyzed in a straightforward way (ref. 39). Let the structure be represented by a linear, partial differential equation:

$$S(w) + c\dot{w} + m\ddot{w} = p - p_s \tag{8}$$

where S is a linear differential operator representing structural stiffness. For example, for an isotropic flat plate, $S = D\nabla^4$, where D is bending stiffness and ∇^4 is the biharmonic operator. The second term on the left side of equation (8) represents a damping contribution, c being the viscous damping coefficient, and the third term is the structural inertia, m being structural mass per unit area. On the right side are two pressure loadings, the first due to the cabin acoustics and the second due to some specified external noise source. For a modal solution, the structural deflection $w(\bar{x}, t)$ is taken as the series:

$$w(\bar{x}, t) = \sum_m q_m(t)\Psi_m(\bar{x}) \tag{9}$$

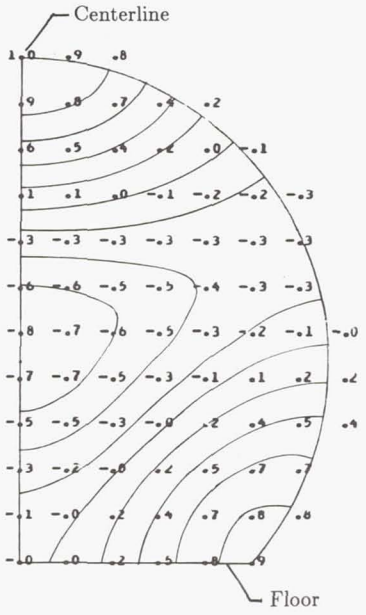

Figure 14. Acoustic mode shape of a cylindrical fuselage with an integral floor, calculated using finite difference method (ref. 48). Numbers are modal amplitudes.

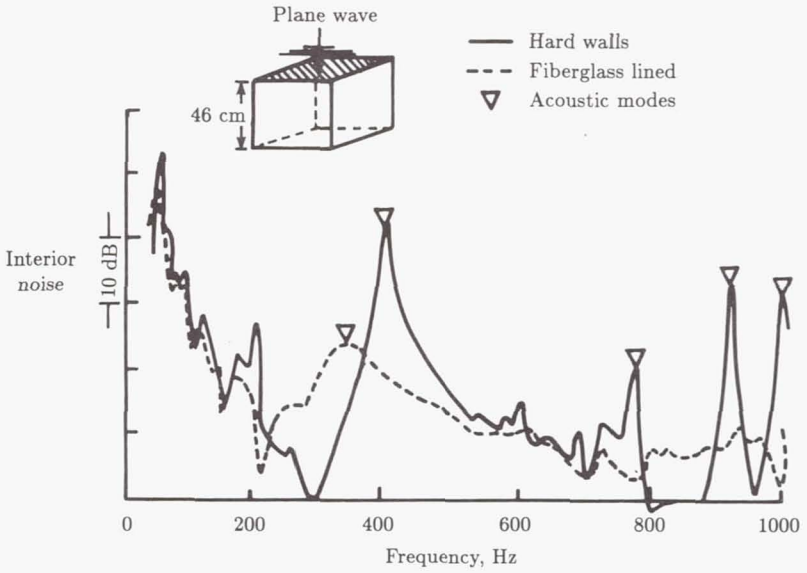

Figure 15. Effect of fiberglass sound-absorbing material on noise transmitted into an enclosure through a 0.32-cm-thick rubber panel (ref. 49).

where q_m are the structural generalized modal coordinates. The mode functions Ψ_m are defined on the flexible region of the enclosure wall and satisfy the eigenvalue equation obtained by setting the right side of equation (8) to zero. Solution of equation (8) is obtained by substituting the structural modal series (eq. (9)) and the acoustic modal series (eq. (4)) and making use of the orthogonality properties of the structural modes. The result is

$$M_m \ddot{q}_m + c_m \dot{q}_m + M_m \omega_m^2 q_m - \rho_o c_o^2 \sum_n C_{mn} P_n = Q_{ms} \tag{10}$$

In this equation M_m, c_m, and ω_m are the generalized mass, damping, and frequency of the structural modes. The coefficients C_{mn} couple the structural and acoustic responses and are given by

$$C_{mn} = \int_{A_F} F_n \Psi_m \, dA / M_{an} \tag{11}$$

The term Q_{ms} is the generalized force acting on the mth structural mode due to the known external source and is given by

$$Q_{ms} = - \int_{A_F} p_s(\bar{x}, t) \Psi_m (\bar{x}) \, dA \tag{12}$$

Equations (10) and (5) form a set of coupled differential equations in time to be solved for the structural and acoustic mode coefficients q_m and P_n due to the action of known acoustic forces $Q_{ms}(t)$. The complete coupled equations have been solved in only a few cases for simple configurations. Coupling was found to be important in a case where the forcing frequency was equal to the resonance frequency of an acoustic mode in the enclosure (ref. 39). The effect of the coupling was to limit the magnitude of the acoustic pressure in the enclosure to a value that did not exceed the exterior source pressure. The acoustic mode acted, in effect, as a vibration absorber and caused the structural panel deflection to approach zero. Coupled equations have also been used to analyze a cylindrical shell model with dimensions appropriate for a light aircraft (ref. 53). The effect of acoustic coupling was found to be small. In most analyses of the vibration of aircraft fuselage structures the coupling terms in equation (10) are dropped. The structural motions can then be determined in a straightforward way without acoustic effects, and the structural motions can then be used as known quantities to solve equation (5), as has been described previously.

Calculation of noise transmitted into an idealized enclosure using modal methods (ref. 54) is illustrated in figure 16. Test results were obtained using a sinusoidal acoustic wave applied at normal incidence at 100 dB onto a thin aluminum panel. The panel was attached to a specially constructed box that allowed noise transmission only through the panel. The panel was flat with uniform properties and the enclosure was rectangular with hard walls so that accurate modes could be obtained by closed-form analysis. The modal behavior of the system is clearly shown by the sharp resonance peaks. The noise levels at the acoustic modes do not exceed the source level of 100 dB, as described by the theory. The interior levels at structural modes, however, exceed the exterior source levels by as much as about 18 dB, a phenomenon

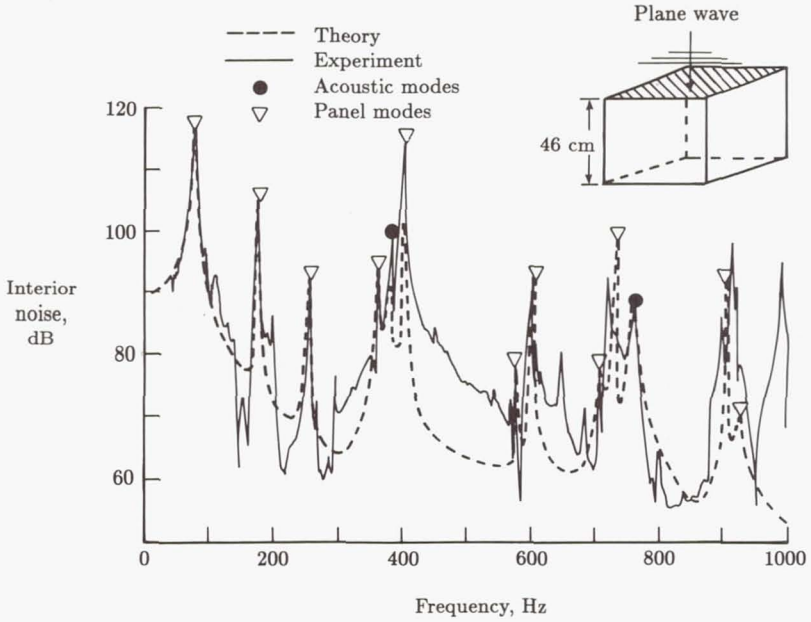

Figure 16. Noise transmitted into a hard-wall enclosure through a 0.08-cm aluminum panel. Source level = 100 dB. (From ref. 54.)

also described by the theory. The agreement between theory and test is good, indicating that modal analysis is a useful solution method.

The frequency range and number of modes shown in figure 16 are in the range of values of practical importance for many full-scale aircraft applications. For aircraft, however, the configurations of the structure and cabin geometry, as well as the presence of absorption on the walls, add sufficient complication that major efforts are required to determine the mode shapes and frequencies. Thus it is now appropriate to consider the practical applications of airborne noise transmission analysis.

Simplification of Analysis Methods

In applying theoretical principles to the calculation of aircraft cabin noise, simplifications are usually made to reduce the numerical processing to a manageable level. The essential features of the noise transmission process must be retained, however, for accurate predictions. Simplified and rapid procedures also are advantageous for displaying trends, for generating insight into noise level variations with system parameters, and for use in design or noise control. Assumptions made in a particular theoretical method tend to reduce its range of application, but a number of methods have been developed covering most of the aircraft situations of interest. The representations of the source and cabin acoustics differ for each method to be discussed in later sections of this chapter. The structural models and approach to treatment, however, are similar.

Representation of Fuselage Structure

As indicated in figure 17, a typical aircraft fuselage consists of longitudinal and circumferential stiffeners that support a thin skin. The stiffeners are normally closely spaced compared with the overall fuselage dimension. Detailed mathematical modeling of each skin panel and stiffener element for calculations throughout the acoustic frequency range is beyond current capabilities. However, it is feasible to apply different simplified models to different frequency ranges (ref. 55). Measurements on the aircraft illustrated in figure 17 have shown that at low frequencies the skin and stiffeners tend to vibrate with about the same magnitude (ref. 36) and the modal wavelengths are long compared with the stiffener spacing (ref. 56). This behavior leads to a low-frequency orthotropic model wherein the actual structural properties are averaged over a large sidewall area. At high frequencies the stiffener motions tend to become small compared with the panel motions and the modal wavelengths become short. This leads to a high-frequency panel model wherein the stiffeners are assumed motionless and all noise is transmitted only through the vibrating skin panels. At intermediate frequencies, both panel and stiffener motions have to be modeled. These models are more difficult to analyze, and results for the mid-frequency region are occasionally obtained by interpolating results obtained from low- and high-frequency models. The frequency range where each model is applicable depends on the particular aircraft being considered.

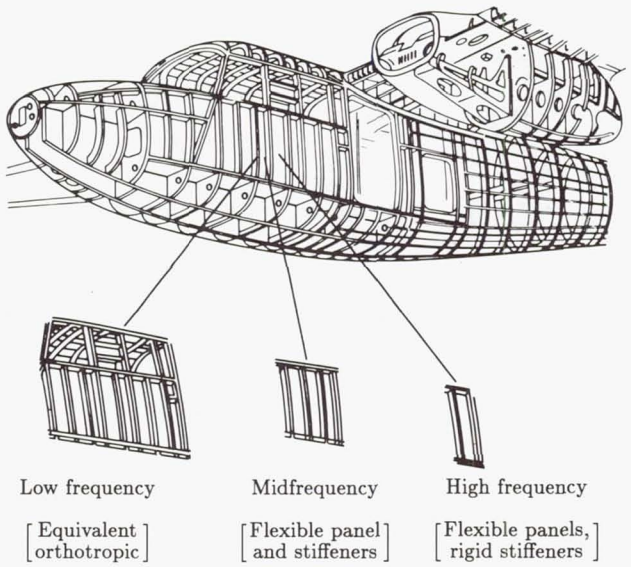

Figure 17. Simplified mathematical models of aircraft fuselage structure for interior noise prediction.

A simple illustration of this structural modeling approach can be found in acoustic transmission loss measurements (fig. 18) made on a flat, aircraft-type panel in a laboratory transmission loss facility (ref. 38). The panel was 1.22 m by 1.52 m and was stiffened by 4 frame stiffeners and 10 stringers. The panel was full-scale in

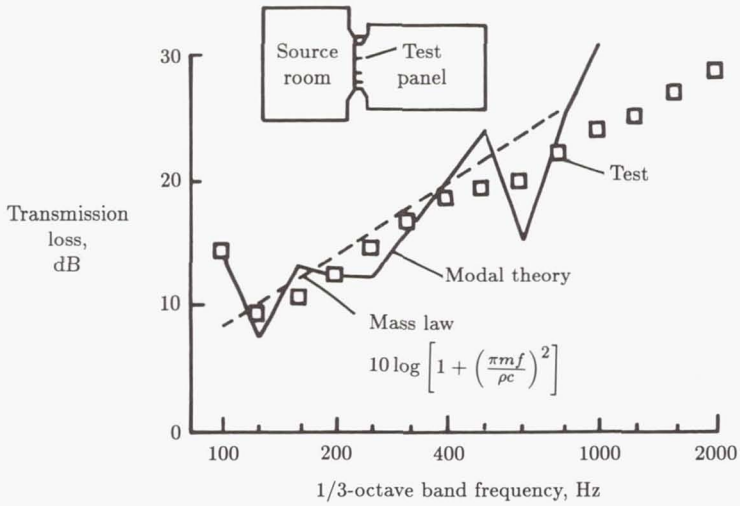

Figure 18. Noise transmission loss of an aircraft-type panel for a diffuse reverberant source noise in a laboratory transmission loss facility. Skin and stiffener mass $m = 5.5$ kg/m^2. (From ref. 38.)

that the material thicknesses and stiffener spacings are representative of full-scale general-aviation-class aircraft.

Test results give transmission losses (TL) at frequencies between 125 and 400 Hz that are only slightly less than mass law predictions using the total mass of skin and stiffeners. The results, along with measured panel mode shapes, suggest that significant motion of both skin and stiffeners is taking place and that panel wavelengths are large compared with stringer spacing. Such behavior is appropriately modeled with the low-frequency, equivalent orthotropic model used in the modal theory results shown in the figure. While the mass law is somewhat closer to the test data, the modal theory is close enough to establish its validity, and it also has the advantage of sufficient flexibility to handle configurations not treatable with the mass law approach.

At frequencies higher than 400 Hz the test results fall below the mass law curve shown. This indicates that the stiffener motion has become small and that the transmission is being controlled by the skin motion. The high-frequency panel model (fig. 17) would be more appropriate in this frequency region.

The panel considered in figure 18 has mass and structural values that are quite similar to the values for aircraft 2 in figure 10. Figure 18 indicates a TL of about 10 dB at frequencies below 200 Hz, whereas figure 10 indicates noise reduction of more than 20 dB at these frequencies. This difference in transmission is thought to be due primarily to differences in the excitation pressure fields; however, differences in structure, structural support conditions, or backing cavity may also contribute. Laboratory TL testing is useful for evaluating theories, because of the controlled test conditions, and for comparing treatment effects, but results should be used with caution because the TL values may not be representative of sidewall noise transmission behavior in an actual aircraft in flight.

Representation of Sidewall Treatment

The elements of importance to interior noise transmission include the fuselage structure and the acoustic treatment in the cabin. A calculation procedure that can rigorously handle these elements and their interactions is not yet available. Therefore approximate methods are required, such as that illustrated in figure 19, which was developed for a particular calculation procedure (ref. 57). Similar approaches are used in other methods. The approach is to calculate the noise transmission through each element separately and then combine the results additively. Thus, noise transmission through the cylindrical structure is calculated without treatment or absorption. Transmission through a skin panel with treatment is calculated separately using methods developed for an incident plane wave and a flat panel of infinite extent (ref. 58). The increment in transmission loss provided to the panel by the treatment is then added to the loss provided by the untreated cylinder, to obtain a combined treated cylinder noise reduction (NR). This NR is then combined with the cabin average absorption coefficient (α) to obtain the noise reduction of the treated fuselage with cabin absorption. The equation used to include absorption is obtained from diffuse room acoustics considerations, and when TL is large, the equation can be written as

$$\mathrm{NR} = \mathrm{TL} + 10\log(\alpha \mathrm{A}_\alpha / \mathrm{A}_t) \tag{13}$$

where A_α and A_t are the areas of absorbing and transmitting surfaces, respectively. These areas may differ in an aircraft due to the presence of floors, bulkheads, seats, and baggage compartments. This equation has been used with reasonable accuracy to relate treatment TL and α measured using laboratory methods (ref. 33) to treatment insertion loss measured in light aircraft cabins (refs. 32 and 59).

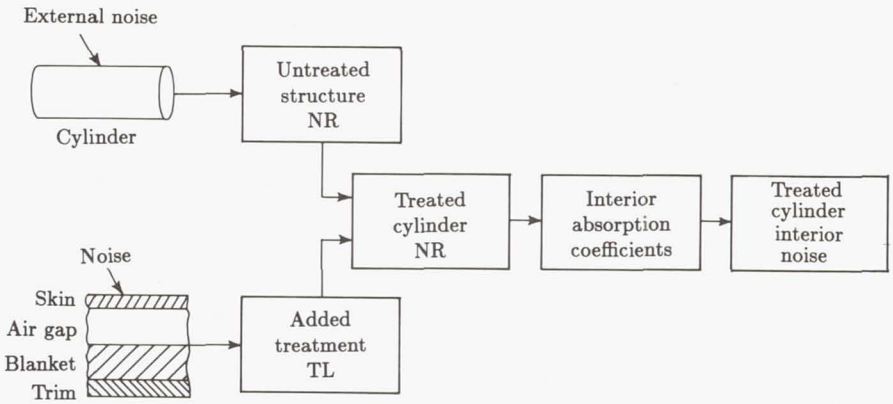

Figure 19. Approach for combining structure, treatment, and cabin absorption for theoretical prediction of aircraft interior noise (ref. 57).

Laboratory TL testing of add-on acoustic treatments has the advantages that test conditions can be accurately controlled, many treatment configurations can be tested at relatively low cost, and treatment effects can be studied separately from other factors (such as structure-borne noise) that can affect cabin noise. TL testing

is commonly used, therefore, for evaluating aircraft cabin noise control treatments (refs. 57, 60, and 61). Figure 20 illustrates treatment insertion loss obtained from TL tests and from theoretical predictions (ref. 38). The structural panel was the one used for figure 18. The treatment consisted of fiberglass and a trim panel located at a distance from the skin just large enough to avoid hard contact with the 7.6-cm-deep frames. Both test results and theory indicate that the insertion loss is negative at frequencies just above 100 Hz, meaning that the treatment increases the noise transmitted compared with the noise transmitted by the untreated panel. This phenomenon is caused by a resonance of the double-panel system. The frequency of this resonance can be predicted, approximately, by modeling the panels as having only mass with surface densities m_1 and m_2 separated by an air gap of thickness d. The resonance frequency is

$$f_d = \frac{1}{2\pi \cos\theta} \left[\frac{\rho_o c_o^2 (m_1 + m_2)}{d m_1 m_2} \right]^{1/2} \tag{14}$$

where θ is the angle of incidence of the acoustic wave. This negative effect can be a disadvantage in practice if significant noise levels exist at frequencies near the double-panel resonance.

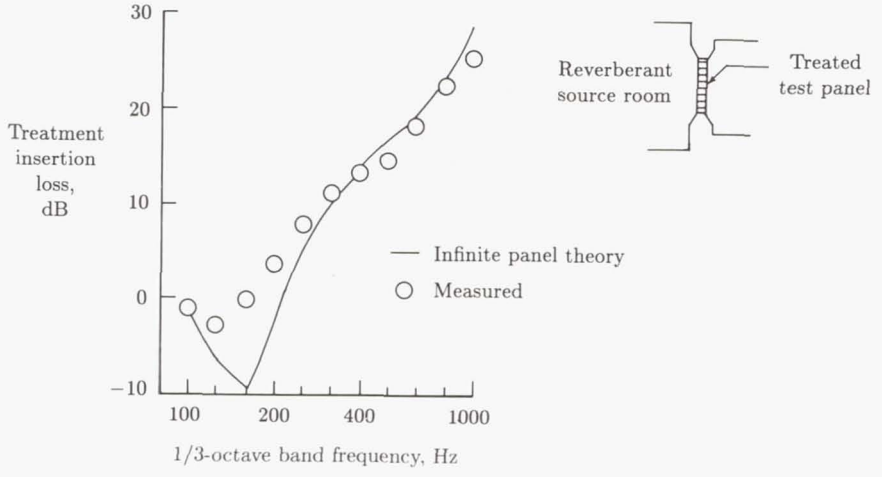

Figure 20. Insertion loss of fiberglass batt and trim panel treatment added to an aircraft panel. Laboratory TL test. (From ref. 38.)

At frequencies above 200 Hz the insertion loss rises rapidly with increasing frequency and quickly exceeds the insertion loss that would be obtained by adding the treatment mass directly to the structure. Thus, a double-wall treatment may have a weight advantage if the negative effects of the double-wall resonance can be avoided and if sufficient cabin absorption can be added to compensate for the usually low absorption characteristics of trim panels. Trade-off analysis is required to determine the best combination of treatments for a particular application (ref. 38).

The theoretically predicted insertion loss is much lower than test results at frequencies between 100 Hz and 200 Hz, where the double-wall resonance is important.

This difference is thought to be caused by the infinite representation of the treatment used in the theory. Theoretically, acoustic waves are allowed to travel parallel to the skin surface, whereas in the aircraft panel the frames form a barrier that prevents such parallel travel. Improvements to the theory have been examined (refs. 38 and 62), but they increase the difficulty of the solution. A rigorous (and manageable) analysis of double-wall treatment has not yet been developed, so most analysis methods use the infinite-panel theory. As shown in figure 20, the theory agrees well with test data at frequencies well above the double-wall resonance, where design attention should be focused anyway because of the double-wall advantage.

Acoustic Power Flow Into an Enclosure

The overall analysis of noise transmission into an airplane fuselage can be considered in terms of acoustic power flow. This approach is quite general and allows different analysis methods to be combined to cover an extensive frequency range. For example, finite element analysis can be performed at low frequencies and statistical energy analysis at high frequencies. Acoustic power flow has been used in varying forms, including the prediction of rocket noise transmission into the payload bay of the Space Shuttle orbiter (ref. 47) and propeller noise transmission into high-speed (ref. 63) and general aviation (ref. 48) aircraft.

The basic concept of the acoustic power flow approach is that of power balance; power flow into a system must be balanced by power flow out of the system and power absorbed within. Thus,

$$P_{\text{in}} = P_{\text{diss}} \tag{15}$$

where P_{in} is the net, time-averaged power flow into the structure and receiving volume, and P_{diss} is the net, time-averaged power dissipated in the structure and on the interior walls. Since P_{in} is the *net* inflow of power, it takes into account any acoustic power that flows back from the fuselage interior to the exterior. In principle, acoustic energy can be stored only in resonant modes, but it has been shown that nonresonant response can also be considered in the analysis (ref. 64).

Statistical Energy Analysis

Statistical energy analysis (SEA) was first developed in 1959 (ref. 65); the original theory was presented with considerable generality so that it would be applicable to a wide variety of physical problems (ref. 66). A number of early applications involved spacecraft launch vehicles, and since about 1974 (ref. 67), the method has been applied to the prediction of noise transmission into aircraft. Certain assumptions inherent in the method mean that SEA is valid only at high frequencies, although the definition of "high" frequency is fairly flexible and varies from one application to another. However, because of this restriction, SEA is often used in conjunction with other methods, particularly modal methods which can be used at low frequencies. This joint application of SEA and modal methods is particularly suitable when the modal approach involves the concept of acoustic power flow. SEA depends explicitly on the concept of power or energy flow in the derivation of the analytical model.

General Concepts of SEA

SEA views a particular system, such as a specific aircraft cabin, as a sample drawn from a statistical population with random parameters. Statistical estimates of

average response parameters, such as acoustic pressure averaged over time and space (e.g., cabin volume), are derived starting with modal equations such as equation (10). The advantage of this approach can be seen by considering the calculation of the response of a complex structure such as that shown in figure 17 at high frequencies using the classical modal methods described in previous sections. As previously mentioned, it takes great effort to calculate the large number of modes that may be required to describe response to a broadband input. In some cases computing capacity and cost limit the number of modes that can be accurately computed (ref. 46). Manufacturing tolerances and variations in material properties may also affect the high-frequency modes; such variations would be impractical to define. The SEA approach is to avoid consideration of the detailed structural characteristics and, instead, focus attention on the use of energy conservation principles to develop relations between acoustic and structural responses that depend on average modal properties over a frequency band.[6] This procedure leads to comparatively simple solutions that depend on structural and acoustic parameters (such as modal density, radiation resistance, and coupling loss factors) that are unique to SEA (refs. 65 and 69). In some problems the answers are independent of many structural details. Major activities in a typical SEA calculation are modeling the system and evaluating the SEA parameters for the system (ref. 70). If the analysis is initiated early in the development of a vehicle, successive improvements to the model and parameter values can lead to good predictions of interior noise for quite complex vehicles (ref. 47).

SEA of Aircraft Sidewall

The first step in an SEA calculation is the synthesis of a model (ref. 70). A model used for an aircraft interior noise analysis (ref. 67) is shown in figure 21. The elements of an SEA model consist of interacting energy storage systems composed of resonant modes. In figure 21 each box represents a single physical element of the sidewall, but this correspondence is not necessary. For example, the torsional and flexural modes of a beam might be represented in separate boxes if they interact differently with neighboring elements. Transmission by nonresonant modes that do not store appreciable energy is represented only by the dashed lines in figure 21. The synthesis of an SEA model might be suggested by previous work, but judgment is required for reliable modeling of each new system.

Energy balance relations are then written for each element of the model. For the fuselage skin, the energy balance is

$$P_{s,e} + P_{s,d} + P_{s,w} + P_{s,f} = 0 \tag{16}$$

where

$P_{s,e}$	power flow from skin to exterior
$P_{s,d}$	power dissipated within skin
$P_{s,w}$	power flow from skin to wall cavity
$P_{s,f}$	power flow from skin to frame

[6] Dowell and Kubota (ref. 68) have developed a new high-frequency approach utilizing asymptotic analysis.

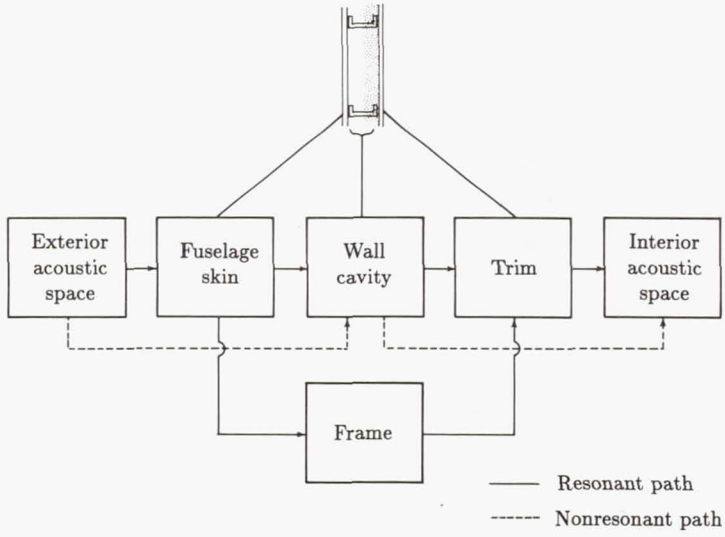

Figure 21. Model of sidewall noise transmission used in statistical energy and power flow theories for aircraft interior noise prediction. (From ref. 67.)

Expressions similar to equation (16) are written for each box in figure 21 and form a set of linear algebraic equations that must be solved simultaneously, in general. For simplified analysis the skin response is determined assuming no power flow to the wall cavity or frame.

Analysis of modal energy shows that the power dissipated in the structure is proportional to the total mean square energy E_s by the relation

$$P_{s,d} = 2\pi f \eta_s E_s \tag{17}$$

where η_s is the damping loss factor. The power flow from the exterior to the skin is found to be proportional to the difference between the energy of the two systems[7]

$$P_{s,e} = 2\pi f n_s \eta_{s,e} \left(\frac{E_s}{n_s} - \frac{E_e}{n_e} \right) \tag{18}$$

where

n_s	modal density of the skin
$\eta_{s,e}$	coupling loss factor defining the power flow from skin to exterior
E_e	energy in exterior field
n_e	modal density of exterior field

[7] The similarity of this equation to the equations for heat and electrical flow leads to the use of thermal and electrical analogies in the development of SEA results (ref. 66).

The energies in the exterior field (modeled as reverberant) and the skin are given by

$$E_e = \frac{V_e}{\rho_o c_o^2} < p_e^2 > \tag{19}$$

$$E_s = \frac{\rho_s V_s}{(2\pi f)^2} < a_s^2 > \tag{20}$$

where

$< p_e^2 >$	space-time mean-square pressure in reverberant field
$< a_s^2 >$	space-time mean-square skin acceleration
V_e, V_s	volumes
ρ_o, ρ_s	density of acoustic medium and skin

Substitution of equations (17) to (20) into equation (16), with $P_{s,w} = P_{s,f} = 0$, leads to the expression for skin acceleration resulting from the exterior pressure:

$$< a_s^2 > = \left[\frac{(2\pi f)^2 V_e}{\rho_s V_s \rho_o c_o^2}\right] \left(\frac{n_s}{n_e}\right) \left(\frac{\eta_{s,e}}{\eta_{s,e} + \eta_s}\right) < p_e^2 > \tag{21}$$

Further solution of equation (21) requires evaluation of the modal densities n_s and n_e and the loss factors η_s and $\eta_{s,e}$. Evaluation of these parameters is a major area of effort in SEA calculations. For simple physical systems such as uniform flat plates or cylinders, modal densities can be accurately calculated using theoretical methods. For complex systems (fig. 17) direct theoretical calculation would be impractical; therefore modal densities are usually estimated from known results for simple configurations. Catalogs of modal densities of many types of systems have been compiled for such estimation purposes (ref. 71). Damping loss factors η_s involve internal dissipation and usually must be measured or estimated from available test results from similar structures. Coupling loss factors $\eta_{s,e}$ can be calculated with reasonable accuracy using theoretical methods for simple configurations, but may have to be estimated or measured for complex systems. Coupling of mechanical systems (plates and shells) with acoustic media can be expressed in the relation

$$\eta_{s,e} = \frac{\rho_o c_o}{2\pi f \rho_s h} \sigma_{s,e} \tag{22}$$

where h is skin thickness, and $\sigma_{s,e}$, known as radiation efficiency, is the ratio of the actual power radiated to the power radiated by an infinite flat plate (with the same mean-square velocity) generating a plane wave. Extensive calculations have been carried out to determine radiation efficiencies of common practical structures (ref. 72).

Solution of the power balance equations for each element in the model of figure 21 leads to an expression for mean-square cabin pressure as a function of exterior pressure and the parameters of each system element. SEA has been applied in

various forms to a number of aircraft and aircraft model configurations (refs. 4, 8, 47, 48, 63, 67, 73, and 74) and found to give results that agree with other analytical methods and with test results.

Analysis of Rectangular Fuselage

A number of aerospace vehicles are characterized by fuselage sidewalls having large areas with little or no curvature and nearly rectangular fuselage cross sections. Many of the vehicles consist of aircraft driven by propellers that generate the major part of the cabin noise by transmission through the sidewall, but the category also includes the Space Shuttle orbiter where the sources of noise in the payload bay at lift-off are the rocket exhausts.

Propeller-Driven Aircraft

The sketches in figures 9 and 10 show a configuration associated with propeller-driven aircraft. Modal theory has been applied to the prediction of cabin noise in these aircraft (ref. 42). The sidewall is modeled as flat, the structural models indicated in figure 17 are used, and the cabin is modeled as rectangular with equivalent modal damping of the acoustic modes. Effects of add-on acoustic treatments are included using an approach like the one illustrated in figure 19 and using infinite-panel theory to calculate treatment effects. Variations of propeller noise over the surface of the sidewall are accounted for by averaging the propeller noise level over each panel and then assuming in the analysis that the average level acts uniformly over that panel.

At midfrequencies the theory considers the sidewall to consist of an array of stiffened panels (fig. 17). In one application of modal theory, three skin panels and four flexible stiffeners are analyzed together as one stiffened panel (ref. 75). The modes of such a stiffened panel are complicated and require considerable effort to calculate accurately (ref. 76). The exterior noise is assumed to act uniformly over each stiffened panel. The cabin noise at any position is obtained by summation on an rms basis of the contribution from each stiffened panel (this assumes that the contributions are area-related). Predictions using this theory have been compared with test results, as illustrated in figure 22 (ref. 77). The exterior noise was directed onto one stiffened panel at a time using an "acoustic guide." For the example shown in the figure, agreement between test and theory is excellent at frequencies below about 250 Hz.

Study of a complete aircraft fuselage in the laboratory has advantages over TL or flight testing. The panel area under study can interact with the noise source, adjacent structure, and cabin acoustics in a realistic manner, but test conditions can be carefully controlled and a variety of tests can be performed at relatively low cost (ref. 78). For example, tests such as that illustrated in figure 22 showed that different stiffened panels transmitted different amounts of noise, and this result was then used to tailor the distribution of treatment over the sidewall to provide a minimum-weight treatment (ref. 75). The acoustic guide has been used to isolate the transmission of noise through a window, thus providing data to support theory for double-pane windows (ref. 77).

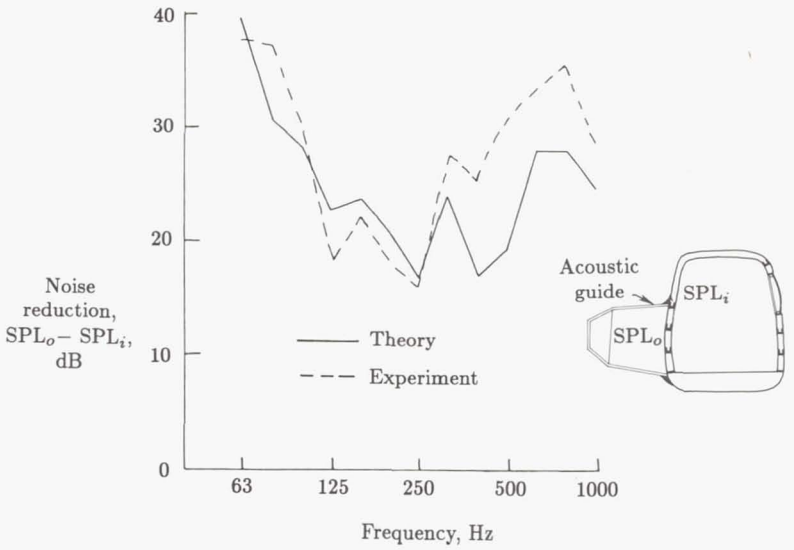

Figure 22. Noise reduction through a light aircraft fuselage using a localized source noise. Laboratory test. (From ref. 77.)

Comparison With Flight Measurements

Measured and predicted interior noise for flight conditions is compared in figure 23 (ref. 5). The aircraft is a twin-engine turboprop weighing about 5080 kg and was operated at an altitude of about 9000 m with a pressurized cabin and nominal cruise engine power settings. The cabin contained seats for pilot, copilot, and test engineer but no other furnishings. Several sidewall treatments were tested; the results shown are for an experimental configuration having several layers of mass-loaded vinyl septa and fiberglass blankets. The analysis (ref. 75) used experimental information for propeller and boundary layer source noise to establish levels on 12 stiffened panel areas of the sidewall. Structural vibration modes of these 12 panels, 6 of which were windows, were determined using detailed finite element strip methods and/or transfer matrix methods. The cabin was modeled as a rectangular enclosure with absorption included as "equivalent" damping of the acoustic modes. The effects of sidewall treatment were included by adding insertion loss values determined from infinite-panel theory, as discussed previously. Figure 23 shows that the theory predicts the overall trend of the flight data quite well. In making a detailed comparison of measured and predicted levels at individual frequencies, one must consider both theoretical approximations and measurement precision, either of which could account for the differences shown.

Treatment Design for Airplane Cabin

The modal methods described above have been used to search for optimum combinations of structural and add-on treatments that satisfy a target interior noise level with the least added weight (refs. 42 and 75). Structural modifications considered included increased skin thickness, addition of stiffeners, addition of mass

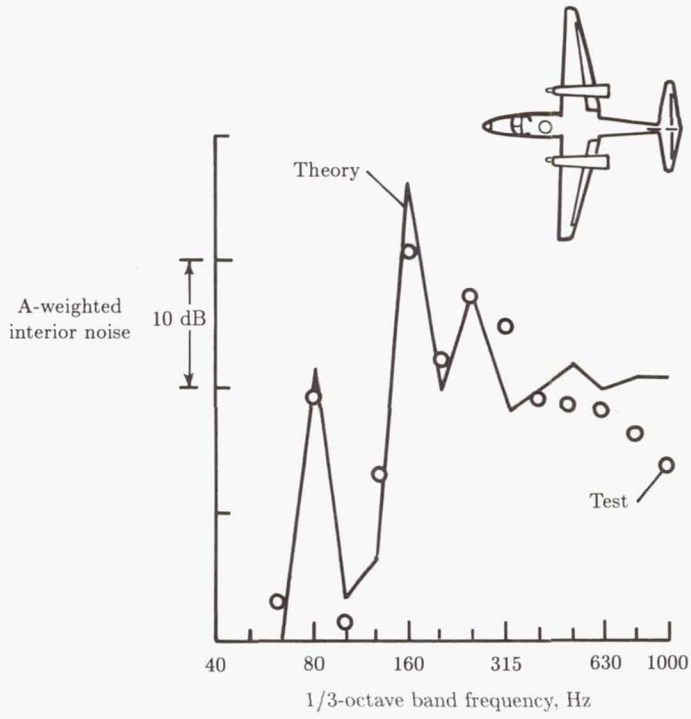

Figure 23. Predicted and measured interior noise in a light aircraft in flight. (From ref. 5.)

or damping layers to the skin, and addition of honeycomb stiffening panels to the skin. Add-on treatments considered included fiberglass blankets, lead-vinyl septa, and trim panels in numerous combinations. Treatment designs were studied for two twin-engine propeller-driven aircraft, one of which was flight tested to obtain the results shown in figure 23.

An example of parameter studies conducted for structural treatments is shown in figure 24 (ref. 79). The interior noise level at zero added weight is the calculated value for an untreated interior. The figure shows that different treatments provide different amounts of reduction in interior noise for a given value of added weight, indicating that there is substantial benefit potential in optimum choice of treatment. For each treatment the curve tends to flatten as weight increases, so that benefits tend to diminish as greater weight of treatment is added. In such a case the alternative to a large weight penalty is to use some other treatment. In the example shown in figure 24 the treatment labeled "damping" would be the best, for that particular noise spectrum and structure, because it provides the lowest noise level for a given weight.

Parameter studies such as that shown in figure 24 have been conducted for a variety of treatments, and several candidate configurations have been developed (ref. 75). Laboratory TL tests of several of these configurations (ref. 80) tend to confirm the ability of the theory to represent the contribution of the treatment elements and to identify a superior treatment combination.

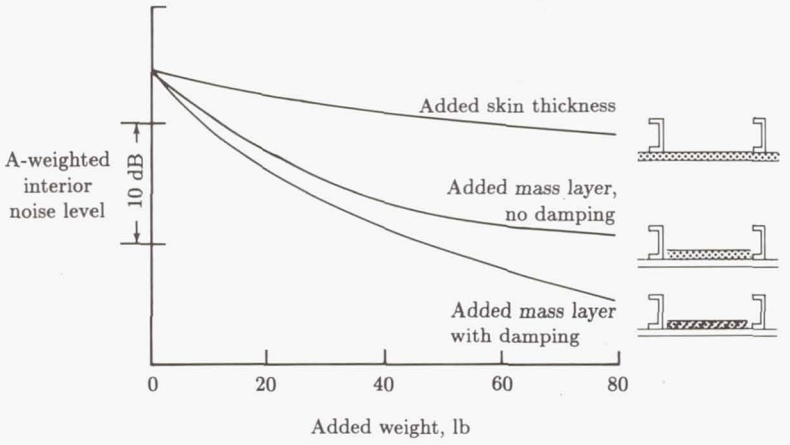

Figure 24. Reduction in aircraft interior noise predicted by modal theory (ref. 79) for three structural treatments.

Space Shuttle Payload Bay

The payload bay of the Space Shuttle orbiter consists of flat sidewalls and bulkheads (forward and aft) and slightly curved bottom structure and bay doors (fig. 25). Thus, the analytical model developed to predict noise transmission into the payload bay envisaged the transmitting structure as an array of flat panels (ref. 47). At low frequencies, below about 60 Hz, the modal characteristics of the structure were predicted using finite element methods. Then, at higher frequencies, where the large number of modes made use of finite element methods very time-consuming, the structure was modeled as equivalent single orthotropic panels. In this case, mass and stiffness of the frames and stringers were averaged over the panel surface to give the structure orthotropic characteristics, and closed-form equations were developed to represent the motion of the panels. The orthotropic model included both frames and stringers until the frequencies exceeded the lowest resonance frequencies of individual panels of a given structural region. At higher frequencies, mass and stiffness of the frames were often excluded from the model.

The coupling between the structure and the excitation field generated by rocket exhaust noise was determined (refs. 11 and 47) by use of the joint acceptance function $j_r^2(\omega)$ for mode of order r. The joint acceptance function is defined by

$$j_r^2(\omega) = \int_{\bar{x}_1} \int_{\bar{x}_2} \frac{S_p(\bar{x}_1, \bar{x}_2; \omega)\Psi_r(\bar{x}_1)\Psi_r(\bar{x}_2)\, d\bar{x}_1\, d\bar{x}_2}{A^2 S_p(\bar{x}_o, \omega)} \tag{23}$$

where

$S_p(\bar{x}_1, \bar{x}_2; \omega)$ the cross spectral density of the "blocked pressure" (ref. 69) on the exterior of the fuselage

Ψ_r eigenfunction (mode shape) of the rth mode of the structure

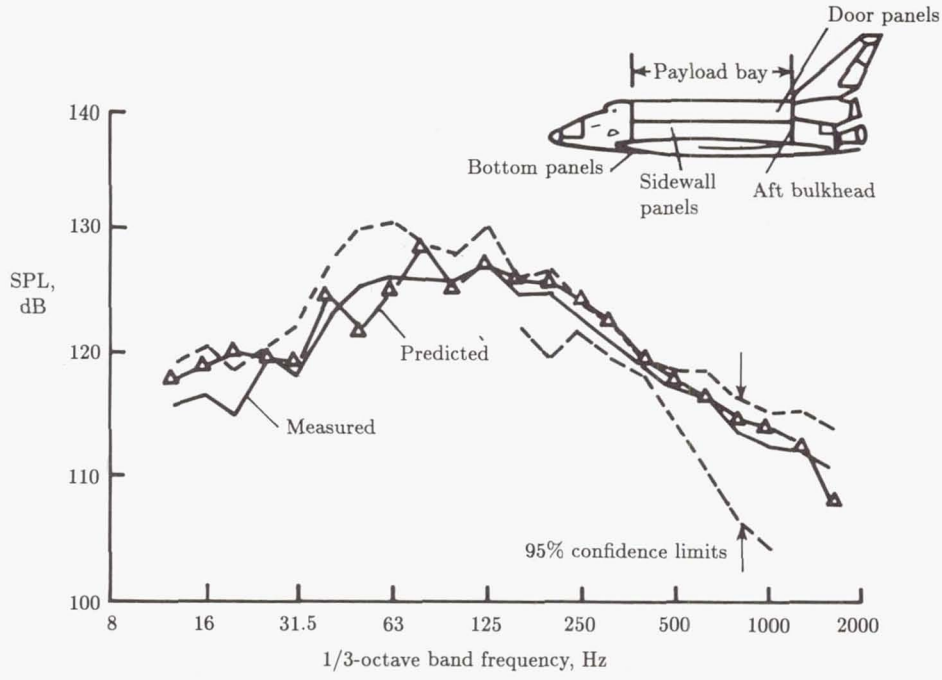

Figure 25. Measured and predicted space-average sound pressure level in the payload bay of the Space Shuttle orbiter (ref. 47).

A	structure area
$S_p(\bar{x}_o, \omega)$	reference value of power spectral density of blocked pressure

The cross spectral density functions of the excitation pressures were obtained from model-scale test data. The pressure field was represented as a convected field with exponential decay of the correlation (ref. 47). In a similar manner, the response of the structure to the acoustic pressure field in the payload bay was predicted from the joint acceptance function with the pressure field assumed to be reverberant. The same approach could be used to predict the response of the payload bay structure to boundary layer excitation during high dynamic pressure conditions on ascent (ref. 11).

Acoustic response of the payload bay was calculated from the coupling of the modes of the structure and the volume. The acoustic modes were predicted for a slightly deformed parallelepiped volume, but at higher frequencies, SEA methods were used. Dissipation of acoustic power in the volume resulted from the absorption of sound by the thermal control material covering the walls of the bay.

During development of the analytical model, ground test and, eventually, launch data were used to evaluate some of the assumptions. This resulted in an analytical model (ref. 81) which could predict the payload bay sound levels with reasonable accuracy, as is shown in figure 25. The model was then used to predict the effect of the presence of a payload on the sound levels in the payload bay.

Analysis of Cylindrical Fuselage

For a large class of aircraft, the fuselage is nearly circular and analysis methods have been developed that consider the transmission of noise into these circular fuselages. The methods differ in the manner in which the fuselage structure is represented and in the analytical model used for the exterior pressure field. In one case, the fuselage is assumed to be infinitely long, since the fuselage length is large relative to both the fuselage diameter and the acoustic wavelength in the frequency range of interest. Furthermore, the exterior pressure field is represented by acoustic plane waves. In another case, the fuselage is assumed to be finite and the excitation pressure field is a detailed representation of that generated by a propeller.

Infinite-Cylinder Analysis

Theories have been developed for analysis of sound transmission into infinitely long cylinders, with the exterior sound field modeled as a plane wave incident to the axis of the cylinder at an angle θ (ref. 82). Because of the geometry of the infinite cylinder, coupling of the shell with the exterior and interior acoustic dynamics, as represented in equation (10) by the C_{mn} terms, can be included without undue difficulty. The effects of external airflow, representing aircraft forward speed, and cabin static pressurization are included in the analysis,[8] and several models of the shell structural dynamics and cabin acoustics have been analyzed.

A theoretical model consisting of an infinite skin that is stiffened at periodic intervals in the direction of a traveling wave has also been applied to aircraft fuselage vibration and noise transmission analysis (ref. 83). The structure behaves as a bandpass filter, responding very efficiently in certain frequency bands (pass bands) but not so efficiently in other frequency bands (stop bands). The model allows a detailed study of the interaction between the skin and stiffener dynamics. Application of this theory to aircraft configurations (ref. 84) has led to development of noise and vibration control concepts involving "intrinsic structural tuning" and damping applied to stringers and frames. Flight test data tend to support the theoretical conclusions, and several operational control devices have been developed and used.

Plane-Wave Transmission Into Cylinder

Figure 26 illustrates cylinder noise transmission as measured and predicted by infinite-cylinder theory (ref. 57). A cylinder of 0.508-m diameter and 1.98-m length was subjected to loudspeaker-generated noise in an anechoic chamber. The skin was unstiffened and the interior contained a core of sound-absorbing foam to simulate the theoretical model of an interior containing only radially inward-traveling waves.[9]

[8] Results have been calculated for a typical narrow-body aircraft with fuselage diameter of 3.66 m, at an altitude of 10 660 m. The results show that forward speed provides a small increase in TL in the mass law region and interacts strongly with the cylinder resonances at lower frequencies. Internal pressure decreases TL slightly, and the acoustic mismatch between external and internal properties increases TL.

[9] The shell interior has also been modeled using acoustic modes (ref. 52).

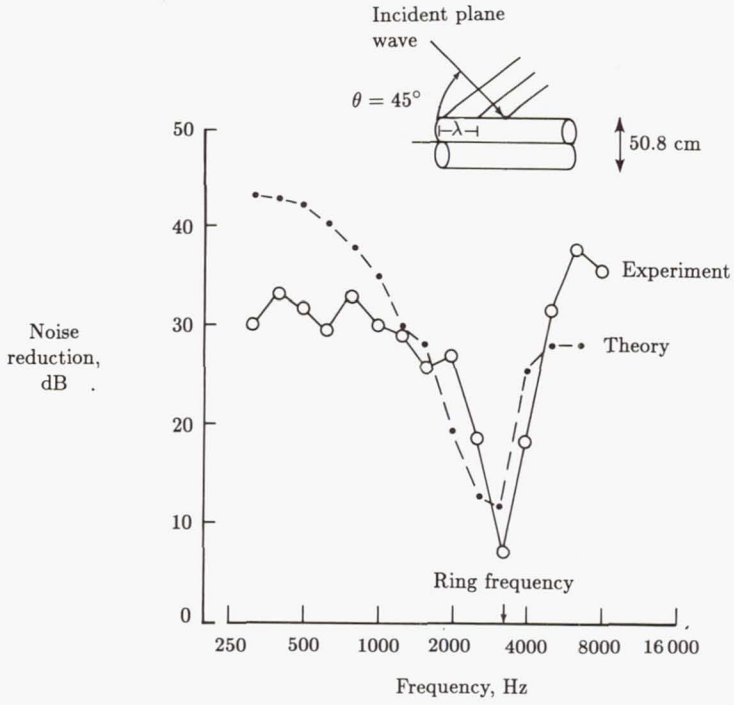

Figure 26. Transmission of sound incident at 45° into an unstiffened cylindrical shell. (From ref. 57.)

Both theory and test show a large decrease in noise reduction at frequencies near the ring frequency for the particular incident angle illustrated. Ring frequency f_r is given by the relation

$$f_r = C_L/\pi D \approx 1700/D \tag{24}$$

where C_L is the longitudinal wave speed in the shell material, D is the cylinder diameter, and the approximate relation applies to aluminum when D is expressed in meters (ref. 85). The mechanism of noise transmission near the ring frequency has been analyzed using statistical methods showing a large concentration of structural modes (ref. 86). Furthermore, some of the structural modes at, and just below, the ring frequency have high acoustic radiation efficiencies. For aircraft, the effects of ring frequency are often not as large as shown in figure 26, probably because of the effects of structural complexities such as stiffeners, floor, or add-on acoustic treatment.

It may be noted that this infinite-cylinder theory is based on incident and transmitted acoustic power and full coupling of acoustic and structural dynamics, in much the same manner as the classical analysis of noise transmission through an infinite flat panel used for architectural TL studies. The effects of curvature have been investigated in comparison with flat panels (ref. 87). The equations presented provide a means of quantitatively estimating curvature effects that may account in part for differences between laboratory TL results and flight results.

Structural Models for Infinite Cylinder

Orthotropic-panel and discrete stiffener structural models have been incorporated in the infinite-cylinder theory (refs. 88 and 89) to explore the influence of these realistic factors on predicted transmission loss. These studies show that the added structural complexity leads to transmission loss characteristics with new features which probably would not have been foreseen based on previous experience and which have not yet been fully explained. The results must therefore be considered preliminary. However, the importance of realistic modeling of ring- and stringer-stiffened aircraft structures and the possible use of fiber-reinforced composites for structural tailoring for noise control make the results of considerable interest.

As an example, the transmission loss (TL) of an orthotropic cylinder is shown in figure 27 for three values of ratio E_ϕ/E_x, where E_ϕ and E_x are Young's moduli in the circumferential and axial directions, respectively. For these calculations, parametric values typical of a narrow-body aircraft fuselage were used, and the ring frequency f_r (and consequently the circumferential stiffness E_ϕ) was held constant at 445 Hz. In this case variations of the ratio E_ϕ/E_x result only from variations of E_x, and E_x is important because it influences the axial bending wave of wavelength λ induced in the cylinder by the incident sound wave.

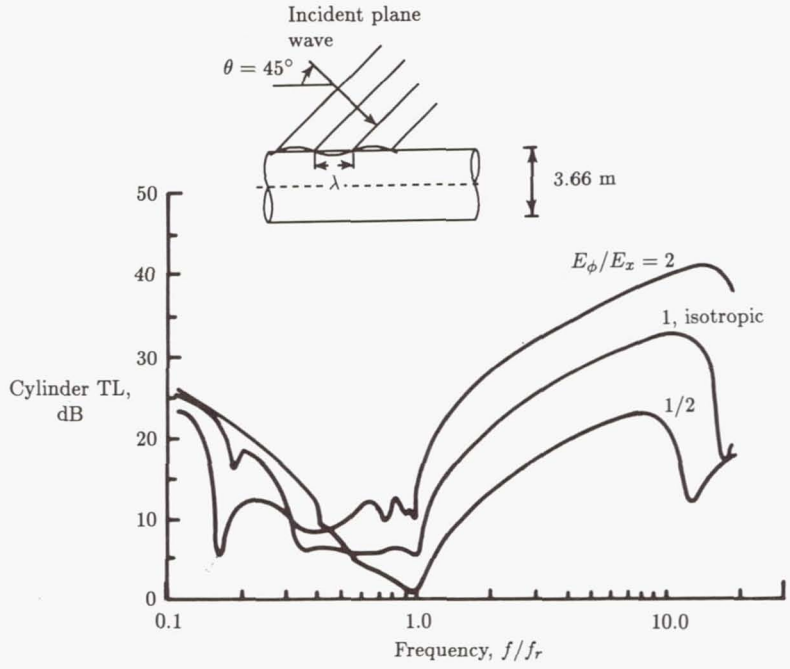

Figure 27. Calculated effect of modulus ratio on transmission loss of a cylindrical shell. (From ref. 88.)

Careful examination of figure 27 reveals the following TL characteristics that are consistent with general experience with flat panels. At low frequencies (in the

stiffness controlled region) the TL increases with decreasing f/f_r at a rate of about 6 dB/octave, and for f/f_r between 1.0 and 10 (often considered the mass controlled region) the TL increases at about 6 dB/octave. The TL dips at the ring frequency, $f/f_r = 1$, and at the coincidence frequency, $f/f_r = 12$ to 20. Increasing the axial stiffness (increasing E_x corresponds to decreasing E_ϕ/E_x) increases the TL at low frequency and reduces the coincidence frequency.

However, the figure also shows other, new features, the main one being the large variation of TL with E_ϕ/E_x for $f/f_r = 1$ to 10. In this frequency region the predicted TL increases by 6 to 8 dB for a doubling of E_ϕ/E_x, indicating that panel mass is not the only controlling parameter. While the analysis of the cylindrical shell (refs. 88 and 89) does not provide a ready explanation of the phenomenon, analysis of an infinite flat plate (ref. 35) shows explicitly that mass and stiffness are coupled and that TL can vary significantly with stiffness. Possibly, the predicted TL for the cylindrical shell involves both resonant and nonresonant (mass law) transmission, and the changes in the acoustic radiation efficiency of the shell associated with change in shell stiffness influence the acoustic transmission.

The choice of orthotropic properties for optimum noise control would have to depend on both the directional and the frequency characteristics of the important noise sources. The calculated results show complex changes in the TL curves with incidence angle (ref. 88). For realistic ring frequencies, important noise sources can be expected to occur at frequencies both above and below f_r. Therefore a detailed analysis of the particular configuration of interest would be required to determine appropriate values of the orthotropic moduli for minimum noise transmission.

Analysis of Aircraft Cabin Treatment

The infinite-panel theory has been combined with add-on treatment and cabin absorption analysis in a manner indicated in the diagram of figure 19. The resulting prediction method has been used to design cabin noise control treatment for high-speed propeller-driven aircraft of three sizes (ref. 57). To handle the propeller source noise having a nonuniform distribution, the fuselage was divided longitudinally into several segments. The average sound pressure level and a range of incidence angles were determined for each segment from estimated propeller characteristics and locations indicated in figure 28. Then sound transmission calculations were performed for several angles of incidence within the range for each segment and an average sound transmission was determined.

The treatment design approach was to estimate the exterior noise generated by a high-speed propeller and then to design a minimum-weight sidewall configuration that would provide an A-weighted cabin sound level of 80 dB. Extensive parametric studies varied sidewall and trim panel weights, configurations, and materials (ref. 57). Results are illustrated in figure 28. As shown by the various shadings in the figure, the treatment varied in several steps along the fuselage length, but was uniform circumferentially except that no treatment was applied below the floor. It was concluded that conventional treatment could provide the required noise reduction provided that sufficient weight was added. The weight required differed for the executive class, narrow-body, and wide-body aircraft studied.

The detailed analysis confirmed weight estimates made earlier using more simplified prediction methods (ref. 90). It was estimated that cabin noise control treatments with added weights up to 2.3 percent of aircraft gross weight, even though

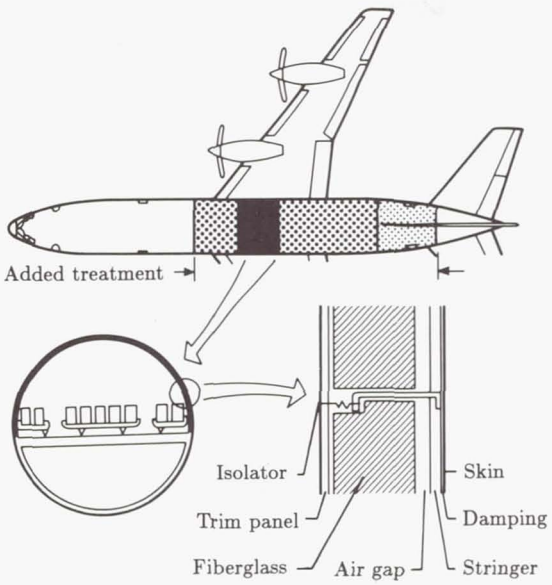

Figure 28. Cabin noise control treatment for a transport aircraft powered by propellers with supersonic tip speed. Weight of treatment required to control propeller noise is 0.75 to 2.3 percent of aircraft gross weight. (From ref. 57.)

much heavier than the more usual value of about 1 percent of gross weight, were not large enough to reduce significantly the advantage in fuel used and direct operating cost obtained by the use of advanced propellers. However the sidewall treatment weights are large enough that worthwhile reductions in fuel consumption would result if treatment weight were reduced. Efforts have been conducted in a search for lighter weight treatment concepts specially suited to the tonal noise spectrum characteristic of propellers (ref. 91).

The detailed analysis also provided an engineering description of the sidewall configurations required. An experimental program was carried out to validate the theoretical prediction methods, to evaluate the sidewall designs developed by the analysis, and to provide experience with the very heavy sidewalls that the theory indicated were necessary for high-speed turboprop application (ref. 92). The test fuselage was a segment taken from an operational commuter aircraft to obtain a realistic structure. The fuselage, a specially designed floor, and the sidewall treatment were designed to be a 43-percent scale model of the narrow-body aircraft design of the theoretical study. Test results were obtained for several sidewall and treatment configurations to obtain trends with weight. Noise reduction results are shown in figure 29 for the configuration representing the design point resulting from the analytical study. The figure indicates that the theory predicts slightly less noise reduction than is measured, suggesting that the weight estimates (ref. 57) are conservative. Test and theory do not agree as well for the other sidewalls, especially at lower frequencies for the lighter weight configurations. Improved representations

of the sidewall structure, the propeller source noise distribution, and the interior acoustics may be required for improvement of the theoretical predictions.

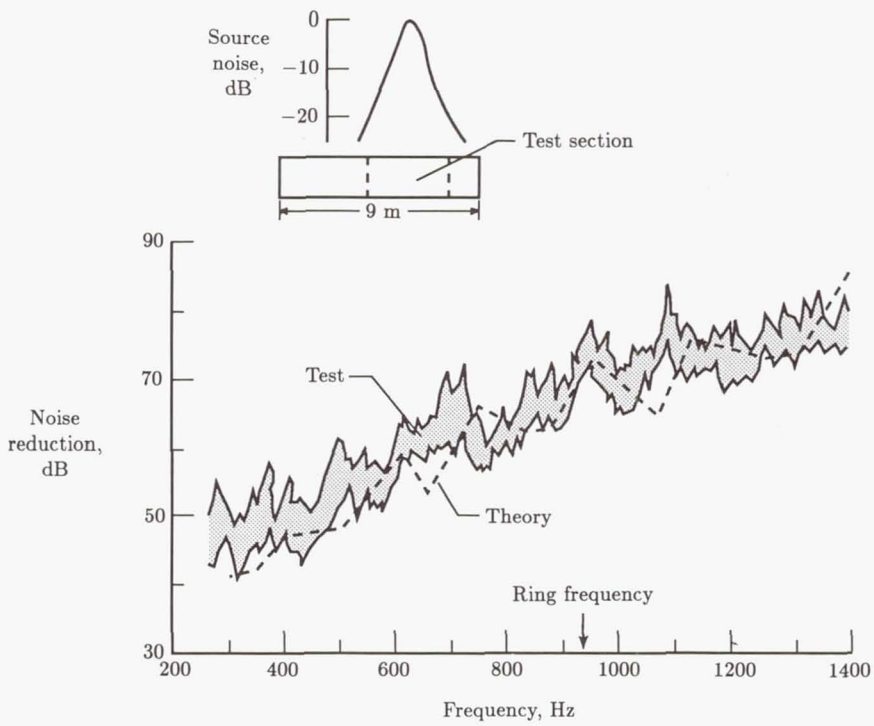

Figure 29. Noise reduction of a 168-cm-diameter aircraft fuselage with double-wall noise treatment (ref. 92). Propeller source noise simulated with a horn. Mass of outer wall was 9.47 kg/m^2; inner wall, 7.13 kg/m^2.

Testing of realistic fuselage and treatments entails substantial cost and time. The theory clearly showed its value in this program by providing candidate treatment configurations at much less cost than would have been required by experimental approaches alone.

Finite-Cylinder Analysis

It is not necessary to model cylindrical fuselages as having infinite length; analyses have been performed wherein the fuselage was considered to have finite length. Those analyses included both model and full-scale situations, and the excitation field was represented as either random or deterministic.

In one approach, transmission of propeller noise into a cylindrical fuselage of finite length has been analyzed using the general method developed for noise transmission into the Space Shuttle payload bay (ref. 63). The fuselage structure was idealized as a series of curved, orthotropic panels with frames and stringers included at low frequencies but not at high frequencies. The fluctuating pressure generated by the propeller was represented as a random, convected pressure field,

but since the pressure field is inhomogeneous, modifications had to be introduced into the analytical model developed initially for the more homogeneous case. The modifications allowed calculation of a joint acceptance function that depends on the distance of a particular panel from the location of maximum excitation pressure. Division of the fuselage structure into several panels allowed calculation of noise transmission through different regions of the cabin and determination of noise control treatments that varied in composition along the length of the cabin. The sidewall treatment was modeled in this approach as an independent module of the analytical procedure.

Transmission of random noise was also considered in another analytical model (refs. 48 and 73), but an important contribution of that study was the detailed representation of propeller acoustic pressures as a deterministic field. Measurements on general aviation aircraft indicate that the harmonic components of propeller noise are essentially deterministic. Furthermore, analytical methods are becoming available to predict the magnitude and phase of each harmonic component. This detailed representation of a propeller acoustic field has been used to calculate the deterministic forcing function on a cylindrical fuselage (ref. 48). In this approach, the region of the fuselage exposed to the acoustic pressure is represented by a grid of points, with the harmonic pressure and phase defined at each point. The grid shown in figure 30 has 160 points on the upper quadrant of the fuselage. The pressure field for the lower quadrant is determined from that of the upper quadrant, with a phase shift introduced to account for the rotational speed imposed by the propeller.

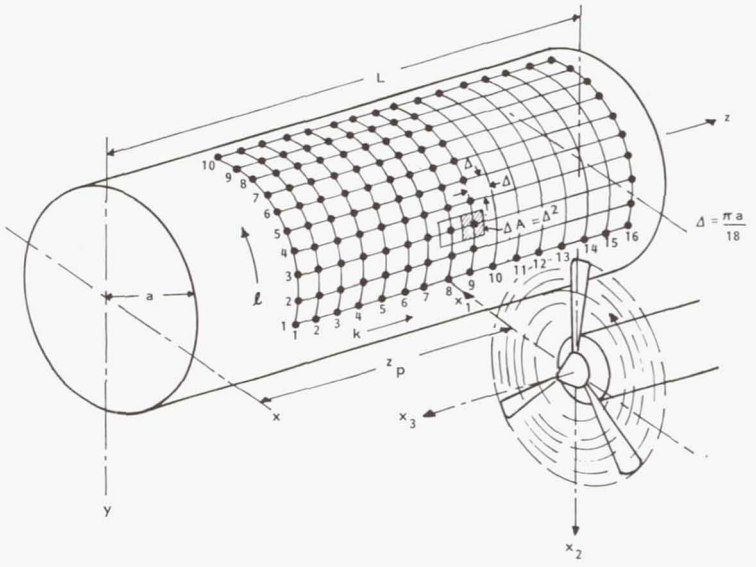

Figure 30. Grid used to couple ANOPP theoretical propeller noise model with cylinder noise transmission in the propeller aircraft interior noise prediction program (ref. 73).

Other important aspects of the analytical model are the representation of the cabin floor as a longitudinal partition and the first attempt to integrate the sidewall treatment into the noise transmission model (ref. 48). The presence of the cabin

floor can strongly influence the dynamic characteristics of the structure and interior volume. For example, the acoustic mode shapes of the cabin may differ from those of a cylindrical volume, as can be seen from figure 14. The floor and shell of the structure can be modeled as an integral unit. Mode shapes can be calculated for such a configuration (refs. 48 and 93), a typical mode shape being shown in figure 31.

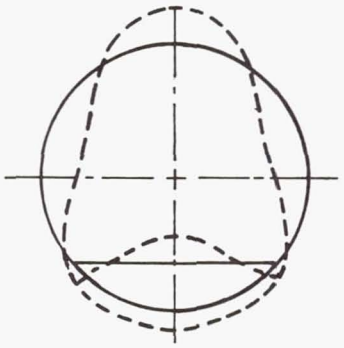

Figure 31. Calculated structural mode of a cylindrical shell with an integral floor. (From ref. 48.)

The analytical model was developed in conjunction with a series of laboratory experiments on test cylinders with diameters of 50.8 to 66 cm and a variety of configurations of circumferential and longitudinal stiffeners, floor structures, and interior acoustic treatments. These cylinders were exposed to broadband random noise and to acoustic pressures generated by a model-scale propeller. As an illustration, figure 32 compares measured and predicted noise transmission spectra for random noise excitation (ref. 73). The agreement between test and theory is good at frequencies below 500 Hz, but deteriorates at high frequencies. In the experiment the treatment consisted of a layer of fiberglass and vinyl about 1.3 cm thick that was attached to the interior of the cylinder wall. The stringer web, however, was 2.5 cm high and, therefore, extended through the treatment into the interior of the cylinder. In the analysis it was possible, using a high-frequency approximation, to estimate the acoustic power flowing through the stringer webs. It was found that at high frequencies the fiberglass-vinyl treatment was very effective and transmitted little noise and that the exposed stringers transmitted the major part of the interior noise. The predicted noise reduction is therefore reduced greatly, as shown in figure 32. In the frequency region between about 500 and 2000 Hz, neither of the theories agrees very well with the test results. However, it can be concluded that relatively small areas of exposed stringer (or ring frame) can be significant noise transmission paths when the skin areas are covered with effective treatment.

The analytical model has also been used to predict sound levels inside a general aviation airplane, for comparison with measured levels (ref. 74). The measurements were performed using a space-averaging technique that was designed to provide space-averaged levels suitable for comparison with the predictions. As shown in figure 33, the predicted sound levels agree closely with the measured results for three of the five harmonic components.

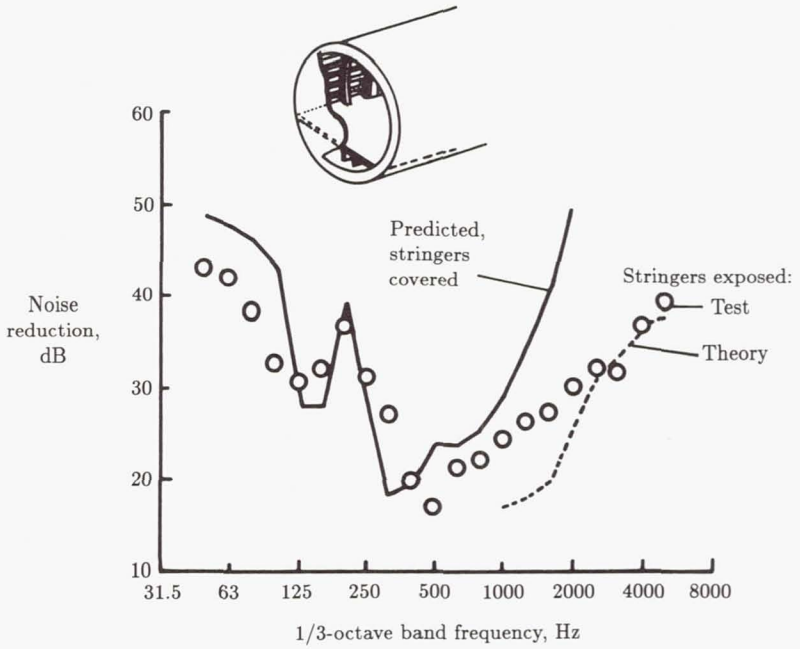

Figure 32. Predicted noise reduction of a stiffened cylinder with acoustic treatment and an integral floor. Power flow theory (ref. 73).

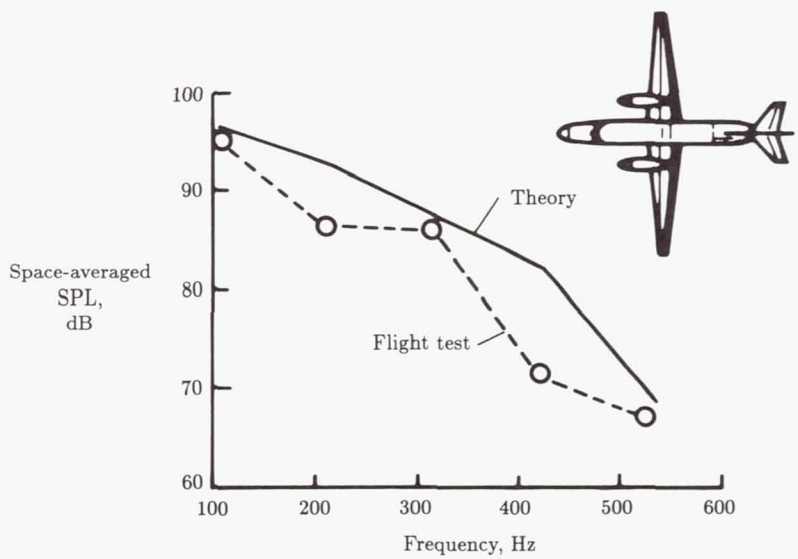

Figure 33. Prediction of cabin noise at propeller tones in flight of a light twin-engine aircraft. Power flow theory (ref. 74).

Structure-Borne Noise

Not all the sound in an aircraft interior is associated with airborne transmission. Some components of the interior acoustic field are the result of mechanical forces or aerodynamic pressures acting on distant regions of the airframe. The resulting vibrational energy is transmitted through the structure and then radiated into the fuselage interior as sound. These components of the interior sound field are referred to as "structure-borne sound."

It has long been recognized that structure-borne sound transmission could contribute to interior sound levels in certain types of aircraft. Bruderline (ref. 94) in 1937 and Rudmose and Beranek (ref. 95) in 1947 observed that structure-borne vibration from wing-mounted reciprocating engines contributed to interior sound levels. Thus, Bruderline noted that on the DC-4, "rubber supports" were to be provided for the engines, and all controls and conduits were to be flexible between the nacelles and engines. However, in both references, discussion of structure-borne sound transmission is only qualitative, Rudmose and Beranek noting that no scheme existed at that time for estimating quantitatively the amount of structure-borne vibration in an aircraft fuselage.

The situation has changed, with an improved understanding of structure-borne sound transmission in aircraft, ground vehicles, ships, and buildings. These activities have been the subject of several review papers (refs. 96 and 97) which provide numerous references associated with a wide range of aerospace and nonaerospace applications. The discussion in this section is directed specifically to the topic of structure-borne sound in aircraft, an application that is probably not as well developed as in some other fields.

Structure-Borne Sound in Aircraft

In general, structure-borne sound in aircraft is associated with discrete frequency components. This does not mean that broadband structure-borne sound is not present; however, if it is present, it has not been identified, probably because of masking by broadband airborne noise. The occurrence of structure-borne sound is not limited to propeller-driven aircraft with reciprocating engines; the sources could be turboprop, turbojet, or turbofan engines, air-conditioning systems, hydraulic pumps, and other rotating or reciprocating equipment.

One of the best documented studies of structure-borne sound in an airplane with turbofan engines is that of the DC-9 (refs. 28 and 98), but the phenomenon has been observed on other aircraft that have turbojet or turbofan engines mounted on the rear of the fuselage. For example, figure 34 shows a narrow-band sound pressure level spectrum that was measured in the cabin of a business jet airplane powered by two twin-spool turbofan engines (with geared fan) mounted on the rear of the fuselage (ref. 29). The spectrum contains a number of discrete frequency components that can be associated with the rotational frequencies of the fan, low-pressure compressor and turbine, and high-pressure compressor and turbine. These discrete frequency components are associated with structure-borne sound, whereas the broadband components result from airborne transmission, mainly due to the turbulent boundary layer on the exterior of the fuselage. Various tests have been performed to demonstrate that the discrete frequency components are definitely associated with structure-borne transmission. The tests have included ground

experiments with engines disconnected and changes to engine mounts for repeated flight tests. Also, external acoustic measurements and analysis show that acoustic radiation from the engine inlet would not generate sufficiently high sound pressure levels to be the dominant source. Structure-borne sound is present also in aircraft with wing-mounted turbojet or turbofan engines, but the sound pressure levels may not be significant except in some aircraft with large turbofan engines.

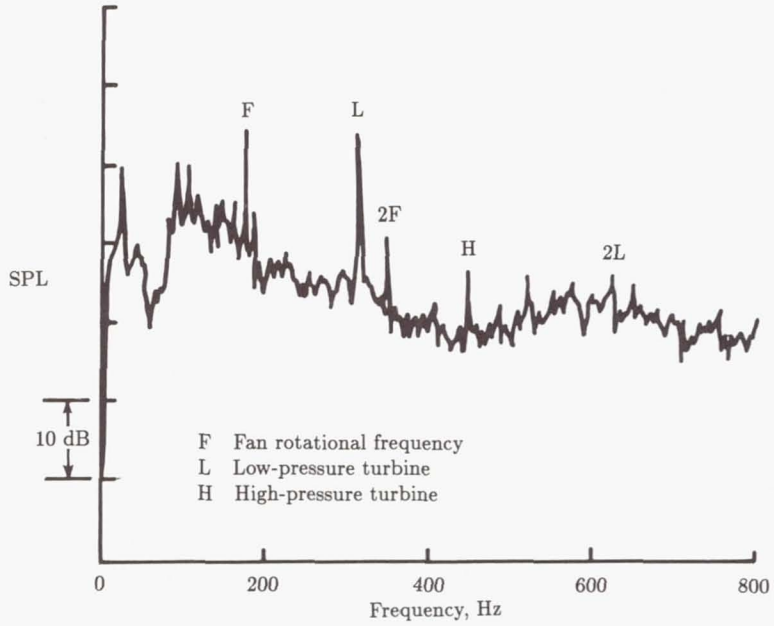

Figure 34. Discrete frequency structure-borne components in sound levels in the cabin of a business jet airplane. (From ref. 29. Copyright 1982 SAE, Inc.; reprinted with permission.)

Structure-borne sound can be a major contributor to the sound pressure levels in the cabin of a helicopter (refs. 99 and 100). For example, an investigation of the noise sources contributing to the acoustic environment in an eight-seat helicopter indicated that structure-borne noise from the engine and gearbox dominated cabin sound levels at frequencies above about 3000 Hz, as shown in figure 35. In this respect the helicopter differs from the fixed wing airplane. Structure-borne sound in helicopters is mainly high frequency, whereas it is usually low frequency in fixed wing airplanes. This difference can influence the choice of analysis method and noise control procedure used for each type of aircraft.

The preceding discussion has been concerned with the direct transmission of mechanical vibration from the engine and associated machinery into the airframe. A second path may also be present, although its importance has not yet been established. This path involves impingement of a propeller wake on the surface of a wing or empennage, with subsequent transmission of vibration energy into the cabin. Such a structure-borne path is difficult to identify, even under ground test conditions. Measurements on a twin-engine general-aviation airplane with a high

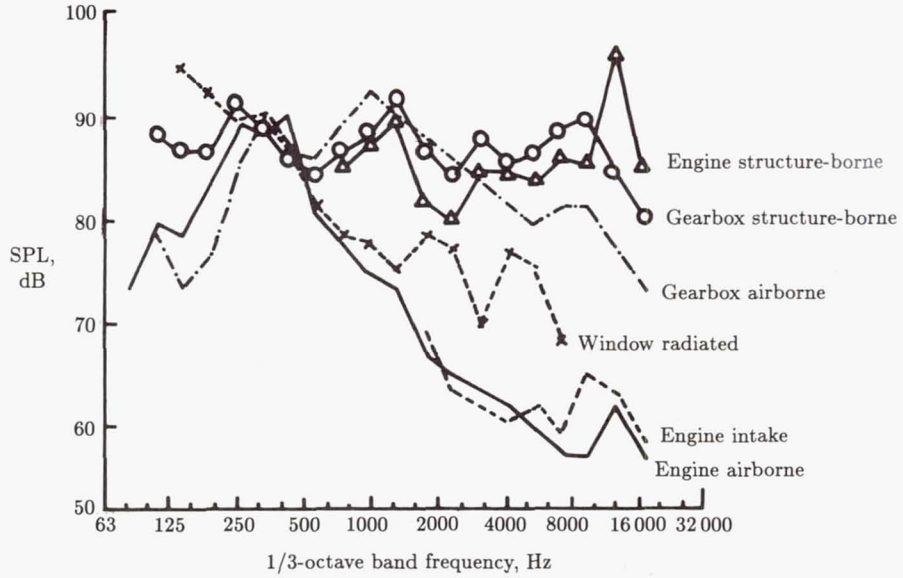

Figure 35. Noise source contributions to sound pressure levels in a helicopter cabin. (From ref. 100.)

wing (ref. 101) suggest that, at least under ground test conditions, the importance of the propeller wake as a noise source could be significant at high propeller torque (fig. 36).

Although most examples of structure-borne sound are associated with the main propulsion system of an airplane, other examples exist, although they are often of short duration. Air cycle machines in air-conditioning systems can transmit discrete frequency vibration which radiates sound into the cabin. Also, vibration can be transmitted from hydraulic pumps into the fuselage structure, with eventual radiation as sound into the cabin.

Usually, structure-borne sound components cannot be measured directly and have to be deduced from other measurements. Exceptions to this general rule occur if the airborne components can be removed (ref. 101), but it is often only the structure-borne path that can be broken and, then, only in ground tests (ref. 102). There still remains the problem of determining the structure-borne components during flight conditions.

Analysis of Structure-Borne Sound Transmission

An analysis of structure-borne sound in aircraft can be divided into three main parts: excitation, transmission, and acoustic radiation. The precise role played by each part depends on the particular aircraft configuration, but the general approach can be discussed using the example of an airplane with wing-mounted turboprop engines and propellers (fig. 37). The main components associated with structure-borne sound transmission are identified in figure 38. For this aircraft the excitation is in two forms: a mechanical component that is associated with out-of-balance forces in

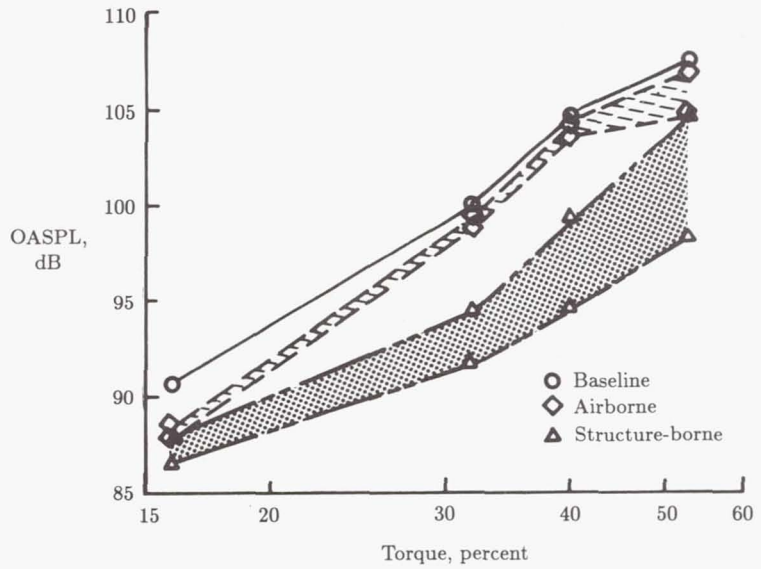

Figure 36. Airborne and structure-borne sound levels deduced from measurements in passenger compartment of a twin-engine, propeller-driven airplane. (From ref. 101.)

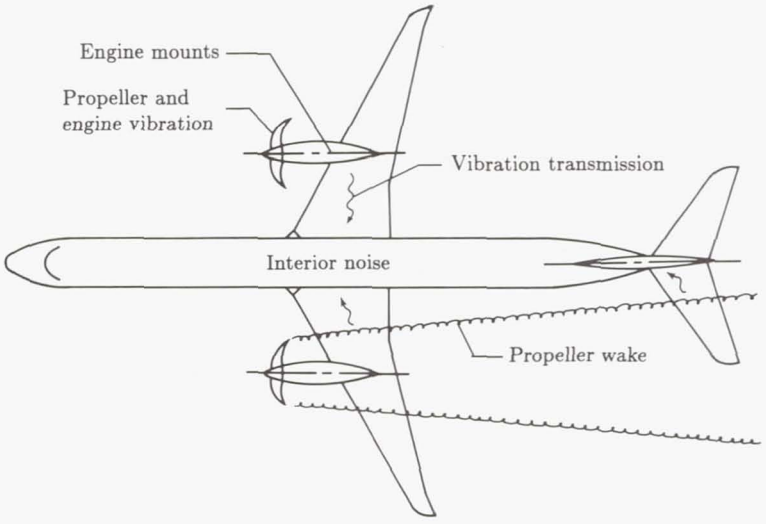

Figure 37. Sources and paths of structure-borne sound in twin-engine, propeller-driven airplane.

the engine and propeller and an aerodynamic component generated by the propeller wake on the wing. The out-of-balance forces are transmitted through the engine mounts (which may be rigid or include vibration isolators) into the wing structure, whereas the aerodynamic pressures act directly on the wing skin. Structure-borne transmission along the wing occurs in the spars and skin, although it is possible that different paths are important for different frequency components.

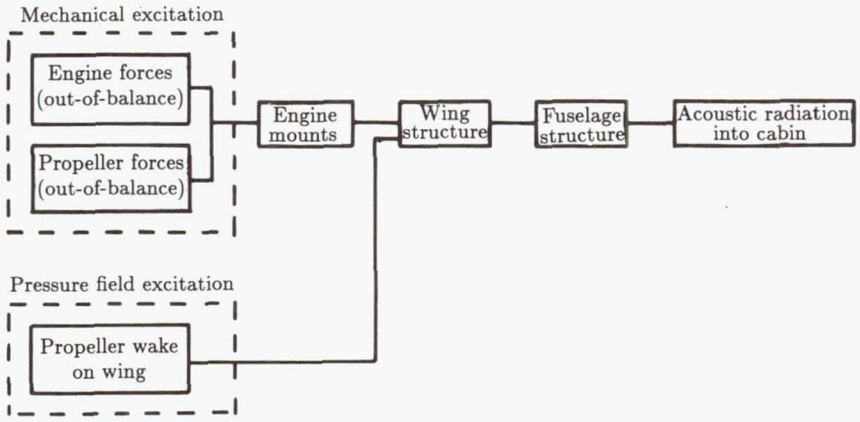

Figure 38. Main components of structure-borne sound transmission path for twin-engine airplane.

Excitation

When the excitation is generated by mechanical forces, the vibrational power P flowing into the airframe structure can be estimated by use of the impedances of the various structural components (ref. 98). Thus, typically,

$$P = \mathrm{Re}\{FV^*\} = \frac{|Z_s|^2}{|Z_s + Z_f|^2}\mathrm{Re}\{Z_f\}V_s^2 \tag{25}$$

where F and V are, respectively, the force and velocity at the connection between the source and the structure, an asterisk denotes the complex conjugate, Z_s is the impedance looking into the source, Z_f is the impedance looking into the airframe, and V_s is the "free velocity" of the source (i.e., the engine vibratory velocity for the hypothetical case when the engine is not constrained).

When an isolator is introduced, the power flow equation becomes more complicated. For the simplest case of a massless isolator with impedance Z_i,

$$P = \frac{|Z_s|^2|Z_i|^2}{|Z_iZ_f + Z_fZ_s + Z_sZ_i|^2}\mathrm{Re}\{Z_f\}V_s^2 \tag{26}$$

The value of V_s cannot be measured directly, but a practical approach is to measure the velocities on an engine or on an airframe during engine operation

when no vibration isolators are present (ref. 98). Impedances can be obtained from measurements (ref. 103) or calculations (ref. 104).

If the excitation is a pressure field, such as the wake generated by the propeller, the loading on the structure can be estimated if the characteristics of the pressure field and the excited structure are known (ref. 105). This can be accomplished using techniques similar to those used to predict the response of fuselage structures to acoustic or aerodynamic excitation, as discussed earlier.

Energy Transmission

The transmission of vibrational energy in a structure involves the participation of several types of waves (ref. 106)—flexural, longitudinal, and transverse (plane and torsional). Thus the analysis is more complicated than for transmission through air. Longitudinal and transverse waves are nondispersive, their propagation speed being independent of frequency; flexural waves are dispersive, the phase speed being proportional to the square root of frequency. A complete estimate of energy transmission has to include contributions from all wave types. The situation is further complicated because at any discontinuity in the structure, such as a frame or stiffener, energy can be transferred from one wave type to another. For example, when a flexural wave in a plate is incident on an unsymmetrically attached mass, the resulting wave system includes transmitted and reflected flexural waves and transmitted and reflected longitudinal waves (ref. 107).

Various analytical approaches can be used to predict structure-borne transmission, but the choice may depend to some extent on the frequency range of interest. At high frequencies, where the vibrational wavelengths are small relative to the structural dimensions, statistical energy analysis methods have been used (refs. 99 and 107) since the requirement of high modal density is satisfied. An alternative approach has used the theory of waveguides (ref. 105). At low frequencies, where the wavelengths of the vibration are long relative to local structural dimensions and the modal density is very small, SEA methods are no longer valid. However, it is then practical to use finite element or other methods (refs. 108 and 109).

In some cases it is appropriate to apply empirical or semiempirical methods to supplement the analysis. For example, empirical methods were applied in the determination of transfer functions relating the forces induced by engine vibration to sound pressure in the cabin of a small, single-engine airplane (ref. 102). Also, experimental techniques have been used to determine transmission paths by disconnecting the engine from the fuselage structure (ref. 102) or by replacing vibration isolation mounts with rigid connections (ref. 110). To some extent, these experimental methods are more correctly considered as source-path identification methods, to be discussed later.

Acoustic Radiation

The final component in the determination of structure-borne sound in aircraft is the radiation of acoustic energy into the receiving volume. This is equivalent to airborne sound transmission except that in structure-borne transmission the structural response is only resonant, whereas in airborne transmission the response can include nonresonant contributions (which may be the major contributions). As was true for the analysis of vibration transmission, different analytical methods may

be applicable for different frequency ranges. SEA methods have been used where the acoustic modal densities in the receiving volume were high (ref. 99), and finite element methods where the acoustic modal densities were low (refs. 45 and 108). One example of the latter situation is the analysis of engine-induced noise in small general aviation airplanes.

Source-Path Identification

Aircraft cabin noise is generated by a variety of sources, such as turbulent boundary layers, jet exhaust, propellers, and engine unbalance forces. Noise from different engines or different locations, such as turbulent boundary layers on forward and aft regions, can be considered separate sources. Transmission can be airborne or structure-borne, but either can propagate along a variety of paths. For example, airborne noise can enter through windows, side panels, or ceiling panels, and structure-borne noise from a propeller wake can enter through excitation of wing panels or horizontal tail surfaces.

The need to minimize the weight of noise control devices requires that the contributions from various sources and paths be known in some detail. Then the cabin noise and structural weight limits may be satisfied by controlling only the dominant source-path combinations, by locating treatments where several sources or paths are affected, or by locating treatments at a position in the path where maximum noise reduction can be obtained with minimum treatment weight.

No single identification method is available that satisfies all situations. A number of methods have been developed, however, and it is usual that several are needed for any particular noise control application. Many identification methods have been developed originally for architectural and surface vehicle applications, and there is extensive literature available (refs. 111 and 112). Identification methods and results for aircraft applications are described in the following sections.

In-Place Measurement Methods

Identification measurements made with an aircraft in an operational flight condition are potentially the most reliable and accurate because all noise sources are present and are interacting in the actual manner to be controlled. Flight tests are expensive, however, and the interactions may not allow separation of the various sources and paths. Development of new measurement techniques and equipment that can operate without interference but in conjunction with other required testing is important for reduction of cost.

Frequency Separation

When the spectral characteristics of the dominant sources are distinctly different, their contributions can be identified from a spectrum of the cabin noise. This is illustrated in figure 9. The principal noise generated by the propeller occurs at the tones, whose frequencies can be obtained from the propeller rpm and number of blades. For this aircraft it is known that no other source produces this spectral characteristic, so the tones are identified as of propeller origin. The propeller broadband noise levels are low, so the broadband spectrum at about 70 dB is associated with the aerodynamic boundary layer. The measurement

of instrumentation noise floor and exterior sound levels on the fuselage (fig. 4) supports this conclusion. The appearance of a tone in the cabin at about 670 Hz associated only with an engine turbine speed suggests the presence of engine-generated structure-borne noise (ref. 4). The spectrum does not separate the contribution from the two propellers, however. For aircraft with piston engines the tone spectra from the propeller and pulsating exhaust usually overlap. Then, exhaust and propeller contributions can be separated only if the propeller is geared to operate at an rpm different from that of the engine (ref. 21) or if some engine tones occur at frequencies between the propeller tones (refs. 110 and 113).

Correlation

Where several sources are present having broadband or overlapping tonal spectra, the contributions can sometimes be separated by correlating the characteristics of the cabin noise with those of the sources.[10] The method requires simultaneous measurement of cabin noise and source noise so that a measured signal can be obtained for each source that contains information for only that one source. Extensive statistical theory has been developed for the separation of the source contributions (ref. 6), and methods of this type have been evaluated for surface-radiated noise (ref. 114), gas turbine combustion noise (ref. 115), and aircraft cabin noise (refs. 116 and 117). Use of coherent output power methods enabled separation of contributions from the right and left propellers, as they occurred at slightly different frequencies (ref. 117). The separation of the contributions from five fuselage panels was only a limited success (ref. 116). Only 35 percent of the sound energy at the copilot's position was attributed to the five panels, and this 35 percent resulted from the coherent motion of the panels, rather than from their independent motions. More extensive evaluation of the fuselage vibration might have been obtained through measurements at additional locations.

These methods require an understanding of fairly sophisticated statistical concepts and the use of a digital computer for processing of the data. Modern self-contained, portable, special purpose hardware for fast Fourier transform (FFT) analysis greatly facilitates such data handling.

Intensity

The distribution of sound radiated into the cabin by the enclosing walls is of interest for laying out the sidewall treatment distribution and for locating "hot spots" that indicate acoustic leaks in a finished cabin. Occasionally a trained observer can identify such hot spots simply by listening or with the aid of a microphone. Recent advances in instrumentation, however, have made possible the measurement of acoustic intensity for identifying the distribution of sound radiated from a vibrating surface (ref. 118).

Acoustic intensity measurements make use of a pair of carefully matched and calibrated microphones that are mechanically held at a fixed distance apart (ref. 119), as shown in figure 39. The pair is then sensitive to intensity flowing along the line joining the microphones and is much less sensitive to intensity flowing in

[10] Two deterministic, discrete frequency sources of precisely the same frequency will always be completely correlated so that this approach is not useful.

other directions. The signals from the microphones are summed to obtain pressure and subtracted to obtain velocity (from the slope of pressure). The complex product yields acoustic intensity. Such measurements are only widely practical through the use of special purpose FFT analysis hardware. The availability of such instrumentation has stimulated a surge in research on intensity methods (ref. 120) and has led to development of special equipment and procedures for measurements on aircraft in flight (ref. 121). Intensity methods have been applied to aircraft panels (ref. 122) and a complete aircraft fuselage in laboratory studies (ref. 123).

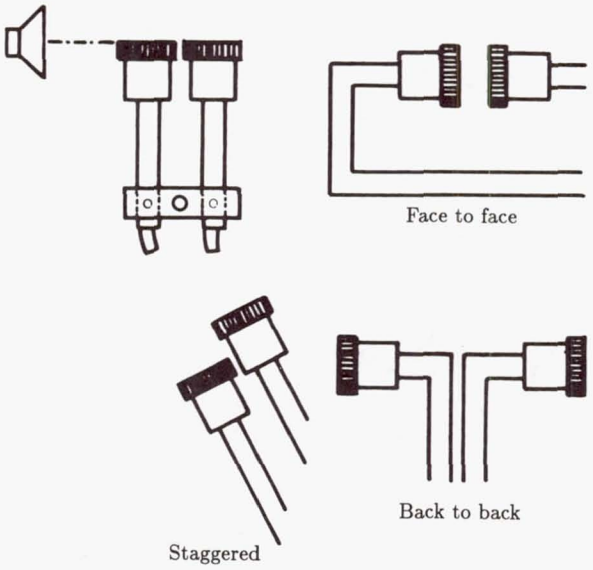

Figure 39. Microphone arrangements for acoustic intensity measurement. (From ref. 119.)

Measurement of sidewall noise transmission (ref. 123) is illustrated in figure 40. A fuselage of a light aircraft was suspended in a semianechoic chamber and a pneumatic driver with a rectangular horn was used to simulate the localized sound field of a wing-mounted propeller. Total acoustic power transmitted through each of four panel areas was measured by sweeping the two-microphone probe over the interior of the panel while the instrument system integrated the instantaneous intensity signal. Incident power was obtained using the same two-microphone technique with the fuselage removed and sweeping over the area previously occupied by the panel. For some tests, measurement results were improved by installing fiberglass absorption blocks in the fuselage when measuring power transmitted. Transmission loss obtained from incident and transmitted power for a window area is shown in figure 40. The measured TL of the plastic window agrees with infinite-panel mass law, and the technique is shown to detect changes in TL due to addition of a window shade such as might be used for noise control purposes. At low frequencies the measurements showed differences from the mass law, as would be expected from the finite nature of the window area. Special efforts have been directed toward design of two-microphone

systems for use in the low-frequency region of importance to propeller aircraft. It was shown that the TL values for the four panel areas could be used to obtain the sound pressure level in the cabin and that changes in SPL due to changes in TL of one panel area could be reasonably well predicted.

The two-microphone method can be expected to cause minimal change in the vibration and acoustic behavior of the fuselage and therefore should produce accurate results.

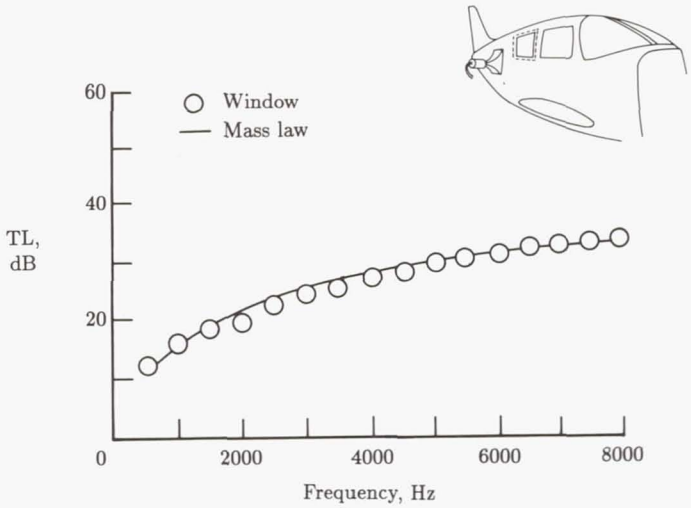

Figure 40. In-place measurement (ref. 123) of aircraft window noise transmission loss using acoustic intensity.

Holography

Near-field acoustic holography (NAH) is a new technique for studying the sound radiation of vibrating surfaces (ref. 124). The technique is quite similar to conventional acoustical holography and is based on the same principles. There are differences, however, that allow NAH to provide significantly more information. Measurements are made as close as possible to the vibrating surface to detect both the radiating and the nonradiating pressure components. For example, one system uses a 16×16 plane array of 256 inexpensive electret microphones located just a few centimeters from the vibrating surface (fig. 41). Processing these data using FFT algorithms to evaluate Rayleigh's integral formulas (ref. 125) allows calculation of the pressure, the velocity, and the vector intensity at any point in the acoustic field. The method has been used to study sound radiation from flat plates (fig. 41) and displays unique "source" and "sink" features of the intensity field.

System Modification Methods

Information on sources and paths can be obtained by modification of some feature of the aircraft operation or configuration. For example, changing the rpm of one engine (when both are normally operated at the same rpm) separates the tones in

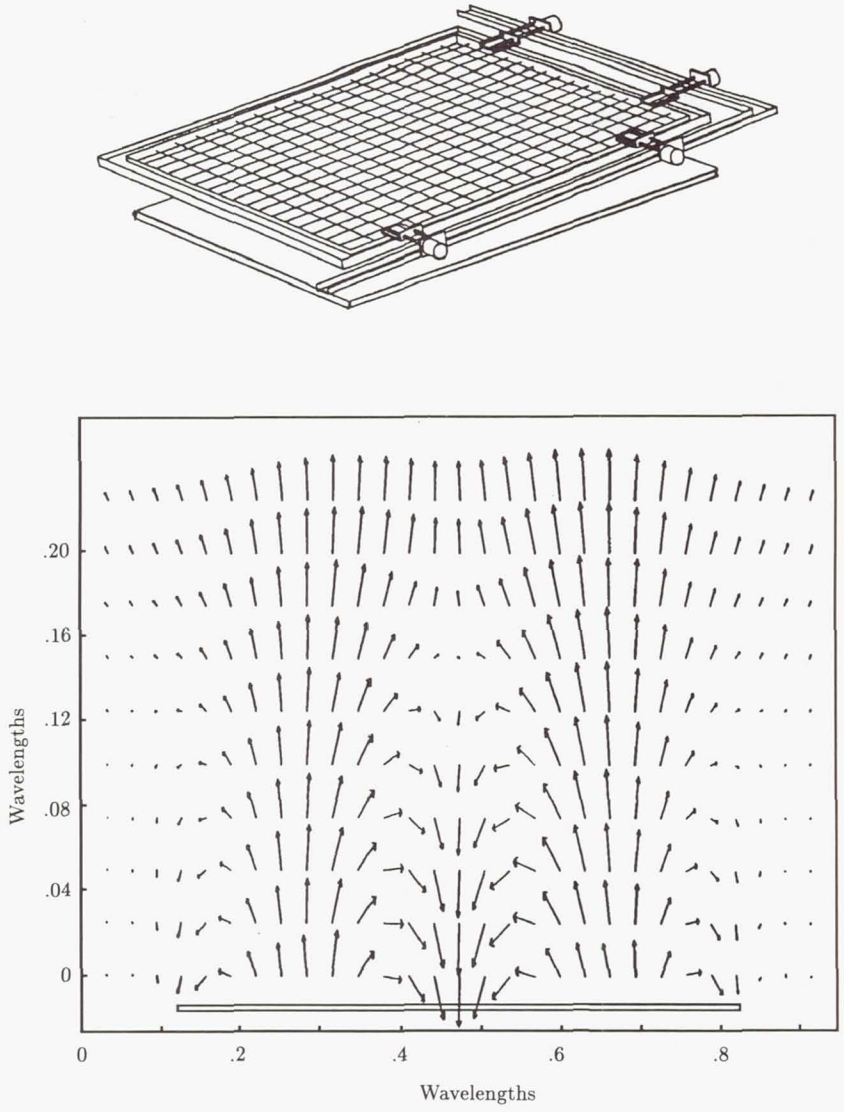

Figure 41. Vector acoustic intensity field of a vibrating plate using near-field acoustic holography. (From ref. 124.)

the frequency spectrum so that the contribution of each engine can be identified, as shown in figure 4. For the analysis to be rigorous, it should be shown that the modification does not change the source strength, the path characteristics, or their interactions. For the rpm change (fig. 4), a number of rpm values for both engines could be investigated to determine the effect of rpm changes. In most cases, however, the effect of the modification cannot be rigorously determined, so the results must be considered only estimates.

The precision obtainable by source-path modification is suggested by figure 42 (ref. 110). A variety of identification techniques, including modification methods, were used to determine the cabin noise contributions from various sources and paths (fig. 42(a)). The component contributions were added to obtain a computed cabin noise level. This is compared with the actual measured noise level in figure 42(b). The overall shape of the spectrum is predicted quite well, but differences of several decibels appear at many frequencies.

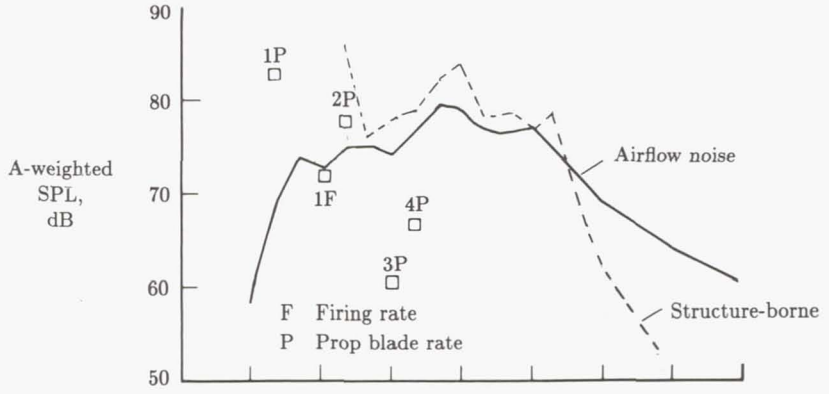

(a) Component contributions.

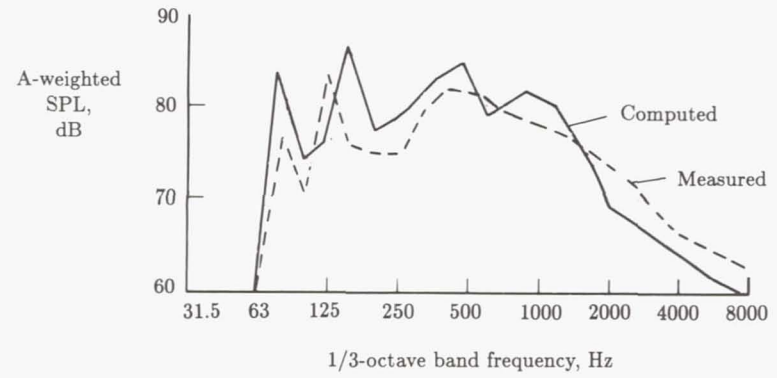

(b) Summation.

Figure 42. Cabin noise contributions for a twin-engine light aircraft in cruise flight. (From ref. 110.)

Turning Off Sources

If one of the noise sources can be turned off, then the reduction in cabin noise that occurs can be considered the contribution of that source. This is true provided

that turning off a source does not change the output of the remaining sources. For example, turning off one engine of a twin-engine aircraft can be expected to reduce airspeed and thus reduce both the aerodynamic noise and the noise of the remaining engine and propeller. These effects can be evaluated either by special tests or by theoretical considerations.

When a source is turned off, it sometimes happens that the cabin noise level is not reduced; it may increase. Such results can occur when two sources have a phase relation that results in cancellation, so that the two sources together make less noise than either one alone. Synchrophasing of multiple propellers and active noise control are intended to reduce cabin noise by such cancellation.

The strength of aerodynamic sources of cabin noise in several light aircraft has been estimated by operating in flight with the engines partly or completely shut down (ref. 110) and some results are shown in figures 43 and 44. As reported by the authors,

> Similar dive tests were carried out with several twin-engine aircraft, on which propellers and engines could be brought completely to a stop without creating unusual propeller wakes which would excite the fuselage in an uncharacteristic manner. In most cases, the dive speed did not reach the cruise velocity. Therefore, a scaling relationship was needed to extrapolate nonpropulsion noise measured at a low speed to the cruise velocity for comparison with "all sources." ... [Figure 43] shows the results of one such scaling test, where data taken at 110 kt is scaled to closely match the 150 kt data using a V^4 relationship [where V is velocity], which is normally associated with the scaling of mean-square pressures in a turbulent boundary layer, wake, or jet when the turbulence structure remains basically unchanged over the speed (and Reynolds number) range of interest .... These 150 kt data are then scaled to the 178 kt cruise condition by a V^4 relationship; the comparison with "engine on" noise levels is shown in ... [figure 44.] Again, the nonpropulsion contribution to the broadband spectral levels is found to be substantial. In this case, the only major uncertainty is whether or not the flow field over the aircraft was identical between the dive and cruise conditions.

Path Blocking

If a transmission path can be blocked, or cut, so that it transmits little or no noise or vibration, then the resulting reduction in cabin noise can be attributed to that path.[11]

Structure-borne noise from engine vibration has been investigated (ref. 102) by detaching the engine from the fuselage in ground tests (fig. 45). The engine support frames were in place for both tests so that the aerodynamic flow noise would be the same, and the tires were partly deflated to minimize any vibration transmission through the ground. When the engine was detached from the fuselage, both engine and cowl were moved forward about 5 cm so that there would be no mechanical connection. All engine loads were then carried by the support frames. The space between the cowl and fuselage at the detachment line was covered with soft adhesive tape that would maintain the aerodynamic lines of flow but not transmit structural

[11] Note the cautions described above that other sources and paths should not be altered and that acoustic cancellation may occur.

vibrations. The reduction of 3 dB for the overall cabin noise (fig. 45) indicates that the noise transmitted through the engine attachments was equal to the noise from all other sources in that test setup. Larger reductions in some 1/3-octave bands indicate that the proportion is larger at those frequencies, and significant structure-borne noise is evident throughout the frequency range.

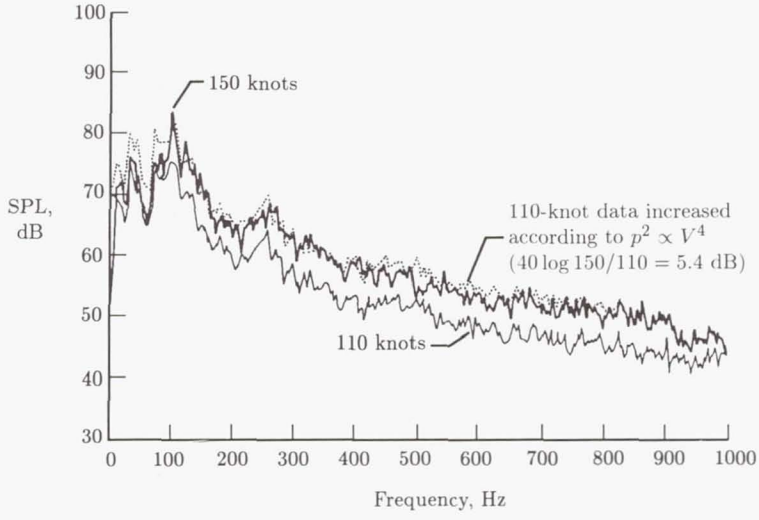

Figure 43. Estimation and scaling of cabin noise due to airflow using engine-off dive tests of a large twin-engine light aircraft. (From ref. 110.)

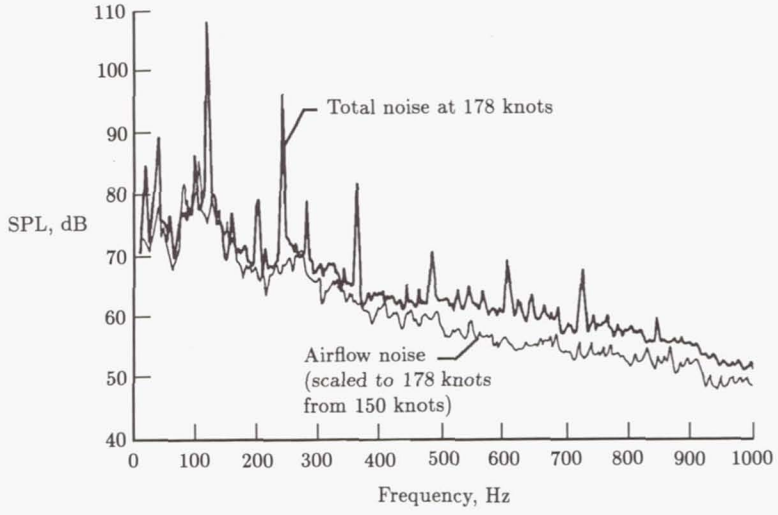

Figure 44. Airflow noise relative to total noise in the cabin of a large twin-engine light aircraft. (From ref. 110.)

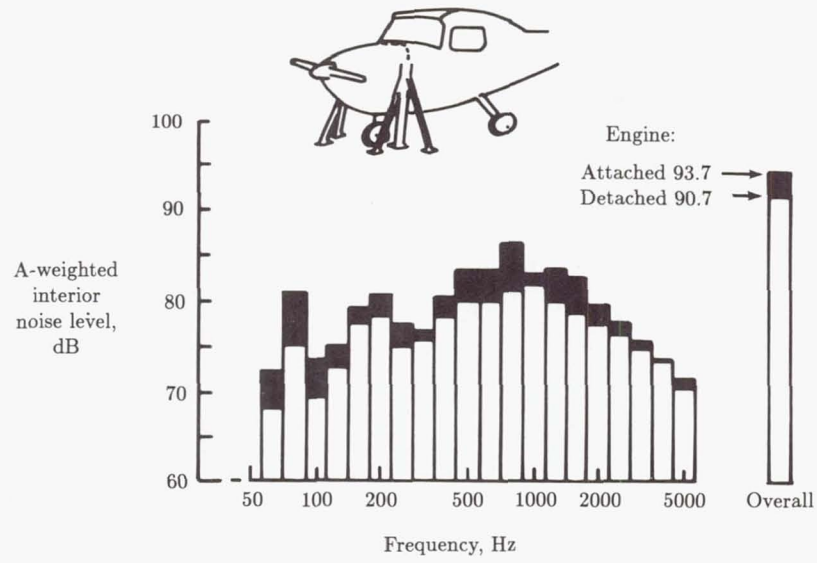

Figure 45. Determination of structure-borne noise by engine detachment method. (From ref. 102.)

Airborne paths are often studied using a heavy mass-loaded vinyl material to cover the surface (fig. 46). Vinyl sheets of 5 to 10 kg/m^2 have been used with soft foam or fiberglass between the vinyl and the surface to minimize the effects on the dynamics of the fuselage structure. Transmission through windows was studied in a reverberation room (ref. 126) by testing with windows uncovered and then covered, as illustrated in figure 46(a). The objective of covering the windows was to eliminate the sound transmission. The results showed that the covering effect depended on frequency; at some frequencies the interior noise was higher with the windows covered, but the overall sound level decreased by 3 dB with the windows covered. Transmission through the fuselage sidewall and the wing structure was studied in ground tests of a light aircraft with engines running (ref. 101). The covered areas are sketched in figure 46(b). The fuselage and wing coverings consisted of one or two layers of foam and septum material weighing 3.08 kg/m^2 each. The entire wing surface was covered from the fuselage to a position outboard of the region where the propeller wake impinged on the wing. By testing with a variety of combinations of fuselage and wing coverings, it was concluded that the propeller wake interaction with the wing surface was a significant structure-borne noise source in the cabin.

Surface covering is an often used and seemingly straightforward approach to path identification. However, unexpected results are sometimes observed, for example the increase in noise level when windows were covered in reverberation room tests (ref. 126), and the reduction in cabin noise level when a window was opened in a propeller aircraft ground test (ref. 127). Explanation of these effects of path changes would require a more in-depth analysis than has been applied yet.

Acoustic enclosures of several kinds can be used to limit the area on the exterior of the fuselage over which the source noise impinges or to limit the sidewall area on

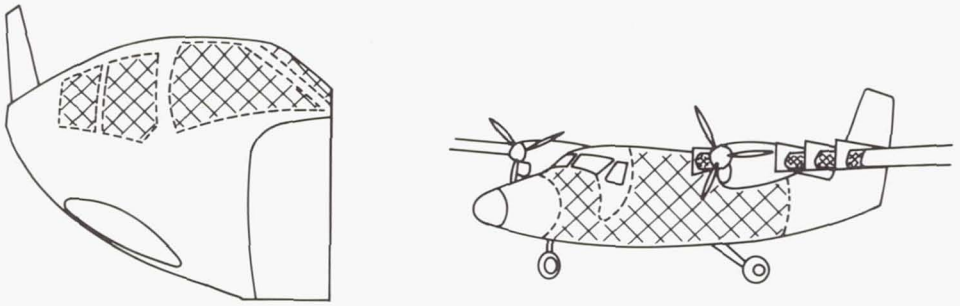

(a) Windows covered. *(b) Fuselage and wing covered.*

Figure 46. Surface covering for path identification by the path blocking method (refs. 101 and 126).

the interior of the aircraft from which the radiated noise is measured. The use of an exterior acoustic guide to measure the noise transmitted through an aircraft window (ref. 77) is illustrated in figure 47. The acoustic guide is constructed of plywood and mass-loaded vinyl walls so that noise generated by the speaker in the enclosure is directed only onto the window. A soft material is applied where the guide walls meet the fuselage surface to provide an acoustic seal but to minimize the effect on vibration behavior. Test results showed that the noise level outside the enclosure was 30 dB less than the level inside. The test results indicate good agreement between the measured and predicted transmission through the window. Location of the acoustic guide at various positions on the fuselage exterior, on the wings, or on tail surfaces would provide information on the relative sensitivity of cabin noise to source noise position.

Parameter Variation

When a transmission path cannot be completely blocked, either by disconnecting structure or by adding mass, then a change in transmission properties may alter the transmitted noise enough to infer the importance of the path. As an example, the structure-borne noise in a single-engine light aircraft has been studied using this technique (ref. 110). The aircraft engine was run on the ground in two test configurations, one using the standard soft rubber engine isolation mounts and the second using solid metal blocks in place of the soft isolators. Cabin noise and acceleration at the four mount locations were measured. For one frequency band the test results obtained were

	Average mount acceleration, dB (re $1g$)	Cabin noise level, dB (re 20 μPa)
Hard mounts	10	88
Soft mounts	−3	84

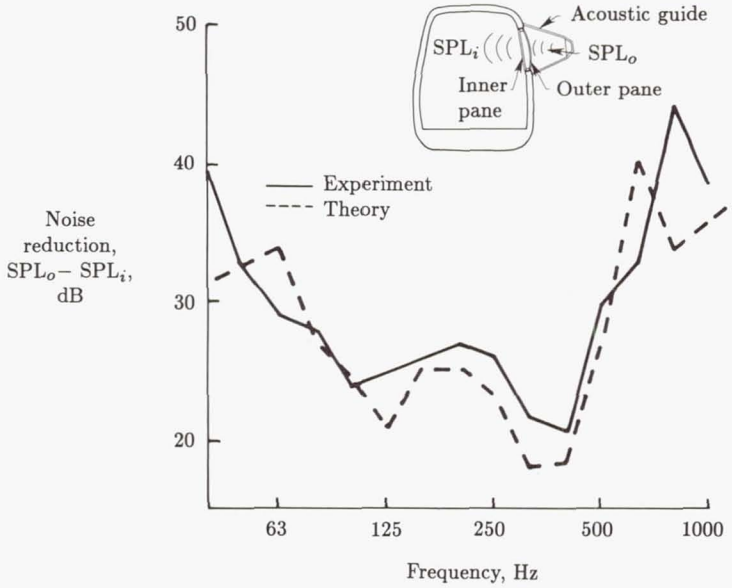

Figure 47. Identification of window noise transmission using an acoustic guide. (From ref. 77.)

Airborne and structure-borne noise were assumed to be independent and therefore to add in the cabin according to the relation,

$$< p^2 >_{\text{total}} = < p^2 >_{\text{air}} + < p^2 >_{\text{struct}} \tag{27}$$

where

$< p^2 >_{\text{total}}$ mean square total acoustic pressure

$< p^2 >_{\text{air}}$ mean square airborne component

$< p^2 >_{\text{struct}}$ mean square structure-borne component

The structure-borne component is then assumed to be proportional to the average acceleration $< a >$ at the engine mounts:

$$< p^2 >_{\text{struct}} = < (ka)^2 > \tag{28}$$

The measured mount accelerations and cabin noise were then used in these expressions to obtain two equations that were solved to obtain the following result for the sound pressure contributions in the frequency band:

	Airborne noise level, dB	Structure-borne noise level, dB
Hard mounts	83.7	86
Soft mounts	83.7	73

The structure-borne noise is seen to be considerably greater with the hard mounts, as would be expected.

Transfer Function Methods

Transfer function methods for source-path identification consist of three steps. First the transfer function between the cabin noise and the source of interest is obtained. Measurements usually are done in a nonoperational environment where no other sources are present and input and cabin noise can be accurately measured. Theoretical methods may also be used (refs. 99 and 110). The second step is to measure the source noise in the operational flight condition. Finally, the product of the transfer function and the flight input noise gives an estimate of the interior noise in flight due to the source of interest.

The structure-borne noise measurements described in the previous section may be considered as an example. The factor k in equation (28) that multiplies mount acceleration to give structure-borne cabin noise is the transfer function for the engine vibration source. The simultaneous equations obtained by using the ground-measured data for hard and soft mounts can be solved for the transfer function k (as well as the airborne component). The use of flight-measured mount accelerations along with k would then yield the estimate of cabin noise in flight due to engine vibration sources.

Radiation Efficiency

Another method developed for separating airborne and structure-borne noise is based on their differing radiation characteristics and relies on the ability to measure radiated intensity (ref. 128). In certain frequency ranges, structure-borne noise and airborne noise have different associated radiation efficiencies because they generate differing types of structural vibration. The first step in the method therefore is to measure the radiation efficiencies, σ_a and σ_s, defined as

$$\sigma_a = \frac{|\mathbf{I}_a|}{\rho c < v_a^2 >} \tag{29}$$

for airborne noise and

$$\sigma_s = \frac{|\mathbf{I}_s|}{\rho c < v_s^2 >} \tag{30}$$

for structure-borne noise. As indicated in figure 48, the radiation efficiency of a skin panel or window is measured with an intensity probe to determine average radiated intensity $|\mathbf{I}|$ and an array of accelerometers to determine mean-square panel velocity $< v^2 >$. Airborne radiation efficiency σ_a is measured with only the speaker in operation, and structure-borne radiation efficiency is measured with only the shaker in operation. When both sources are in operation, the total panel velocity $< v^2 >$ and radiated intensity $|\mathbf{I}|$ are measured and the components of radiated power P are determined using the relations

$$P_a = \rho c A \sigma_a \frac{\sigma_s < v^2 > - |\mathbf{I}|/\rho c}{\sigma_s - \sigma_a} \tag{31}$$

for airborne power P_a and

$$P_s = \rho c A \sigma_s \frac{\sigma_a < v^2 > - |\mathbf{I}|/\rho c}{\sigma_a - \sigma_s} \tag{32}$$

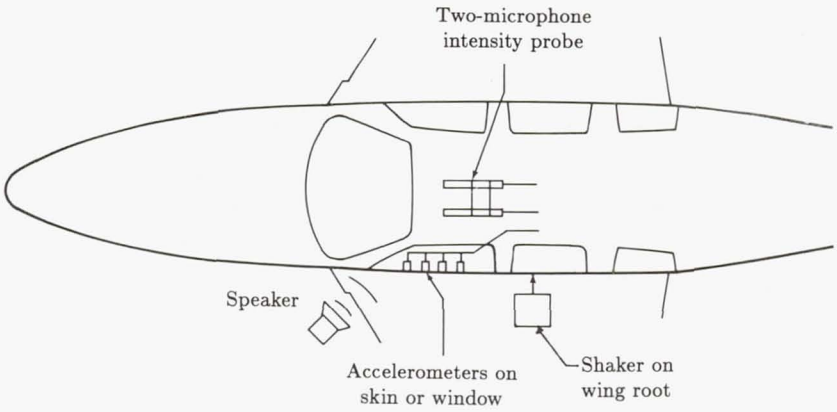

Figure 48. Setup for separating airborne and structure-borne noise using radiation efficiency method (ref. 128).

for structure-borne power P_s, where A is panel area, and certain simplifying assumptions are valid (ref. 128).

The method has been investigated using a number of aircraft panels in a transmission loss setup and using an aircraft fuselage with laboratory sources, as indicated in figure 48. Both coherent and incoherent sources were used. In general the method successfully separated airborne and structure-borne components and determined the proportions of radiated acoustic power. Limitations of the method were identified as (1) a requirement that the radiation efficiencies σ_a and σ_s differ, (2) some unexplained overestimation of the airborne contribution at some frequencies, (3) possible difficulties in determining the separate radiation efficiencies σ_a and σ_s for complex aircraft sources in flight, and (4) a restriction to low frequencies because, above the coincidence frequency of the panel, σ_a and σ_s are expected to be equal. This low-frequency limitation may not be serious because in many aircraft configurations the coincidence frequency can be expected to be well above the frequency of important noise sources. Several significant advantages of the method were also identified. No changes in the aircraft structure or operation are required, in contrast to the system modification methods. The studies indicate that the method is quick and inexpensive and that it works for a variety of stiffened-skin structures. The method was successful when the acoustic and vibrational sources were fully coherent, in contrast to the previously discussed correlation methods, which may not be able to separate contributions from several highly coherent sources. Finally, there are no limitations in principle to the use of this method in flight.

Reciprocity

Application of reciprocity principles to aircraft cabin noise transmission has been explored with the objective of identifying noise sources and transmission paths (ref. 129). The reciprocity principle envisions two configurations of the aircraft, as illustrated in figure 49. The first configuration represents the operational situation for which results are sought. In figure 49(a) the cabin noise due to external sources, represented as speakers, is the information desired. In the second configuration,

referred to here as the "reciprocal configuration" (fig. 49(b)), the positions of speakers and microphones are interchanged, and the exterior noise due to a speaker in the cabin is measured. The principle of reciprocity states that the transfer functions obtained in the two configurations are equal. In mathematical terms,

$$(\mathrm{SPL}_{\mathrm{in}} - Q_{\mathrm{out}})_a = (\mathrm{SPL}_{\mathrm{out}} - Q_{\mathrm{in}})_b \tag{33}$$

where Q is the volume-acceleration level of the speaker output and subscripts in and out indicate measurements inside and outside. The subscripts a and b refer to configurations shown in figure 49. Similar reciprocal relations have been developed for the cabin noise due to a mechanical excitation on the exterior of the fuselage (ref. 129). The advantage of using the reciprocal configuration is that the measurements may be more convenient or more feasible to make. For example, the configuration of figure 49(b) may be required so as to limit the noise levels radiated to nearby test activities. In the case of mechanical forces, a typical engine compartment does not have room for bulky shakers, but accelerometers can usually fit in.

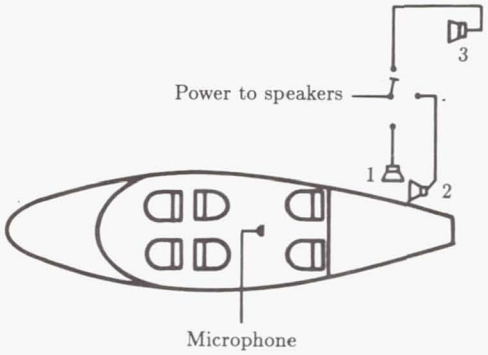

(a) Operating configuration.

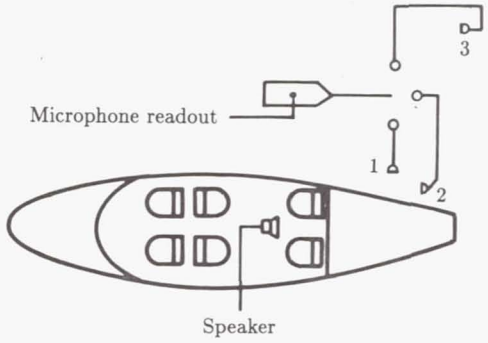

(b) Reciprocal configuration.

Figure 49. System configurations for reciprocity measurements (ref. 129).

Investigations completed using a light aircraft fuselage and special omnidirectional speakers in laboratory tests (ref. 129) have verified the validity of reciprocal transfer functions when applied to the complex structure, damping treatments, sound-absorbing material, and cabin furnishings of the aircraft interior. These results suggest that the assumptions of reciprocity, such as the requirement that the system be linear and time invariant, are satisfied for the fuselage. These results were valid for both single inputs of mechanical or acoustic type and multiple correlated mechanical inputs acting simultaneously.

Theoretical Methods

Some theoretical methods for interior noise prediction are formulated in a manner that provides information on transmission path sensitivity (refs. 45, 79, and 130). As an example, figure 50 illustrates interior noise prediction for an aircraft fuselage. In this method the fuselage sidewall is divided into a number of units, each consisting of one to three skin panels and up to two internal stiffeners. The horizontal edges are simply supported and the vertical edges of each panel unit are supported by flexible stiffeners. The cabin noise is calculated separately for each panel unit, and the contributions from all panel units are added to obtain the total interior noise. As shown in the figure, the noise transmitted through the different panel units varies considerably in the baseline configuration. The addition of damping tape to the skin panels reduces the noise transmitted through all panel units except number 9, so that with damping tape the contributions of all units are more nearly equal. Such information could be useful in identifying which sidewall areas most need additional treatment or in determining the sensitivity of transmitted noise to the addition of various types of treatment to different sidewall regions.

Noise Control Application

General Approach

Interior noise levels can be reduced by noise control at the source or by attenuation during transmission. In principle, noise control at the source is the most desirable approach, but it may be extremely difficult or expensive unless the techniques are incorporated in the basic design of the airplane. Consequently, noise attenuation in the transmission path is also required in most aircraft.

The methods used to reduce noise generation depend on the nature of the source. For propeller noise, the methods could include increasing the clearance between the propeller tip and the fuselage, lowering the propeller rotational speed, locating the propeller plane away from the occupied region of the fuselage, synchrophasing the propellers, and changing the direction of rotation of the propeller (ref. 131). The first three methods involve the basic design of the airplane, although there may be some benefit in retrofitting different engines and propellers. Propeller synchronization involves accurate control of the propeller speed in multiengine configurations. In turbojet and turbofan aircraft, structure-borne noise can be controlled by reducing the out-of-balance forces generated by the rotating components; and airborne noise can be controlled by locating jet exhausts well away from the fuselage. Turbulent boundary layer pressure fluctuations can be reduced by avoiding flow separation,

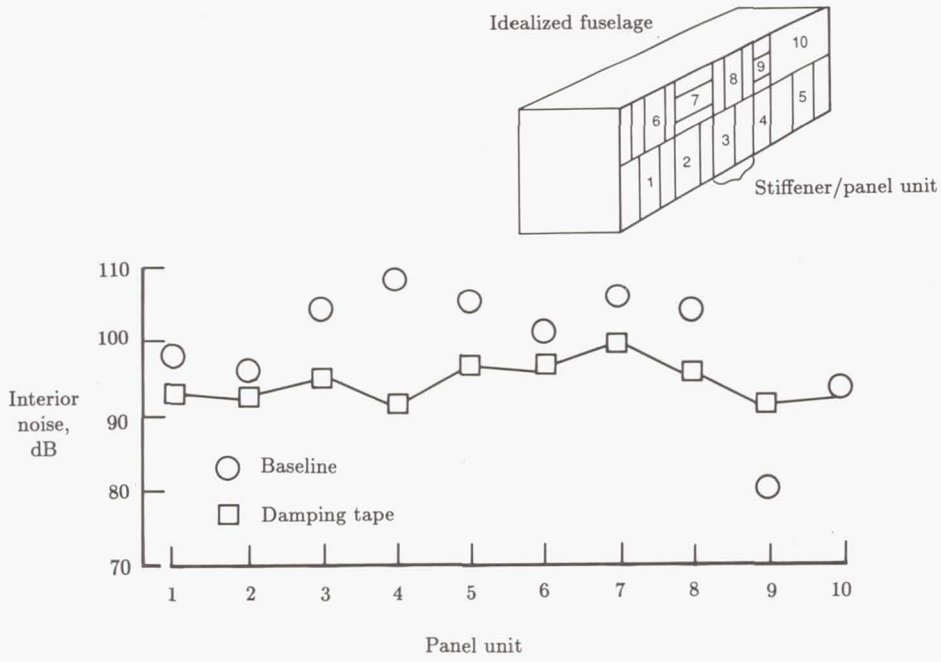

Figure 50. Interior noise contributions of panel areas of a fuselage as determined by theoretical analysis (ref. 79).

but the main reductions can be achieved only by removing the turbulent boundary layer itself, a solution that has not yet been accomplished. With the exception of propeller synchronization and direction of rotation, reduction at source is not considered further in this chapter.

Descriptions of noise control methods applied to aircraft of various configurations (refs. 28, 61, 100, and 132–141) show that the most common approach is to utilize cabin sidewall treatments that reduce interior sound pressure levels to the desired values. A typical sidewall treatment, from a large modern jet aircraft, is shown in cross section in figure 51. The sidewall is a multielement system with fiberglass blankets, impervious septa, an interior decorative trim, and multipane windows. Damping materials are applied to the fuselage skin. This type of treatment reduces both airborne (transmission through the fuselage skin) and structure-borne (radiated by the skin) noise, although the effectiveness may differ for the two components. Dynamic vibration absorbers are used in several cases to reduce structure-borne noise from turbofan engines (ref. 28) or airborne propeller noise (refs. 136 and 142). Various noise control methods are reviewed in the following sections.

Multielement Sidewall

The sidewall treatment has to satisfy both thermal and acoustic requirements, although adequate thermal insulation can usually be achieved with less treatment than is needed for noise control. In addition, the acoustical treatment has to have minimum weight and volume, should not readily absorb moisture, should be resistant

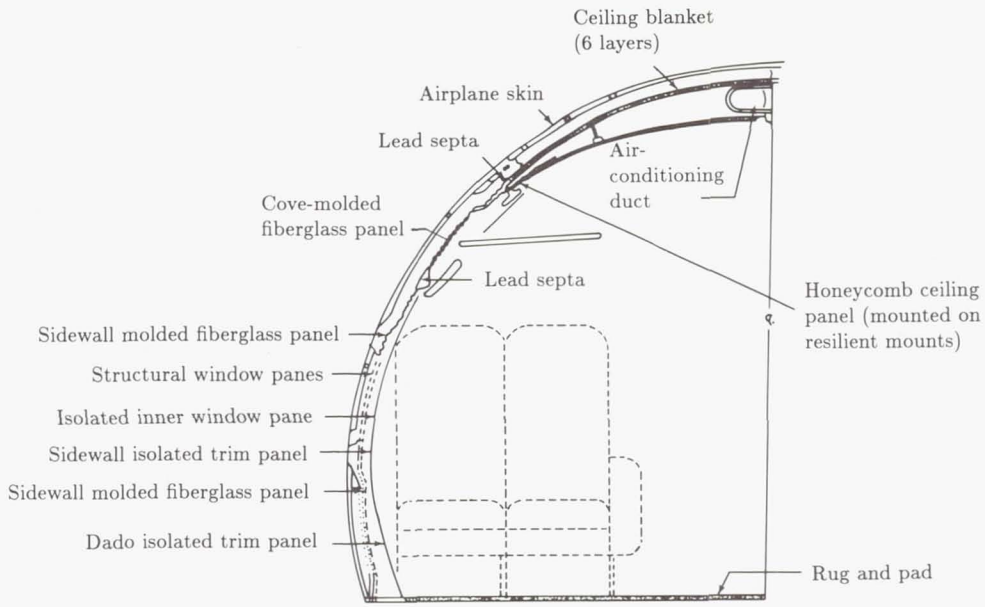

Figure 51. Typical sidewall cross section of a large passenger transport aircraft. (From ref. 133. Copyright AIAA; reprinted with permission.)

to flame, and should not give off smoke or toxic fumes. Laboratory measurements have shown that fiberglass blankets satisfy these criteria and are more effective than other materials in terms of noise reduction per unit weight. The fiberglass is available in various densities, such as 6.4, 8, and 24 kg/m^3, and the lowest density material is preferred unless there is a very stringent space limitation. Typically, the fibers have diameters of about 0.00013 cm and are bonded together by a resin material that constitutes about 15 percent of the total weight of the blanket. The fiberglass material is enclosed in very thin impervious sheets to protect it from moisture.

Typical examples of multielement sidewalls in large commercial airplanes are shown in figure 52, which compares sections through sidewall treatments for standard-body (3.6-m-diam) and wide-body (5.8-m-diam) (ref. 135) airplanes. The standard-body treatment consists of a fiberglass blanket filling the depth of the ring frame stiffener and a relatively thin blanket between the cap of the ring frame and the interior trim panel. Attachment of the interior panel to the frame causes compression of the thin blanket and thereby degrades the acoustic insulation of the sidewall. The wide-body treatment uses the same type of low-density glass fiber but provides a thicker blanket between the frame and the interior trim panel and an air gap between the two blankets.

The acoustic design of the sidewall treatments has undergone extensive experimental and analytical study over a number of years to optimize the configuration (e.g., refs. 36, 38, 57–60, 62, 63, 92, 95, 132, and 143–146). The studies have investigated not only the use of the fiberglass material, but also the insertion of heavy impervious septa. This is particularly true with respect to the advanced turboprop airplane (refs. 63 and 92) where greater transmission losses are required at low frequencies than are provided by current production sidewall treatments.

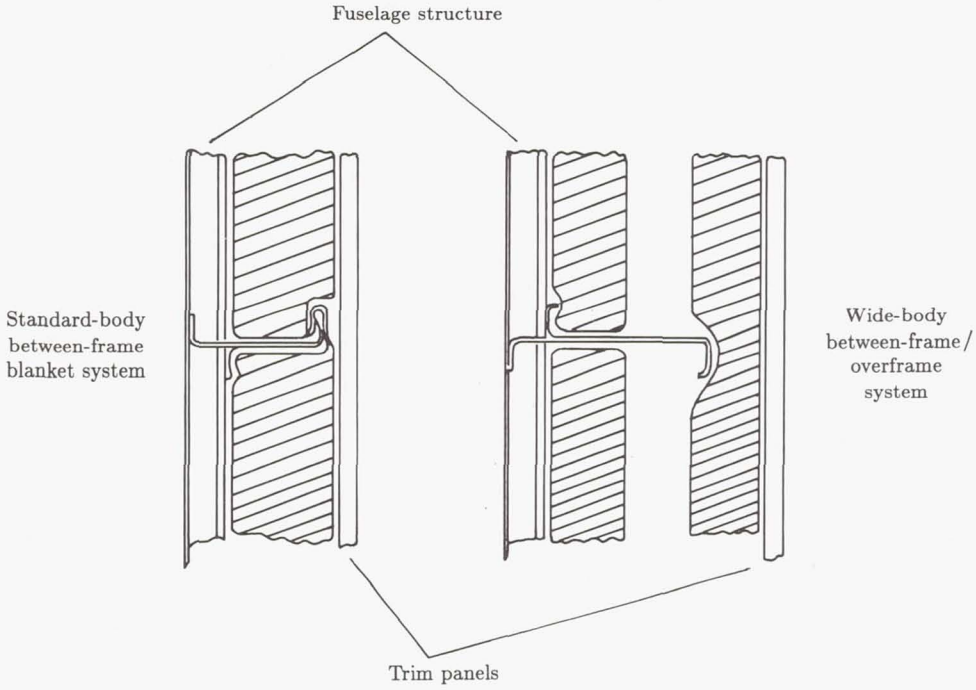

Figure 52. Sections through sidewall treatments used on large passenger aircraft. (From ref. 135.)

Transmission loss characteristics of an idealized double-wall treatment are shown in figure 53, which presents predicted increases in transmission loss relative to the untreated fuselage (ref. 63). Transmission loss spectra are plotted for cases with and without porous material between the two walls. When there is no material in the air gap, the spectra clearly show the predicted decrease in transmission loss at the double-wall (mass-spring-mass) and air gap acoustic resonance frequencies. It is possible that, at some frequencies in the neighborhood of the resonances, the transmission loss for the double-wall system can be less than the original single panel. As the surface mass density m_2 of the inner trim panel increases, the frequency of the double-wall resonance f_d decreases but the air gap acoustic resonance frequency is unchanged. When porous materials are introduced, the effects of the double-wall and acoustic resonances are reduced significantly. Test data show the presence of the double-wall resonance, but the magnitude of the effect can vary considerably. The results in figure 53 refer to a sidewall that is 13 cm thick, thicker than that usually found in a general aviation airplane but typical of larger commercial aircraft. Increasing the distance between the sidewall panels reduces both the mass-spring-mass and the air gap resonance frequencies, a factor that can be important when designing for low-frequency noise control.

The analysis assumes that the trim panel is limp, since all the components of the multielement sidewall are assumed to be locally reacting. In practice, trim panels are usually stiff, such as 2.08-mm-thick aluminum panels, 6.35-mm-thick honeycomb, or 2.03-mm-thick crushed-core honeycomb (ref. 61). Thus, the assumption of limpness

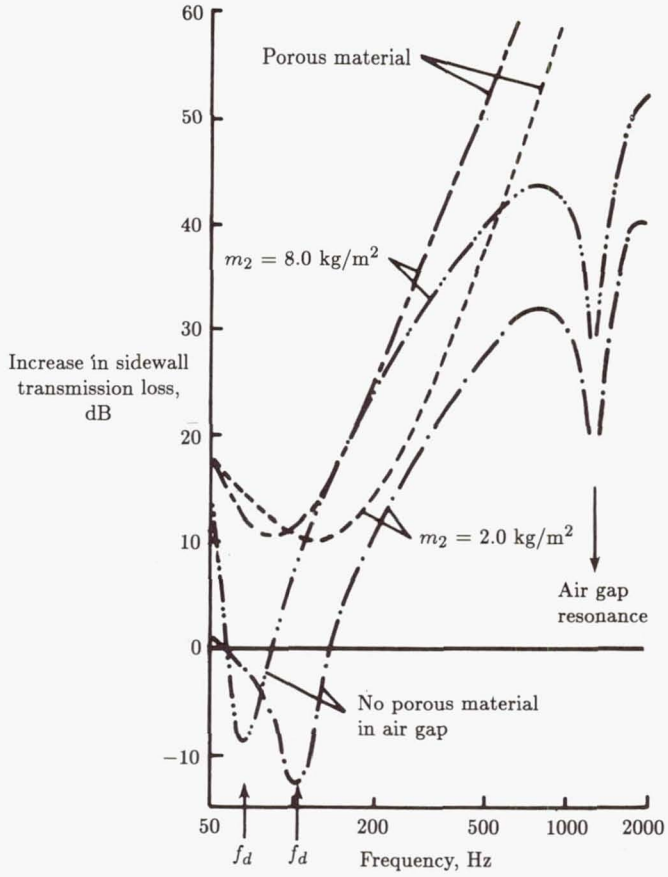

Figure 53. Predicted increase in sidewall transmission loss due to addition of a trim panel or fiberglass treatment. (From ref. 63.)

is not necessarily valid. However, an approximation to a limp panel can be achieved by addition of damping material to the trim panel (ref. 134). Alternatively, a mass-loaded septum, such as vinyl impregnated with lead or iron oxide, can be inserted between the fiberglass blankets and trim panel (refs. 61 and 133).

Mass-loaded septa can also be inserted between the various layers of fiberglass blankets in an attempt to optimize transmission loss and weight (refs. 50 and 144). However, when using multiple layers it is necessary to avoid multiple mass-spring-mass resonances that can degrade the transmission loss in the frequency range of concern.

Experimental and analytical studies of the transmission loss provided by multi-element treatments assume that the interior trim panel is mounted so that no structure-borne path for noise transmission exists. Any such path would degrade the acoustic insulation provided by the treatment. In practice, the conventional trim panel has to be mounted to the fuselage structure in such a manner that the attachment will not collapse under shock loading yet will be soft enough to provide insulation at low frequencies. These opposing requirements could be satisfied by

using mounts with snubbers, provided that the snubbers are not activated by the normal static loads. The attachment of the trim panel to the fuselage structure usually occurs at fuselage ring frames; figure 54 shows an example of a trim panel vibration isolation mount used to attach a trim panel to the cap of a ring frame (ref. 61). The vibration and acoustic performance of typical trim mounts is illustrated in figures 55 and 56. In one case, the vibration reduction provided by two mounts was measured in the laboratory when each mount was subjected to a static load of 0.45 kg (ref. 29). Figure 55 shows that at low frequencies neither mount provides isolation (there may even be an increase in the transmitted vibration at the resonance frequency of the mount), and at high frequencies the stiffer the mount, the lower the vibration isolation. Figure 56 illustrates acoustic performance in terms of the noise reduction through a double-wall system with the panels connected by mounts of various stiffnesses (ref. 61). Stiff mounts provide little improvement over a rigid connection, whereas soft mounts can provide a good simulation of the completely uncoupled system, at least for high frequencies.

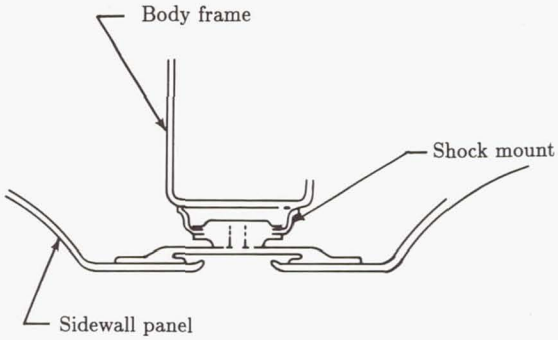

Figure 54. Vibration isolation mount for sidewall trim panel in large passenger aircraft. (From ref. 61. Copyright 1981, SAE, Inc.; reprinted with permission.)

Since there is a practical limit to the vibration isolation that trim panel mounts can provide at low frequencies, it may sometimes be necessary to consider the installation of an interior trim panel that is a self-supporting structure with a minimal number of attachment points to the fuselage (ref. 134). Examples of possible applications are cases where significant noise reductions are required at low frequencies (50 to 200 Hz) associated with propeller noise or structure-borne noise from engine out-of-balance forces. Finally, any discussion of multielement sidewall treatments should include mention of items such as windows and doors that can be weak links in a noise control approach. Windows are typically multipane systems so that an adequate transmission loss can be achieved, the innermost pane being part of the trim panel. Doors have low transmission loss because the presence of opening and closing mechanisms limits the space available for acoustic treatment and acoustic leaks can occur around the door seals. One solution is to provide sound-absorbing panels in entry areas (refs. 61 and 133).

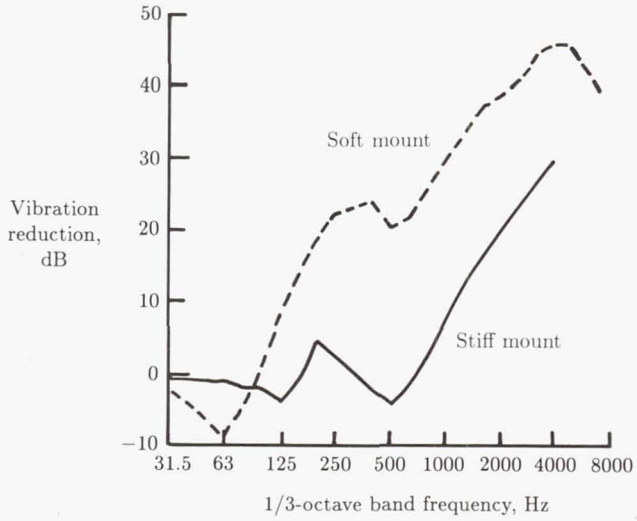

Figure 55. Vibration attenuation provided by two trim panel mounts. Static load of 0.45 kg. (From ref. 29. Copyright 1983, SAE, Inc.; reprinted with permission.)

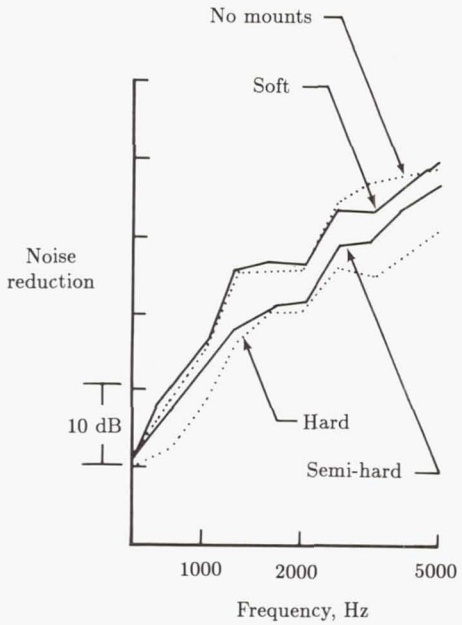

Figure 56. Noise reduction across a double-wall sidewall with several mount configurations. (From ref. 61. Copyright 1981, SAE, Inc.; reprinted with permission.)

Additions to Structure

In addition to the use of sidewall treatments, the noise transmission and acoustic radiation characteristics of the fuselage structure can be modified by the addition of mass, damping, or stiffness. Of the three alternatives, damping is the method most commonly used in production aircraft; mass and stiffness changes have been investigated mainly on an experimental basis.

The addition of damping material to the skin can significantly reduce cabin noise levels if the sound transmission or radiation is controlled by resonant response of the structure and the existing damping is not high. Below the fundamental frequency of the skin panel the response of an individual panel is stiffness controlled so that increasing the damping of the panel has a negligible effect on sound transmission.[12] Also, damping is not very effective for mass-law-controlled transmission except near the critical frequency, which is often above the frequency range of interest for airplane interior noise.

Damping material has been used in production turbojet (refs. 134, 140, and 141) and turboprop (ref. 136) aircraft, and experimental installations can be found in a variety of airplanes and helicopters (refs. 147–150). In many examples the damping material is aluminum-backed tape, the aluminum foil acting as a constraining layer to generate the damping through shear strain within the viscoelastic material, which also provides the adhesive. In some cases the tape includes a thin layer of foam between the viscoelastic material and the aluminum foil. The foam displaces the foil away from the viscoelastic material and thereby augments its constraining action. In other examples the damping material is unconstrained tiles. The damping material is applied only to the skin in all the preceding examples, usually covering only part (roughly 80 percent) of the skin area.

Measurements on a large, modern jet aircraft (ref. 148) showed that the addition of damping tape reduced interior sound pressure levels by 3 to 8 dB at frequencies above about 800 Hz (fig. 57). It was estimated that the addition of the damping material would increase the total damping factor of the panels from about 0.01 to about 0.05. In this application, the sound pressure levels were associated with external turbulent boundary layer excitation, and the skin structural response was resonant. The presence of the damping tape would also have some effect on the stiffness-controlled response because of the weight of the tape; it was estimated that the frequency of the fundamental mode of the panel was reduced from 625 Hz to 595 Hz. The effectiveness of damping tape could, perhaps, be extended to lower frequencies by application to stringers and ring frames (ref. 84) as well as to the skin panels. Damping material can also attenuate structure-borne sound, when resonant bending modes dominate radiation (ref. 100). Analysis of a helicopter structure indicated that panel loss factors could be increased from about 0.01 to about 0.07, resulting in noise reduction of approximately 7 dB.

One important parameter affecting the acoustic performance of a given damping material is the damping coefficient at low temperatures; fuselage skin temperatures during cruise conditions can be −29°C (ref. 15) or lower. Many damping materials are most efficient at room temperatures, so that suitable materials must be selected carefully.

[12] This assumes that the panel weight is small compared with average sidewall weight and that damping is increased without adding weight.

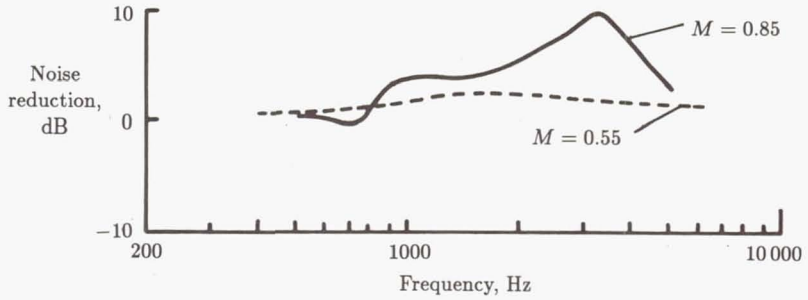

Figure 57. Noise reduction provided by damping tape on fuselage skin. Boundary layer excitation, flight test. (From ref. 149.)

The use of damping material need not be restricted to the fuselage skin and stiffeners. It can be applied to other structures if sound transmission or radiation is dominated by resonant response of those structures. For example, damping material has been applied in a recent installation (ref. 134) to the sidewall trim panel as well as the fuselage skin. Also, additional damping has proven effective in reducing acoustic radiation from gearboxes in helicopters (ref. 149).

Increasing the basic stiffness of a fuselage structure may appear to be an attractive way of decreasing low-frequency sound transmission. However, several factors must be considered. First, the overall low-frequency response of the fuselage structure should be understood, so that the frequency range associated with stiffness response can be determined. Second, if the fuselage is pressurized during flight, the effective stiffness of the structure is already much higher than that of the unpressurized fuselage. Third, increasing the stiffness with only a negligible weight increase lowers the critical frequency. Consequently, the decreased transmission loss associated with coincidence occurs at lower frequencies.

The main application of structural stiffness in noise control has been concerned with the modification of existing structures by the addition of honeycomb material to the skin (refs. 36, 79, 149, and 151). In practice, the honeycomb material can be applied only in relatively small panels, because of the obstructions presented by longitudinal and circumferential stiffeners on the fuselage. Since the honeycomb panel can reduce vibration (and, hence, noise) only when the flexural wavelengths in the fuselage skin are small relative to the planform dimensions of the honeycomb panel, the method is effective only at relatively high frequencies. This is illustrated in figure 58, which contains data from an experimental installation on a pressurized cylindrical fuselage under cruise conditions (ref. 149). At low frequencies, where the dimensions of the honeycomb panel are small relative to the flexural wavelengths, the honeycomb material acts mainly as additional mass and has little or no noise control capability.

In figure 58 the honeycomb panels provide essentially no vibration reduction at frequencies below about 400 Hz. Vibration and noise reductions at lower frequencies were obtained in ground tests of a general aviation airplane (refs. 36 and 151), but in that case the fuselage panels were flat rather than curved and the fuselage was unpressurized during the tests. The panel fundamental frequency was 69 Hz compared with a corresponding frequency of about 400 Hz for the untreated skin panels associated with the data in figure 58. Noise reductions of up to 10 dB were

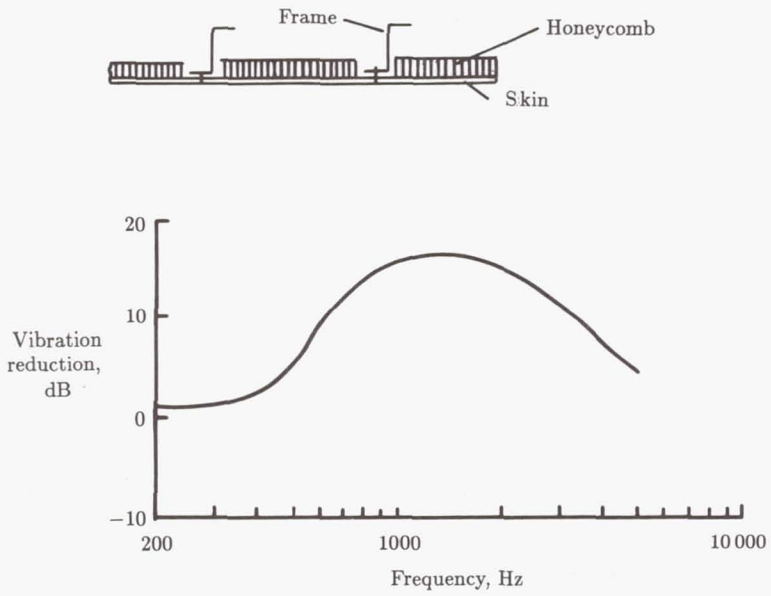

Figure 58. Vibration reduction provided by honeycomb panels attached to skin. Honeycomb thickness = 1.9 cm, Weight = 1.2 kg/m^2. (From ref. 149.)

measured in the frequency range from 100 to 600 Hz during ground tests (refs. 36 and 151), even though it is possible that the data were contaminated by noise transmission through flanking paths (no flight tests were performed).

Dynamic Absorbers

Dynamic vibration absorbers can alter the vibration characteristics of a system, particularly at frequencies in the neighborhood of the resonance frequency of the absorber. However, devices of this type are useful only when the vibration to be controlled is dominated by a single constant frequency. The absorber is tuned to this frequency by adjusting the absorber mass and stiffness until the resonance frequency of the absorber equals the frequency to be attenuated. The vibration of the system at the attachment point of the absorber can then be reduced significantly, since the absorber provides a force that acts against the vibration of the system.

Dynamic absorbers have been used to attenuate structure-borne and airborne sound associated with engines operating at constant speed during cruise conditions. For a jet airplane with rear-mounted engines (ref. 28), dynamic absorbers were attached to the fuselage structure close to the turbofan engine mounts to reduce structure-borne sound transmission. Two sets of absorbers were tuned to the rotational frequencies of the low- and high-pressure compressors of the turbofan engine, 120 and 180 Hz, respectively. Noise was reduced by 5 to 10 dB in flight tests.

Propeller noise has been controlled in turboprop aircraft by installing dynamic absorbers on the ring frames of the fuselage (refs. 136 and 142) and by attaching absorbers to cabin trim panels (ref. 136). Absorbers were tuned to the fundamental, first harmonic, or second harmonic of the propeller blade-passage frequency. For

a twin-engine aircraft (ref. 136), absorbers tuned to the blade-passage frequency of 88 Hz were attached to the ring frames to reduce noise by about 10 dB for a weight penalty of 30 kg. Also, three sets of absorbers tuned to frequencies of 88, 176, and 264 Hz and attached to the interior trim panels reduced the A-weighted sound level by about 2 dB for a weight penalty of 25 kg.

Vibration Isolators

Vibration isolators are widely used in engine mounting systems to attenuate structure-borne sound associated with engine out-of-balance forces. This is particularly true for reciprocating engines where significant levels of vibration can be transmitted into the fuselage structure, but it is also true for turboprop and turbofan installations. Vibration isolators are constructed from elastomeric material or metal, the choice being influenced to some extent by the thermal conditions to which the mounts will be exposed. Isolators usually have nonlinear characteristics and the system stiffness has to be chosen so that the required vibration reduction is achieved under the normal static load conditions. The static loads are imposed by engine thrust and weight and by aircraft maneuvers; snubbers are provided for extreme load conditions. The operating stiffness range is chosen so that there is adequate attenuation at the frequencies of concern.

Design of vibration isolators involves a large number of factors in addition to the vibration and acoustic transmission characteristics (ref. 152). An engine has several mounts, each having to provide vibration isolation in more than one direction. Furthermore, the overall isolation performance of the mounting system is no better than the performance of the least effective isolator. The vibration isolation of engine mounts has been investigated for a single-engine propeller-driven airplane with reciprocating engine (ref. 153). It was found that isolator stiffness is a strong parameter in controlling noise transmission while isolator damping is a much weaker parameter. Interior noise level was reduced by up to 10 dB by using experimental isolators in laboratory tests.

Acoustic Absorption

Noise control methods are successful only if an adequate amount of acoustic absorption exists within the airplane cabin. The absorption can be provided on the interior surfaces of the cabin—sidewall, bulkheads, and floor—or within the volume by, for example, the seats. If there is little or no absorption, the space-averaged sound pressure levels are high and there are strong spatial variations (ref. 50). However, the benefits of increased absorption soon reach a stage of diminishing returns. For example, increasing absorption coefficient from 0.80 to 0.95 reduces noise, on the average, by less than 1 dB, whereas the same change of 0.15 in coefficient from 0.20 to 0.35 would reduce noise by about 2.5 dB. Thus, it is useful in some cases to add sound-absorbing material only in local areas such as close to the heads of passengers.

The design of a sidewall trim panel is usually dictated by factors other than high acoustic absorption. The trim panels are selected for resistance to mechanical damage and ease of cleaning as well as appearance and acoustic performance. This often results in a surface that has a low acoustic absorption coefficient, except perhaps at low frequencies where there may be some absorption due to membrane action of the panel. However, there are several surface areas that can be designed with acoustic

absorption in mind. These include ceiling panels, bulkheads, closet doors, and areas of the overhead baggage containers. A typical sound-absorbing panel (refs. 61, 133, and 135) consists of a perforated surface that is exposed to the interior of the cabin, a flow-resistive screen or cloth, a honeycomb core, and an impervious backing sheet (fig. 59). The honeycomb core can be in different thicknesses depending on the space available or the frequency range of interest. The thicker the core, the greater the absorption at low frequencies, but there may be an associated reduction in absorption at higher frequencies. The absorption at high frequencies can be increased by placing low-density fiberglass in the honeycomb core.

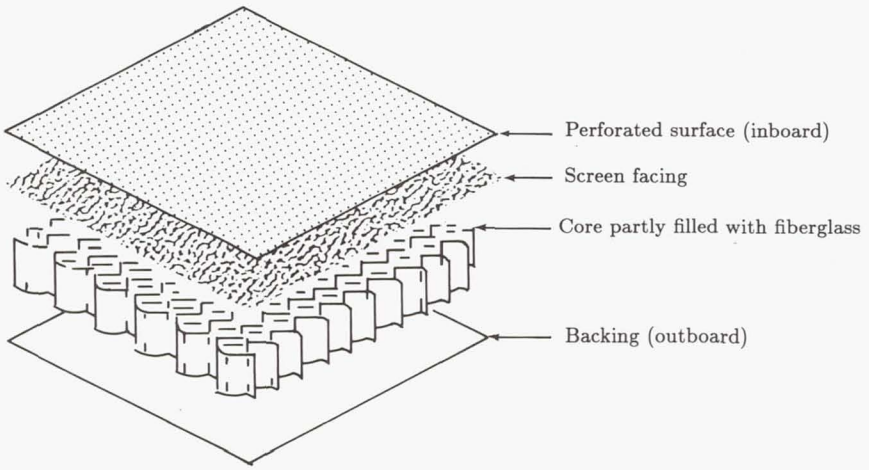

Figure 59. Components of sound-absorbing panel for airplane interior. (From ref. 135.)

In most designs the contributions of transmission loss and absorption have to be considered together and optimized to achieve the maximum noise reduction within the restrictions of space and weight. Sometimes an impervious trim with relatively low absorption may be more desirable than a perforated surface with high absorption but relatively low transmission loss (ref. 132).

Exploratory Concepts

Various methods or designs for interior noise control have been studied on an exploratory basis but not applied to production aircraft. The main objective of the studies has been to further reduce noise transmission through the sidewall without additional weight penalties, particular emphasis being given to the low-frequency regime associated with propeller noise. In general, the proposed methods have been restricted to laboratory measurements or analytical studies, but some have been used in flight tests. The methods include the basic design of the fuselage structure, nonstructural additions to the fuselage skin panels, and new concepts for the sidewall treatment.

Proposed modifications to the fuselage structure include the design of integrally stiffened panels with stiffeners forming a triangular array similar to the isotropic

panels currently used in space vehicle structures (ref. 154). Other approaches involve fuselage structures constructed from honeycomb panels, the use of closely spaced stiffeners, or the use of stiffeners made from composite materials (ref. 155). Also, it has been proposed that fuselage structures can be designed in such a manner that certain frequencies are filtered out during acoustic transmission (ref. 84). This approach is based on analytical studies which show that periodic structures have frequency bands where there is no transmission of flexural waves.

Novel additions to the fuselage skin panels are the bonding of rubber wedges to the panel boundaries (ref. 148) or the use of waveguide absorbers to provide broadband damping (ref. 156). In the first case the wedges were installed in a large jet airplane in a region of the fuselage where the dominant excitation is the external turbulent boundary layer. Multiple blocking masses have been investigated as an alternative to a single mass in the control of structure-borne sound in helicopters (ref. 157). This approach was not a realistic concept for panel-stringer configurations but may have application in parts of the structure, such as the main frames, where the modal density is lower. Sidewall treatments containing resonators located between the fuselage skin and the trim panel have been tested in laboratory conditions (ref. 91) and found to have promise for improved noise transmission with minimum increase in weight.

Active noise control is an electronic means of reducing noise by the cancellation, or partial cancellation, of the noise of interest. The method has been demonstrated successfully in duct acoustics and in certain other environments with a relatively compact source. In potential aircraft applications, two general approaches are being pursued. One method provides local control for each occupant of the cabin by providing headsets for the flight crew of a helicopter (ref. 158) or by providing loudspeakers in the headrest of the seat of each occupant (ref. 159). The second method is directed toward reduction of the general noise levels in the cabin by the judicious placement of noise-cancelling sources (refs. 160 and 161).

References

1. Beranek, Leo L., ed.: *Noise and Vibration Control.* McGraw-Hill Book Co., Inc., c.1971.
2. Harris, Cyril M.; and Crede, Charles E., eds.: *Shock and Vibration Handbook,* Second ed. McGraw-Hill Book Co., c.1976.
3. Leatherwood, Jack D.; Clevenson, Sherman A.; and Hollenbaugh, Daniel D.: *Evaluation of Ride Quality Prediction Methods for Helicopter Interior Noise and Vibration Environments.* NASA TP-2261, AVSCOM TR 84-D-2, 1984.
4. Wilby, John F.: Propeller Aircraft Interior Noise. *Propeller Performance and Noise, Volume 2,* VKI-LS-1982-08-VOL-2, Von Karman Inst. for Fluid Dynamics, 1982.
5. Mixson, John S.; and Powell, Clemans A.: Review of Recent Research on Interior Noise of Propeller Aircraft. *J. Aircr.,* vol. 22, no. 11, Nov. 1985, pp. 931–949.
6. Bendat, Julius S.; and Piersol, Allan G.: *Random Data: Analysis and Measurement Procedures.* John Wiley & Sons, Inc., c.1971.
7. Ungar, E. E.; Wilby, J. F.; Bliss, D. B.; Pinkel, B.; and Galaitsis, A.: *A Guide for Estimation of Aeroacoustic Loads on Flight Vehicle Surfaces—Volume 1.* AFFDL-TR-76-91-Vol. 1, U.S. Air Force, Feb. 1977. (Available from DTIC as AD A041 198.)
8. Wilby, E. G.; and Wilby, J. F.: *Application of Stiffened Cylinder Analysis to ATP Interior Noise Studies.* NASA CR-172384, 1984.

9. Bhat, W. V.: Flight Test Measurement of Exterior Turbulent Boundary Layer Pressure Fluctuations on Boeing Model 737 Airplane. *J. Sound & Vibration,* vol. 14, no. 4, Feb. 22, 1971, pp. 439–457.
10. Wilby, J. F.; and Gloyna, F. L.: Vibration Measurements of an Airplane Fuselage Structure: I. Turbulent Boundary Layer Excitation. *J. Sound & Vibration,* vol. 23, no. 4, Aug. 22, 1972, pp. 443–466.
11. Wilby, J. F.; and Piersol, A. G.: Analytical Prediction of Aerospace Vehicle Vibration Environments. ASME Paper 81-DET-29, Sept. 1981.
12. Hubbard, Harvey H.; and Houbolt, John C.: Vibration Induced by Acoustic Waves. *Engineering Design and Environmental Conditions, Volume 3* of *Shock and Vibration Handbook,* Cyril M. Harris and Charles E. Crede, eds., McGraw-Hill Book Co., Inc., c.1961, pp. 48-1–48-57.
13. Farassat, F.; and Succi, G. P.: A Review of Propeller Discrete Frequency Noise Prediction Technology With Emphasis on Two Current Methods for Time Domain Calculations. *J. Sound & Vibration,* vol. 71, no. 3, Aug. 8, 1980, pp. 399–419.
14. Hanson, D. B.; and Magliozzi, B.: Propagation of Propeller Tone Noise Through a Fuselage Boundary Layer. AIAA-84-0248, Jan. 1984.
15. Wilby, J. F.; McDaniel, C. D.; and Wilby, E. G.: *In-Flight Acoustic Measurements on a Light Twin-Engined Turboprop Airplane.* NASA CR-178004, 1985.
16. Zorumski, William E.: *Propeller Noise Prediction.* NASA TM-85636, 1983.
17. Goldsmith, I. M.: *A Study To Define the Research and Technology Requirements for Advanced Turbo/Propfan Transport Aircraft.* NASA CR-166138, 1981.
18. Šulc, J.; Hofr, J.; and Benda, L.: Exterior Noise on the Fuselage of Light Propeller Driven Aircraft in Flight. *J. Sound & Vibration,* vol. 84, no. 1, Sept. 8, 1982, pp. 105–120.
19. Magliozzi, B.: Acoustic Pressures on a Prop-Fan Aircraft Fuselage Surface. AIAA-80-1002, June 1980.
20. Barton, C. Kearney; and Mixson, John S.: Characteristics of Propeller Noise on an Aircraft Fuselage. *J. Aircr.,* vol. 18, no. 3, Mar. 1981, pp. 200–205.
21. Mixson, John S.; Barton, C. Kearney; and Vaicaitis, Rimas: Investigation of Interior Noise in a Twin-Engine Light Aircraft. *J. Aircr.,* vol. 15, no. 4, Apr. 1978, pp. 227–233.
22. Fuller, C. R.: *Analytical Investigation of Synchrophasing as a Means of Reducing Aircraft Interior Noise.* NASA CR-3823, 1984.
23. Johnston, J. F.; Donham, R. E.; and Guinn, W. A.: Propeller Signatures and Their Use. AIAA-80-1035, June 1980.
24. Willis, Conrad M.; Mayes, William H.; and Daniels, Edward F.: *Effects of Propeller Rotation Direction on Airplane Interior Noise Levels.* NASA TP-2444, 1985.
25. Wilby, J. F.; and Wilby, E. G.: *Analysis of In-Flight Acoustic Data for a Twin-Engined Turboprop Airplane.* NASA CR-178389, 1988.
26. Wilby, J. F.; and Gloyna, F. L.: Vibration Measurements of an Airplane Fuselage Structure: II. Jet Noise Excitation. *J. Sound & Vibration,* vol. 23, no. 4, Aug. 22, 1972, pp. 467–486.
27. Schoenster, James A.; Willis, Conrad M.; Schroeder, James C.; and Mixson, John S.: Acoustic-Loads Research for Powered-Lift Configurations. *Powered-Lift Aerodynamics and Acoustics,* NASA SP-406, 1976, pp. 429–443.
28. Van Dyke, J. D., Jr.; Schendel, J. W.; Gunderson, C. O.; and Ballard, M. R.: Cabin Noise Reduction in the DC-9. AIAA Paper No. 67-401, June 1967.
29. Wilby, John F.: Interior Noise of General Aviation Aircraft. *SAE Trans.,* sect. 3, vol. 91, 1982, pp. 3133–3144. (Available as SAE Paper 820961.)
30. Miller, Brent A.; Dittmar, James H.; and Jeracki, Robert J.: *The Propeller Tip Vortex—A Possible Contributor to Aircraft Cabin Noise.* NASA TM-81768, 1981.
31. Howlett, James T.; Clevenson, Sherman A.; Rupf, John A.; and Snyder, William J.: *Interior Noise Reduction in a Large Civil Helicopter.* NASA TN D-8477, 1977.

32. Mixson, John S.; O'Neal, Robert L.; and Grosveld, Ferdinand W.: *Investigation of Fuselage Acoustic Treatment for a Twin-Engine Turboprop Aircraft in Flight and Laboratory Tests.* NASA TM-85722, 1984.
33. Standard Method for Laboratory Measurement of Airborne Sound Transmission Loss of Building Partitions. ASTM Designation: E 90-85. *Volume 04.06 of 1986 Annual Book of ASTM Standards,* c.1986, pp. 764–775.
34. Piersol, A. G.; Wilby, E. G.; and Wilby, J. F.: *Evaluation of Aero Commander Propeller Acoustic Data: Taxi Operations.* NASA CR-159124, 1979.
35. Mixson, John S.; and Roussos, Louis A.: *Consideration of Some Factors Affecting Low-Frequency Fuselage Noise Transmission for Propeller Aircraft.* NASA TP-2552, 1986.
36. Barton, C. K.; and Mixson, J. S.: Noise Transmission and Control for a Light Twin-Engine Aircraft. *J. Aircr.,* vol. 18, no. 7, July 1981, pp. 570–575.
37. Heitman, Karen E.; and Mixson, John S.: Laboratory Study of the Effects of Sidewall Treatment, Source Directivity and Temperature on the Interior Noise of a Light Aircraft Fuselage. AIAA-86-0390, Jan. 1986.
38. Mixson, John S.; Roussos, Louis A.; Barton, C. Kearney; Vaicaitis, Rimas; and Slazak, Mario: Laboratory Study of Add-On Treatments for Interior Noise Control in Light Aircraft. *J. Aircr.,* vol. 20, no. 6, June 1983, pp. 516–522.
39. Dowell, E. H.; Gorman, G. F., III; and Smith, D. A.: Acoustoelasticity: General Theory, Acoustic Natural Modes and Forced Response to Sinusoidal Excitation, Including Comparisons With Experiment. *J. Sound & Vibration,* vol. 52, no. 4, June 22, 1977, pp. 519–542.
40. Dowell, E. H.: *Aeroelasticity of Plates and Shells.* Noordhoff International Publ. (Leyden, Netherlands), c.1975.
41. Dowell, E. H.: Reverberation Time, Absorption, and Impedance. *J. Acoust. Soc. America,* vol. 64, no. 1, July 1978, pp. 181–191.
42. Vaicaitis, R.: Noise Transmission Into a Light Aircraft. *J. Aircr.,* vol. 17, no. 2, Feb. 1980, pp. 81–86.
43. Van Nieuwland, J. M.; and Weber, C.: Eigenmodes in Nonrectangular Reverberation Rooms. *Noise Control Eng.,* vol. 13, no. 3, Nov./Dec. 1979, pp. 112–121.
44. Wolf, J. A., Jr.; and Nefske, D. J.: NASTRAN Modeling and Analysis of Rigid and Flexible Walled Acoustic Cavities. *NASTRAN: User's Experiences,* NASA TM X-3278, 1975, pp. 615–631.
45. Unruh, J. F.: Finite Element Subvolume Technique for Structural-Borne Interior Noise Prediction. *J. Aircr.,* vol. 17, no. 6, June 1980, pp. 434–441.
46. Unruh, J. F.: Structure-Borne Noise Prediction for a Single-Engine General Aviation Aircraft. *J. Aircr.,* vol. 18, no. 8, Aug. 1981, pp. 687–694.
47. Wilby, John F.; and Pope, Larry D.: Prediction of the Acoustic Environment in the Space Shuttle Payload Bay. *J. Spacecr. & Rockets,* vol. 17, no. 3, May–June 1980, pp. 232–239.
48. Pope, L. D.; Wilby, E. G.; and Wilby, J. F.: *Propeller Aircraft Interior Noise Model.* NASA CR-3813, 1984.
49. Barton, C. Kearney; and Daniels, Edward F.: *Noise Transmission Through Flat Rectangular Panels Into a Closed Cavity.* NASA TP-1321, 1978.
50. Wilby, John F.; O'Neal, Robert L.; and Mixson, John S.: Flight Investigation of Cabin Noise Control Treatments for a Light Turboprop Aircraft. *SAE Trans.,* sect. 4, vol. 94, 1985, pp. 4.614–4.624. (Available as SAE Paper 850876.)
51. Beranek, Leo L.; Nichols, Rudolph H., Jr.; Rudmose, H. Wayne; Sleeper, Harvey P., Jr.; Wallace, Robert L., Jr.; and Ericson, Harold L.: *Principles of Sound Control in Airplanes.* OSRD No. 1543, National Defense Research Committee, 1944.
52. Koval, L. R.: Effects of Cavity Resonances on Sound Transmission Into a Thin Cylindrical Shell. *J. Sound & Vibration,* vol. 59, no. 1, July 8, 1978, pp. 23–33.
53. Howlett, James T.; and Morales, David A.: *Prediction of Light Aircraft Interior Noise.* NASA TM X-72838, 1976.

54. Mixson, John S.; Barton, C. Kearney; and Vaicaitis, Rimas: Interior Noise Analysis and Control for Light Aircraft. SAE Paper 770445, Mar.–Apr. 1977.
55. Cockburn, J. A.; and Jolly, A. C.: *Structural-Acoustic Response Noise Transmission Losses and Interior Noise Levels of an Aircraft Fuselage Excited by Random Pressure Fields.* Tech. Rep. AFFDL-TR-68-2, U.S. Air Force, Aug. 1968.
56. Geisler, D. L.: *Experimental Modal Analysis of an Aero Commander Aircraft.* NASA CR-165750, 1981.
57. Revell, J. D.; Balena, F. J.; and Koval, L. R.: *Analytical Study of Interior Noise Control by Fuselage Design Techniques on High-Speed, Propeller-Driven Aircraft.* NASA CR-159222, 1980.
58. Beranek, Leo L.; and Work, George A.: Sound Transmission Through Multiple Structures Containing Flexible Blankets. *J. Acoust. Soc. America,* vol. 21, no. 4, July 1949, pp. 419–428.
59. Heitman, Karen E.; and Mixson, John S.: Laboratory Study of Cabin Acoustic Treatments Installed in an Aircraft Fuselage. *J. Aircr.,* vol. 23, no. 1, Jan. 1986, pp. 32–38.
60. Grosveld, Ferdinand W.: Noise Transmission Through Sidewall Treatments Applicable to Twin-Engine Turboprop Aircraft. AIAA-83-0695, Apr. 1983.
61. Tate, R. B.; and Langhout, E. K. O.: Aircraft Noise Control Practices Related to Ground Transport Vehicles. *SAE Trans.,* sect. 3, vol. 90, 1981, pp. 2648–2666. (Available as SAE Paper 810853.)
62. Grosveld, Ferdinand W.: Field-Incidence Noise Transmission Loss of General Aviation Aircraft Double-Wall Configurations. *J. Aircr.,* vol. 22, no. 2, Feb. 1985, pp. 117–123.
63. Rennison, D. C.; Wilby, J. F.; Marsh, A. H.; and Wilby, E. G.: *Interior Noise Control Prediction Study for High-Speed Propeller-Driven Aircraft.* NASA CR-159200, 1979.
64. Pope, L. D.; and Wilby, J. F.: Band-Limited Power Flow Into Enclosures. *J. Acoust. Soc. America:*
    Part I. vol. 62, no. 4, Oct. 1977, pp. 906–911.
    Part II. vol. 67, no. 3, Mar. 1980, pp. 823–826.
65. Lyon, Richard H.: Analysis of Sound-Structural Interaction by Theory and Experiment. *Noise and Vibration Control Engineering,* Malcolm J. Crocker, ed., Purdue Univ., c.1972, pp. 182–192.
66. Lyon, Richard H.; and Maidanik, Gideon: Power Flow Between Linearly Coupled Oscillators. *J. Acoust. Soc. America,* vol. 34, no. 5, May 1962, pp. 623–639.
67. Wilby, J. F.; and Scharton, T. D.: *Acoustic Transmission Through a Fuselage Sidewall.* NASA CR-132602, 1975.
68. Dowell, E. H.; and Kubota, Y.: Asymptotic Modal Analysis and Statistical Energy Analysis of Dynamical Systems. *J. Appl. Mech.,* vol. 52, no. 4, Dec. 1985, pp. 949–957.
69. Smith, P. W., Jr.: Response and Radiation of Structural Modes Excited by Sound. *J. Acoust. Soc. America,* vol. 34, no. 5, May 1962, pp. 640–647.
70. Lyon, Richard H.: What Good is Statistical Energy Analysis, Anyway? *Shock and Vibration Dig.,* 1970, pp. 2–10.
71. Hart, F. D.; and Shah, K. C.: *Compendium of Modal Densities for Structures.* NASA CR-1773, 1971.
72. Runkle, Charles J.; and Hart, Franklin D.: *The Radiation Resistance of Cylindrical Shells.* NASA CR-1437, 1969.
73. Pope, L. D.; and Wilby, E. G.: *Analytical Prediction of the Interior Noise for Cylindrical Models of Aircraft Fuselages for Prescribed Exterior Noise Fields. Phase II: Models for Sidewall Trim, Stiffened Structures, and Cabin Acoustics With Floor Partition.* NASA CR-165869, 1982.
74. Beyer, T. B.; Powell, C. A.; Daniels, E. F.; and Pope, L. D.: Effects of Acoustic Treatment on the Interior Noise of a Twin-Engine Propeller Airplane. *J. Aircr.,* vol. 22, no. 9, Sept. 1985, pp. 784–788.

75. Vaicaitis, R.; and Mixson, J. S.: Theoretical Design of Acoustic Treatment for Noise Control in a Turboprop Aircraft. *J. Aircr.*, vol. 22, no. 4, Apr. 1985, pp. 318–324.
76. Vaicaitis, R.; and Slazak, M.: Noise Transmission Through Stiffened Panels. *J. Sound & Vibration,* vol. 70, no. 3, June 8, 1980, pp. 413–426.
77. Vaicaitis, R.; Grosveld, F. W.; and Mixson, J. S.: Noise Transmission Through Aircraft Panels. *J. Aircr.*, vol. 22, no. 4, Apr. 1985, pp. 303–310.
78. Vaicaitis, R.; Bofilios, D. A.; and Eisler, R.: *Experimental Study of Noise Transmission Into a General Aviation Aircraft.* NASA CR-172357, 1984.
79. Vaicaitis, R.; and Slazak, M.: *Cabin Noise Control for Twin Engine General Aviation Aircraft.* NASA CR-165833, 1982.
80. Grosveld, Ferdinand W.; and Mixson, John S.: Noise Transmission Through an Acoustically Treated and Honeycomb-Stiffened Aircraft Sidewall. *J. Aircr.*, vol. 22, no. 5, May 1985, pp. 434–440.
81. Wilby, John F.; Piersol, Allan G.; and Wilby, Emma G.: A Comparison of Space Shuttle Payload Bay Sound Levels Predicted by PACES and Measured at Lift-Off. *Proceedings of the Shuttle Payload Dynamic Environments and Loads Prediction Workshop, Volume I,* JPL D-1347, California Inst. of Technology, Jan. 1984, pp. 113–134.
82. Koval, L. R.: On Sound Transmission Into a Thin Cylindrical Shell Under "Flight Conditions." *J. Sound & Vibration,* vol. 48, no. 2, Sept. 22, 1976, pp. 265–275.
83. SenGupta, G.: Current Developments in Interior Noise and Sonic Fatigue Research. *Shock & Vibration Dig.,* vol. 7, no. 10, Oct. 1975, pp. 3–20.
84. SenGupta, G.; and Nijim, H. H.: Control of Cabin Noise in a Prop-Fan Aircraft by Structural Filtering. AIAA-79-0583, Mar. 1979.
85. Lyon, Richard H.: *Lectures in Transportation Noise.* Grozier Publ. Inc., c.1973.
86. White, Pritchard H.: Sound Transmission Through a Finite, Closed, Cylindrical Shell. *J. Acoust. Soc. America,* vol. 40, no. 5, Nov. 1966, pp. 1124–1130.
87. Koval, Leslie R.: Effects of Air Flow, Panel Curvature, and Internal Pressurization on Field-Incidence Transmission Loss. *J. Acoust. Soc. America,* vol. 59, no. 6, June 1976, pp. 1379–1385.
88. Koval, L. R.: On Sound Transmission Into an Orthotropic Shell. *J. Sound & Vibration,* vol. 63, no. 1, Mar. 8, 1979, pp. 51–59.
89. Koval, L. R.: On Sound Transmission Into a Stiffened Cylindrical Shell With Rings and Stringers Treated as Discrete Elements. *J. Sound & Vibration,* vol. 71, no. 4, Aug. 22, 1980, pp. 511–521.
90. Revell, J. D.; and Tullis, R. H.: *Fuel Conservation Merits of Advanced Turboprop Transport Aircraft.* NASA CR-152096, 1977.
91. May, D. N.; Plotkin, K. J.; Selden, R. G.; and Sharp, B. H.: *Lightweight Sidewalls for Aircraft Interior Noise Control.* NASA CR-172490, 1985.
92. Prydz, R. A.; Revell, J. D.; Balena, F. J.; and Hayward, J. L.: Evaluation of Interior Noise Control Treatments for High-Speed Propfan-Powered Aircraft. AIAA-83-0693, Apr. 1983.
93. Peterson, M. R.; and Boyd, D. E.: Free Vibrations of Circular Cylinders With Longitudinal, Interior Partitions. *J. Sound & Vibration,* vol. 60, no. 1, Sept. 8, 1978, pp. 45–62.
94. Bruderline, Henry H.: Developments in Aircraft Sound Control. *J. Acoust. Soc. America,* vol. 8, no. 3, Jan. 1937, pp. 181–184.
95. Rudmose, H. Wayne; and Beranek, Leo L.: Noise Reduction in Aircraft. *J. Aeronaut. Sci.,* vol. 14, no. 2, Feb. 1947, pp. 79–96.
96. Vaicaitis, Rimas; and Mixson, John S.: Review of Research on Structureborne Noise. *A Collection of Technical Papers, Part 2—AIAA/ASME/ASCE/AHS 26th Structures, Structural Dynamics and Materials Conference,* Apr. 1985, pp. 587–601. (Available as AIAA-85-0786.)
97. Lyon, R. H.; and Slack, J. W.: A Review of Structural Noise Transmission. *Shock & Vibration Dig.,* vol. 14, no. 8, Aug. 1982, pp. 3–11.
98. Rubin, S.; and Biehl, F. A.: Mechanical Impedance Approach to Engine Vibration Transmission Into an Aircraft Fuselage. *SAE Trans.,* vol. 76, 1967, pp. 2711–2719. (Available as SAE Paper 670873.)

99. Yoerkie, C. A.; Moore, J. A.; and Manning, J. E.: *Development of Rotorcraft Interior Noise Control Concepts, Phase 1: Definition Study.* NASA CR-166101, 1983.
100. Bellavita, Paolo; and Smullin, Joseph: Cabin Noise Reduction for the Agusta A-109 Helicopter. *Proceedings of Fourth European Rotorcraft and Powered Lift Aircraft Forum, Volume 2,* Associazione Italiano di Aeronautica ed Astronautica and Associazione Industrie Aerospaziali (Gallarate, Italy), Sept. 1978, pp. 61-0–61-29.
101. Metcalf, Vern L.; and Mayes, William H.: Structureborne Contribution to Interior Noise of Propeller Aircraft. *SAE Trans.,* sect. 3, vol. 92, 1983, pp. 3.69–3.74. (Available as SAE Paper 830735.)
102. Unruh, James F.; Scheidt, Dennis C.; and Pomerening, Daniel J.: *Engine Induced Structural-Borne Noise in a General Aviation Aircraft.* NASA CR-159099, 1979. (Available as SAE Paper 790626.)
103. Ewins, D. J.; and Silva, J. M. M.: Measurements of Structural Mobility on Helicopter Structures. *Proceedings of Symposium on Internal Noise in Helicopters,* Univ. of Southampton (England), 1980, pp. D1 1–D1 19.
104. Eichelberger, E. C.: Point Admittance of Cylindrical Shells With and Without Ring Stiffening. ASME Paper 80-WA/NC-5, Nov. 1980.
105. Junger, M. C.; Garrelick, J. M.; Martinez, R.; and Cole, J. E., III: *Analytical Model of the Structureborne Interior Noise Induced by a Propeller Wake.* NASA CR-172381, 1984.
106. Cremer, L.; and Heckl, M. (E. E. Ungar, transl.): *Structure-Borne Sound.* Springer-Verlag, 1973.
107. Ungar, Eric E.: Transmission of Plate Flexural Waves Through Reinforcing Beams; Dynamic Stress Concentrations. *J. Acoust. Soc. America,* vol. 33, no. 5, May 1961, pp. 633–639.
108. SenGupta, G.; Landmann, A. E.; Mera, A.; and Yantis, T. F.: Prediction of Structure-Borne Noise, Based on the Finite Element Method. AIAA-86-1861, July 1986.
109. Eversman, W.; Ramakrishnan, J. V.; and Koval, L. R.: A Comparison of the Structureborne and Airborne Paths for Propfan Interior Noise. AIAA-86-1863, July 1986.
110. Hayden, R. E.; Murray, B. S.; and Theobald, M. A.: *A Study of Interior Noise Levels, Noise Sources and Transmission Paths in Light Aircraft.* NASA CR-172152, 1983.
111. Royster, Larry H.; Hart, Franklin D.; and Stewart, Noral D., eds.: *NOISE-CON 81 Proceedings—Applied Noise Control Technology.* Noise Control Found., c.1981.
112. Crocker, Malcolm J.: Identification of Noise From Machinery, Review and Novel Methods. *INTER-NOISE 77 Proceedings, Noise Control: The Engineer's Responsibility,* Eric J. Rathe, ed., International Inst. of Noise Control Engineering (Switzerland), c.1977, pp. A 201–A 211.
113. Jha, S. K.; and Catherines, J. J.: Interior Noise Studies for General Aviation Types of Aircraft, Part I: Field Studies. *J. Sound & Vibration,* vol. 58, no. 3, June 8, 1978, pp. 375–390.
114. Kumar, Sudhir; and Srivastava, Narayan S.: Investigation of Noise Due to Structural Vibrations Using a Cross-Correlation Technique. *J. Acoust. Soc. of America,* vol. 57, no. 4, Apr. 1975, pp. 769–772.
115. Strahle, Warren C.; Muthukrishnan, M.; and Neale, Douglas H.: Coherence Between Internal and External Noise Generated by Gas Turbine Combustors. AIAA-77-20, Jan. 1977.
116. Keefe, Laurence: Interior Noise Path Identification in Light Aircraft Using Multivariate Spectral Analysis. AIAA-79-0644, Mar. 1979.
117. Piersol, A. G.; Wilby, E. G.; and Wilby, J. F.: *Evaluation of Aero Commander Sidewall Vibration and Interior Acoustic Data: Static Operations.* NASA CR-159290, 1980.
118. Forssen, Bjorn Henry: Determination of Transmission Loss, Acoustic Velocity, Surface Velocity and Radiation Efficiency by Use of Two Microphone Techniques. Ph.D. Thesis, Purdue Univ., Aug. 1983.
119. Atwal, Mahabir; and Bernhard, Robert: *Noise Path Identification Using Face-to-Face and Side-by-Side Microphone Arrangements.* NASA CR-173708, 1984.

120. Crocker, Malcolm J.; Forssen, Bjorn; Raju, P. K.; and Wang, Yiren S.: Application of Acoustic Intensity Measurement for the Evaluation of Transmission Loss of Structures. Purdue Univ. paper presented at the International Congres on Recent Developments in Acoustic Intensity Measurement (Senlis, France), Sept. 30–Oct. 2, 1981.
121. Dalan, G. A.; and Cohen, R. L.: Acoustic Intensity Techniques for Airplane Cabin Applications. *J. Aircr.,* vol. 22, no. 10, Oct. 1985, pp. 910–914.
122. McGary, Michael C.: *Noise Transmission Loss of Aircraft Panels Using Acoustic Intensity Methods.* NASA TP-2046, 1982.
123. Crocker, M. J.; Heitman, K. E.; and Wang, Y. S.: Evaluation of the Acoustic Intensity Approach To Identify Transmission Paths in Aircraft Structures. *SAE Trans.,* sect. 3, vol. 92, 1983, pp. 3.59–3.68. (Available as SAE Paper 830734.)
124. Maynard, J. D.; Williams, E. G.; and Lee, Y.: Nearfield Acoustic Holography: I. Theory of Generalized Holography and the Development of NAH. *J. Acoust. Soc. America,* vol. 78, no. 4, Oct. 1985, pp. 1395–1413.
125. Williams, Earl G.: Numerical Evaluation of the Radiation From Unbaffled, Finite Plates Using the FFT. *J. Acoust. Soc. America,* vol. 74, no. 1, July 1983, pp. 343–347.
126. Jha, S. K.; and Catherines, J. J.: Interior Noise Studies for General Aviation Types of Aircraft, Part II: Laboratory Studies. *J. Sound & Vibration,* vol. 58, no. 3, June 8, 1978, pp. 391–406.
127. Howlett, James T.; and Schoenster, James A.: An Experimental Study of Propeller-Induced Structural Vibration and Interior Noise. SAE Paper 790625, Apr. 1979.
128. McGary, Michael C.; and Mayes, William H.: A New Measurement Method for Separating Airborne and Structureborne Aircraft Interior Noise. *Noise Control Eng. J.,* vol. 20, no. 1, Jan.–Feb. 1983, pp. 21–30.
129. Ver, Istvan L.: Some Uses of Reciprocity in Acoustic Measurements and Diagnosis. *Inter-Noise 85, Proceedings 1985 International Conference on Noise Control Engineering, Volume II,* Tagungsbericht—Tb Nr. 39, Federal Inst. for Occupational Safety (Munich), Sept. 1985, pp. 1311–1314.
130. Bernhard, R. J.; Gardner, B. K.; Mollo, C. G.; and Kipp, C. R.: Prediction of Sound Fields in Cavities Using Boundary Element Methods. AIAA-86-1864, July 1986.
131. Metzger, Frederick B.: Strategies for Aircraft Interior Noise Reduction in Existing and Future Propeller Aircraft. SAE Paper 810560, Apr. 1981.
132. Goss, Russell P.: Acoustics Program for the Grumman Gulfstream II. AIAA-71-783, July 1971.
133. Gebhardt, George T.: Acoustical Design Features of Boeing Model 727. *J. Aircr.,* vol. 2, no. 4, July–Aug. 1965, pp. 272–277.
134. Holmer, Curtis I.: Approach to Interior Noise Control. *J. Aircr.:*
Part I: Damped Trim Panels, vol. 22, no. 7, July 1985, pp. 618–623.
Part II: Self-Supporting Damped Interior Shell, vol. 22, no. 8, Aug. 1985, pp. 729–733.
135. Marsh, Alan H.: Noise Control Features of the DC-10. *Noise Control Eng.,* vol. 4, no. 3, May–June 1975, pp. 130–139.
136. Waterman, E. H.; Kaptein, D.; and Sarin, S. L.: Fokker's Activities in Cabin Noise Control for Propeller Aircraft. SAE Paper 830736, Apr. 1983.
137. Hunter, Gertrude S.: Sound Reduction Program for Convair-Liner 340. *Noise Control,* vol. 2, no. 1, Jan. 1956, pp. 27–32.
138. Sternfeld, Harry, Jr.: New Techniques in Helicopter Noise Reduction. *Noise Control,* vol. 7, no. 3, May–June 1961, pp. 4–10.
139. Leverton, J. W.; and Pollard, J. S.: Helicopter Internal Noise—An Overview. *Proceedings of Symposium on Internal Noise in Helicopters,* Univ. of Southampton (England), 1980, pp. A4 1–A4 22.
140. Forth, Karl D.: Quiet Interiors. *Aviation Equip. Maint.,* vol. 5, no. 9, Sept. 1986, pp. 30–35.
141. Large, J. B.; Wilby, J. F.; Grande, E.; and Andersson, A. O.: The Development of Engineering Practices in Jet, Compressor, and Boundary Layer Noise. *Aerodynamic Noise,* Univ. of Toronto Press, c.1969, pp. 43–67.

142. Olcott, John W.; Larson, George C.; and Aarons, Richard N.: B/CA Analysis: Gulfstream 1000. *Bus. & Commer. Aviation,* vol. 49, no. 2, Aug. 1981, pp. 49–52.
143. Nichols, R. H., Jr.; Sleeper, H. P., Jr.; Wallace, R. L., Jr.; and Ericson, H. L.: Acoustical Materials and Acoustical Treatments for Aircraft. *J. Acoust. Soc. America,* vol. 19, no. 3, May 1947, pp. 428–443.
144. Mangiarotty, R. A.: An Isolator-Membrane for Soundproofing Aircraft Cabins Exposed to High Noise Levels. *J. Sound & Vibration,* vol. 3, no. 3, May 1966, pp. 467–475.
145. Balena, F. J.; and Prydz, R. A.: Experimental and Predicted Noise Reduction of Stiffened and Unstiffened Cylinders With and Without a Limp Inner Wall. AIAA-81-1968, Oct. 1981.
146. Vaicaitis, R.; and Mixson, J. S.: Theoretical Design of Acoustic Treatment for Cabin Noise Control of a Light Aircraft. AIAA-84-2328, Oct. 1984.
147. Howlett, James T.; and Clevenson, Sherman A.: *A Study of Helicopter Interior Noise Reduction.* NASA TM X-72655, 1975.
148. Bhat, W. V.; and Wilby, J. F.: Interior Noise Radiated by an Airplane Fuselage Subjected to Turbulent Boundary Layer Excitation and Evaluation of Noise Reduction Treatments. *J. Sound & Vibration,* vol. 18, no. 4, Oct. 22, 1971, pp. 449–464.
149. Wilby, J. F.; and Smullin, J. I.: Interior Noise of STOL Aircraft and Helicopters. *Noise Control Eng.,* vol. 12, no. 3, May–June 1979, pp. 100–110.
150. Henderson, John P.; and Nashif, Ahid D.: Reduction of Interior Cabin Noise Levels in a Helicopter Through Additive Damping. *Shock & Vibration Bull.,* Bull. 44, Pt. 5, U.S. Dep. of Defense, Aug. 1974, pp. 13–22.
151. Barton, C. K.: Structural Stiffening as an Interior Noise Control Technique for Light Twin-Engine Aircraft. Ph.D. Thesis, North Carolina State Univ., 1979.
152. Hrycko, G. O.: Design of the Low Vibration Turboprop Powerplant Suspension System for the DASH 7 Aircraft. *SAE Trans.,* sect. 3, vol. 92, 1983, pp. 3.133–3.145. (Available as SAE Paper 830755.)
153. Unruh, J. F.: Specification, Design and Test of Aircraft Engine Isolators for Reduced Interior Noise. *J. Aircr.,* vol. 21, no. 6, June 1984, pp. 389–396.
154. Lorch, D. R.: Noise-Reduction Measurements of Integrally Stiffened Fuselage Panels. AIAA-80-1033, June 1980.
155. Getline, G. L.: *Low-Frequency Noise Reduction of Lightweight Airframe Structures.* NASA CR-145104, 1976.
156. Ungar, Eric E.; and Kurzweil, Leonard G.: *Preliminary Evaluation of Waveguide Vibration Absorbers.* AFWAL-TR-83-3125, U.S. Air Force, Jan. 1984. (Available from DTIC as AD A140 743.)
157. Ellen, C. H.: *A Study of the Use of Blocking Masses in Reducing Helicopter Cabin Noise.* Tech. Memo Aero 1838, Royal Aircraft Establ., Mar. 1980.
158. Wheeler, P. D.; Rawlinson, R. D.; Pelc, S. F.; and Dorey, A. P.: The Development and Testing of an Active Noise Reduction System for Use in Ear Defenders. *INTER-NOISE 78, Designing for Noise Control,* William W. Lang, ed., Noise Control Found., c.1978, pp. 977–982.
159. Keith, S. E.; and Scholaert, H. S. B.: *A Study of the Performance of an Olson-Type Active Noise Controller and the Possibility of the Reduction of Cabin Noise.* UTIAS Tech. Note No. 228, Inst. for Aerospace Studies, Univ. of Toronto, Mar. 1981.
160. Silcox, R. J.; Fuller, C. R.; and Lester, H. C.: Mechanisms of Active Control in Cylindrical Fuselage Structures. AIAA-87-2703, Oct. 1987.
161. Salikuddin, M.; Tanna, H. K.; Burrin, R. H.; and Carter, W. E.: Application of Active Noise Control to Model Propeller Noise. AIAA-84-2344, Oct. 1984.